Exploring Conditions Leading to Self-Heating of Pyrrhotite-Rich Materials

Xinran Wang

Department of Mining, Metals and Materials Engineering

McGill University

Montreal, Canada

August 2007
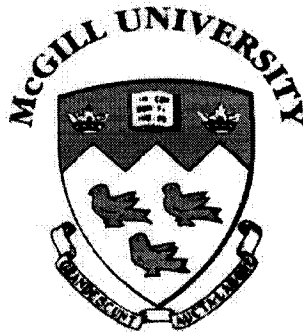
A thesis submitted to McGill University

in partial fulfillment of the requirements of the degree of

Master of Engineering

Abstract

Self-heating of sulphide minerals has a potential for serious impact on environment and safety in mining of ores, and storage and transport of concentrates. A research program, focused on the investigation of the conditions under which the H_2S is produced from pyrrhotite-rich materials, has been initiated using the self-heating facility and technology developed at the Noranda Technology Centre. It is hypothesized that H_2S production could be important in self-heating as the exothermic heat of oxidation of H_2S to SO_2 is greater than that for oxidation of S to SO_2.

The hypothesis of liberation of H_2S was tested using copper (as metal pieces and sulphate solution) as a detector, both in the self-heating apparatus and in a "weathering" apparatus at 40°C. X-ray diffraction and scanning electron microscopy analysis of coatings and precipitates confirmed the formation of copper sulphide and therefore indicated the release of H_2S. Release of H_2S involves acid conditions and the possible origin of the acidity was discussed.

Prior work had suggested that the level of exposure to oxygen was a factor in self-heating. Tests were conducted to explore the role of oxygen level. Three tests were conducted in the weathering apparatus at 40°C with covers of no hole, 3 holes and 128 holes to control access the air. Weight gain was recorded every two days and stage B self-heating tests were conducted on the samples after a month of weathering. Under limited air access (no hole and 3 hole covers), the samples showed higher weight gain, higher degree of

oxidation (by colour change) and higher self-heating rates compared with the sample with more exposure to air (128 hole cover). X-ray diffraction analysis identified the oxidation products elemental sulphur, maghemite and goethite in the samples under the limited air conditions. A series of non-standard self-heating tests were conducted in the self-heating apparatus under different air flow rates of Stage A. These showed that the samples weathered under low air flow rates yielded significantly higher self-heating rates in both stage A and B.

All the experiments indicate that a high level of exposure to air dose not promote self-heating but rather suppress it. Less oxidative conditions play a critical role in the self-heating of pyrrhotite-rich materials.

Résumé

L'auto-échauffement, menant à l'auto-combustion, des sulfures peut avoir de sérieuses conséquences environnementales et de sécurité lors du minage des minerais, du stockage et du transport des concentrés de minéraux sulfurés. Un programme de recherche, dédié à l'étude des conditions sous lesquelles le gaz hydrogène sulfuré est produit par des matériaux riches en sulfures, en utilisant l'équipement et la technologie développés au Centre de Technologie Noranda, a été initié. L'hypothèse selon laquelle la production de H_2S pourrait être importante pour l'auto-échauffement, puisque la chaleur dégagée par l'oxydation de H_2S en SO_2 est supérieure à celle dégagée par la transformation de S^0 en SO_2, a été renforcée.

L'hypothèse de libération de H_2S a d'abord été testée en utilisant le cuivre (sous forme de pièces de métal et de solution cuprique sulfatée) comme détecteur, à la fois dans l'appareil d'auto-échauffement et dans un appareil d'érosion à 40°C. La diffraction des rayons X et l'analyse par microscopie électronique à balayage sur les dépôts et précipités ont confirmé la formation de sulfures de cuivre et ont donc indiqué l'émanation de H_2S. Celle-ci implique des conditions acides et l'origine possible de l'acidité a été discutée.

Des travaux précédents ont suggéré que le degré d'exposition à l'oxygène était un facteur pour l'auto-échauffement. Des tests ont été réalisés pour explorer le rôle du niveau d'oxygène. Trois expériences ont été conduites dans un dispositif d'érosion à 40°C avec des couvercles exempts de trous, avec 3 trous et avec 128 trous pour contrôler l'accès

d'air. Le gain de masse a été enregistré tous les deux jours et après une période de 1 mois d'altération, les échantillons ont été soumis à des tests d'auto-échauffement (étape B à 140°C). Sous des conditions restreintes d'aération (couvercles sans trous et avec 3 trous), les échantillons ont montré un gain de masse, un degré d'oxydation (selon le changement de couleur) et des vitesses d'auto-échauffement plus importants à comparer des échantillons plus exposés à l'air (couvercle avec 128 trous). L'analyse par diffraction des rayons X a permis d'identifier du soufre élémentaire, de la *Maghemite* et de la *Goethite* comme produits d'oxydation. Unes série de tests d'auto-échauffement sous des conditions non-standards, c'est- à -dire sous différents flux d'air lors de l'étape A (à 70°C), a également été réalisée. Ceux-ci ont montré que les échantillons altérés sous des flux d'air faibles présentaient des vitesses de combustion plus élevées à la fois dans l'étape A et B du test.

Acknowledgements

Table of Contents

List of Figures

List of Tables

Chapter 1 Introduction

1. 1 Self-heating of Sulphides

Sulphides refer to several types of minerals containing sulphur in its lowest oxidation state, -2. Self-heating is the spontaneous heating of a material without external heat input. It is well established that sulphides will self-heat on exposure to moisture and oxygen (Farnsworth, 1977; Good, 1977; Rosenblum et al., 2001; Wu and Li, 2005). This process is highly exothermic and if the heat generated is not dissipated, combustion may occur when the temperature reaches the ignition point of the sulphide.

The hazards of sulphide self-heating range from sulphur dioxide release to fires. The literature documents self-heating incidents underground, on ships and trucks transporting sulphide concentrates and in mine waste (tailing) disposal areas. In 1917, 163 miners died in a fire in the Granite Mountain mine shaft, Montana; a fire occurred in 1945 at the Braden Copper mine in Chile killing 355 people, and in 1972 a fire at the Sunshine Mine, Idaho, claimed the lives of 91 miners. All these incidents were due to the spontaneous combustion of sulphides (Stachulak, 1990). Figure 1.1 is taken from the front cover of the CIM JUNE 1977 VOL. 70-NO.782 issue showing an underground fire at the (then) Cominco Sullivan mine, Kimberly, British Columbia. In 1966, at Mount Isa Mines, Australia, temperature of the ore in dumps reached more than 1000° F accompanied by large volumes of sulphur dioxide (Lukaszewski, 1969). Mine face temperatures in the Huelva mine, Spain (Ninteman, 1978) ranged up to 55°C due to heat generation. Mining

at these operations was restricted due to the high temperatures, sulphur dioxide emissions, low oxygen, and dusting caused by air thermals (Headley et al., 1977).
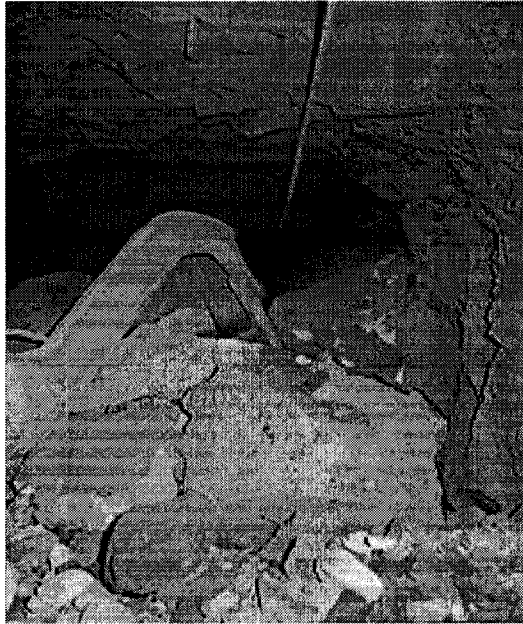
Figure 1. 1 Underground sulphide mine fire (Kimberly, BC, 1977)

The bulk volume of reactive sulphides stored in the open may increase up to 20 percent due to the formation of oxidation products (Ninteman, 1978). After a long period of "weathering", agglomeration occurs and materials become hard to handle because of the self-cementing properties of oxidized sulphides, and this is particularly evident in tailings (Lukaszewski, 1969).

Lukaszewski (1969), Farnsworth (1977), and Good (1977) note that sulphide minerals can act as fuel to promote mine fires. Good (1977) in his study of the Sullivan mine fire found that pyrrhotite was the most significant mineral in self-heating. Based on these findings, sulphide minerals could become classified as hazardous materials making

mining and transport of concentrates subject to increasing regulation. The problem is one the industry is keen to avoid.

Different strategies have been attempted to inhibit the self-heating of sulphide minerals. Since sulphide oxidation produces acid, lime or limestone was added to keep pH alkaline in anticipation of retarding oxidation. Sulphides were mixed with bentonite to try to adsorb oxygen (Good, 1977). Wetting (Lukaszewski, 1969), flooding and cooling by forced ventilation (Bowes et al., 1954) have been tried. Cementing (Rosenblum and Spira, 1981) and compacting to minimize access to air (Rosenblum et al., 2001) have also been investigated. All have met with inconsistent success. Bone-dry materials with moisture content less than 0.3% can be safely stored and shipped (Rosenblum et al., 2001) but this approach is not generally economic.

Developing a methodology to inhibit spontaneous combustion is hampered by the fact that the mechanism of self-heating is poorly understood. A trial and error approach is unlikely to succeed. Moisture and oxygen, as the most important factors affecting self-heating, will be examined in this thesis. Under certain conditions, H_2S gas has been detected (Somot and Finch, 2006). To generate H_2S implies reaction with an acid (Good, 1977; Thomas et al., 2000; Belzile et al., 2004; Gunsinger et al., 2006). Although H_2S was detected by Filippou et al. (1997) in pressure oxidation of pyrrhotite and by Thomas et al. (2000) when dissolving pyrrhotite in perchloric acid, no studies have demonstrated the possible role of H_2S in self-heating.

Somot and Finch (2006) reported results on pyrrhotite-rich tailings (PoT) using the self-heating facility developed at the Noranda Technology Centre (NTC) (Figure 1.2). The PoT sample was diluted with sand to give a range of PoT content. Standard self-heating tests were conducted to give self-heating rates as a function of PoT content (Figure 1.3).

(Room 2440 Flotation Chemistry Laboratory)
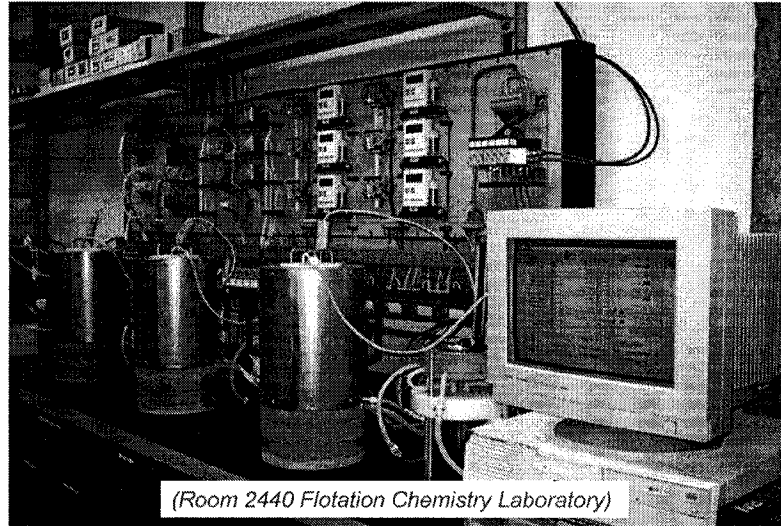
Figure 1. 2 General view of set-up of self-heating apparatus
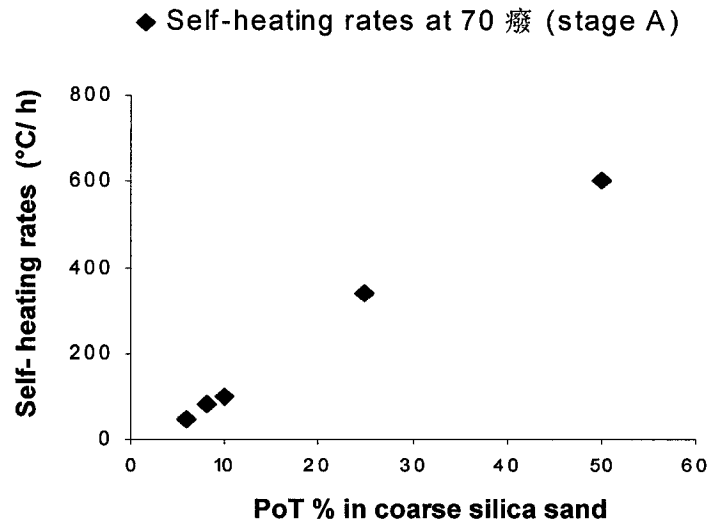
Figure 1. 3 Self-heating rates vs. PoT % (Somot and Finch, 2006)

As expected, the self-heating rates increased with the increasing PoT content. Visually, however, the colour of the samples evolved to suggest a different response (Figure 1.4): the colour of the samples containing 10% or less PoT was orange; the 25% PoT sample was greenish while the 50% PoT sample remained the original grey.
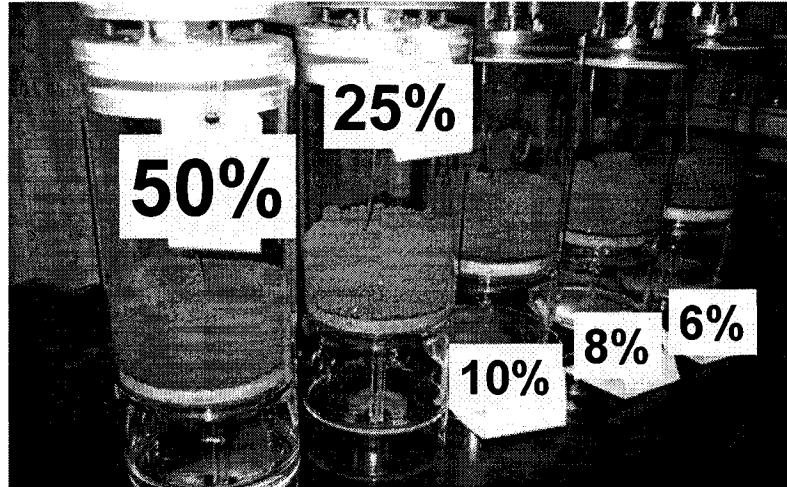
Figure 1. 4 Visual evidence of self-heating rates vs. PoT % (Somot and Finch, 2006)

That is, the samples showing the most visible evidence of oxidation corresponded to those having the lowest self-heating rates ($\leq$ 10% PoT) while that showing the least visible response gave the highest self-heating rate (50% PoT). Somot and Finch (2006) speculated that the high PoT content produced a low oxidizing environment that may favour formation of H_2S and it was formation of and/or subsequent reaction of H_2S that was responsible for the high heating observed. Evidence of H_2S formation was presented.

The current research program focused on testing the hypothesis of H_2S production from pyrrhotite (Po) rich materials under self-heating conditions. The investigation was conducted using the Noranda Technology Centre (NTC) self-heating facility and various

5

"weathering" test set-ups. The materials were characterized by a variety of techniques to aid interpretation. The source of acid needed for H_2S generation was also considered.

1. 2 Objectives

Somot and Finch (2006) proposed that H_2S might be a factor in self-heating. Therefore, the overall objectives of this thesis are:

I.   To test hypothesis that H_2S is formed using the self-heating apparatus with copper pieces and copper sulphate solution as indicators.

II.   To track the source of acid needed for the production of H_2S.

III.   To test liberation of H_2S in "weathering" apparatus to avoid possible artifacts associated with the standard test.

IV.   To test the importance of less oxidative conditions in self-heating of sulphides.

1. 3 Thesis Organization

The thesis consists of five chapters.

Chapter one introduces the problem of self-heating, and the objectives of the research. Chapter two summarizes the findings from the literature regarding the methods to evaluate self-heating, factors and conditions related with self-heating, and the reaction mechanisms. Chapter three outlines the apparatus, techniques, and procedures utilized in the experiments. Chapter four is the results section and discussion of the findings. Chapter five concludes the thesis, assesses the fulfillment of the project objectives and suggests possible future work.

Appendix lists

A1. The self-heating response curves for all the self-heating tests.

A2. The data of weight gain tests.

A3. Interim report on the researches in spontaneous heating of metal sulphide concentrates (II), 1976.

Chapter 2 Literature Review

2.1 Methods to Evaluate Self-heating of Sulphides

It has been known for centuries that self-heating or spontaneous combustion poses serious safety and environmental issues. The following text summarizes the methods established to test the self-heating behaviour of sulphide materials.

Good (1977) developed a procedure to perform combustion tests at Cominco's laboratory in Kimberley, BC, Canada using the apparatus in Figure 2.1. Two gram of -200 mesh sample was heated in a tube furnace in an oxygen stream. A thermocouple connected to a recorder was used to monitor the sample temperature continuously. The sulphur dioxide emissions were monitored up to the ignition point.
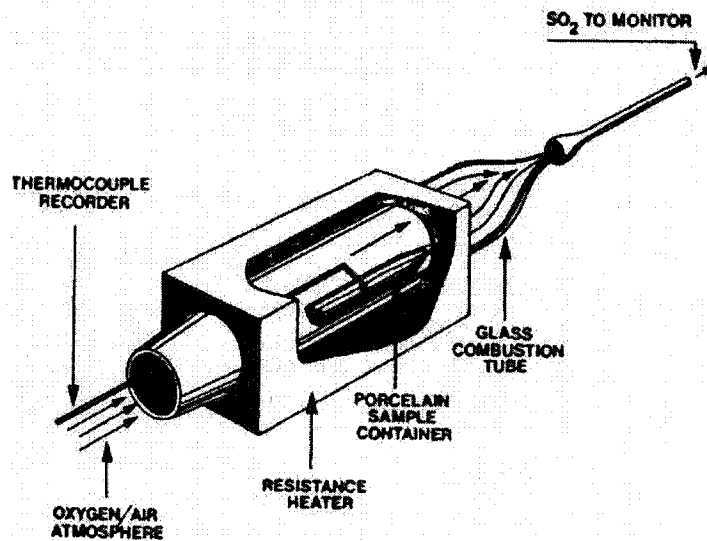
Figure 2. 1 Combustion test apparatus (Good, 1977)

Figure 2.2 is a typical heating response curve with a pyrrhotite sample and the corresponding sulphur dioxide emissions. The ignition temperature of -200 mesh pyrrhotite was 400°C shown as a sharp temperature increase (Good, 1977).
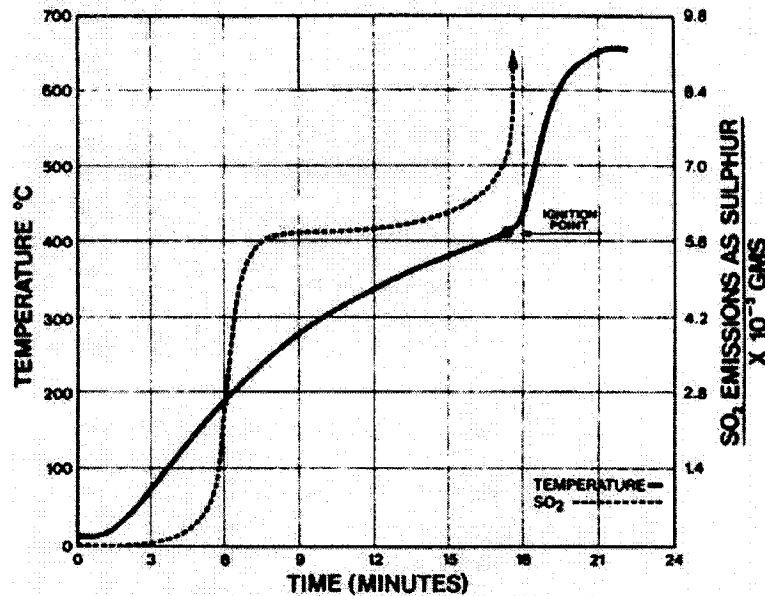
Figure 2. 2 Typical heating curve and SO₂ emissions using apparatus in Figure 2.1

(Good, 1977)

The West German Materials Testing Office (BAM) developed a method based on the principle of temperature rise of samples placed in a wiremesh cylinder. An oven, controlled at 200°C, was used to keep the sample at a constant temperature (Wegener and Schlieper, 1977). If the temperature rise of the sample exceeded 500°C within 48 hours, the material was considered as self-igniting.

A method to predict the spontaneous combustion of sulphide minerals at ambient temperature was created by Wu and Li (2005). In their weight increment test, 40 gram of -40 mesh sample was placed in a chamber set at 40°C and 90% relative humidity. Over 4

9

to 10 days the sample weight was recorded. In their oxygen absorption test, a 100g sample was placed in a sealed container immersed in an isothermal water trough. The container was filled with a known volume of air. During the test period, the quantity of absorbed oxygen was measured. Wu and Li found a linear relationship between the amount of oxygen absorption and the weight increment. Although the weight increment method may indicate reactivity of a sample, it is not an accurate way to predict spontaneous heating potential because oxidation and self-heating are not equivalent.

The Self-Heating Substances Test (DOT/UN Division 4.2) is used to classify materials as spontaneously combustible in accordance with U.S. Department of Transportation (DOT) and United Nations (UN) requirements. This method states introducing a powder sample into a 100 mm x 100 mm x 100 mm stainless steel cubic mesh basket which is set in an oven with temperature of 140 °C for 24 hours. During the experiment, the sample temperature is monitored at several locations.

The above methods are, more precisely, employed to measure self-ignition or reactivity rather than self-heating. An advance in the evaluation of self-heating potential was developed by Rosenblum and Spira (1981) at the Noranda Technology Center (NTC). The technique measured the rate of self-heating of a one kg sample maintained at 38.5°C and monitored the oxygen consumption rate to assess the potential hazard from self-heating of sulphides. The apparatus is shown in Figure 2.3 (Rosenblum and Spira, 1981). The test sample is set in a one litre beaker (reaction vessel) placed inside a sealed five litre Dewar flask which is held within a Styrofoam block. The vessel was surrounded by a copper shield heated by a heating coil.
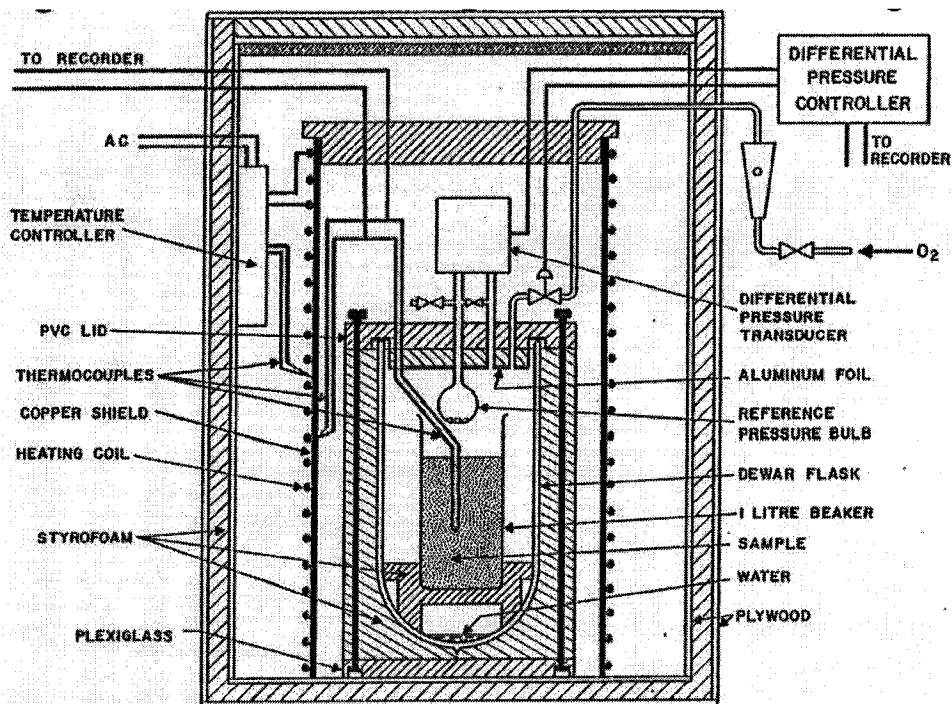
Figure 2. 3 Noranda Technology Center temperature-rise apparatus (Rosenblum and Spira, 1981)

One of the shortcomings of the method is that the samples to be investigated need to be warmed up outside the apparatus to 28°C before being placed in the reaction chamber. Also, the amount of sample seemed to affect the results. Rosenblum and Spira stated that 0.5 kg sample gave 40% higher self-heating rate than 1 kg sample probably because the bottom part of the sample behaved like a heat sink.

A notable advance in the ranking of the self-heating hazard of sulphides was the self-heating apparatus (Figure 1.2). The samples can be tested from room temperature to 500°C. The flow rate of air (or any test gas) is controlled by a flow meter. There are standard and manual operation modes to meet different requirements which make it a

11

very flexible technique to evaluate self-heating potential. Details of the self-heating apparatus used in this thesis will be described in section 3.1.1.

2.2 Factors Affecting the Self-heating of Sulphide Materials

Extensive studies have been conducted to investigate factors involved in sulphide oxidation. The following identifies some of the possible parameters playing a role in the self-heating of sulphide materials, notably: pyrrhotite content, oxygen and moisture level, pH, particle size distribution (or surface area), voidage, temperature, galvanic effects, and presence of ferric iron, trace metals and bacteria.

In the mineral processing industry, another important commodity that can self-heat is coal (Nordon, 1979; Jones and Littlefair, 1997; Jones et al., 1998; Fierro et al., 2001; Wang et al., 2002; Wang et al., 2003). Coal has some common important variables like sulphides, for example, particle size, temperature, moisture, oxygen, but this thesis will focus on sulphides.

2.2.1 Pyrrhotite

Pyrrhotite is the most common iron sulphide mineral in nature after pyrite and both are common minerals present in tailings and waste rock from processing base-metal ores (Cruz et al., 2005). Pyrrhotite is often associated with pyrite, sphalerite, galena, chalcopyrite and pentlandite. The general formula is $Fe_{1-x}S$ ($0 \leq x \leq 0.125$) revealing a non-stoichiometric composition with a disordered NiAs structure (Shaw et al., 1998; Filippou et al., 1997; Janzen et al., 2000; Thomas et al., 2000; Mikhlin et al., 2002). Another way to express the formula is $Fe_{n-1}S$ ($n \geq 8$) (Thomas et al., 2000) and the range is

12

from Fe_7S_8 to $Fe_{11}S_{12}$ with the corresponding ratio of Fe to S from 0.875 and 0.917. Pyrrhotite oxidizes 20-100 times faster than pyrite because of its non-stoichiometric structure (Shaw et al., 1988). Lukaszewski (1973) mentioned that both pyrrhotite and pyrite are highly susceptible to oxidation but the oxidation rate of pyrite under optimum conditions was generally slow enough that heat was lost to the surroundings.

The non-stoichiometry of pyrrhotite is due to a system of ordered vacancies within the Fe lattice (Thomas et al., 2000; Posfai et al., 2000). Arnold (1966) noted a good correlation between structural type and composition. Pyrrhotite with the smallest ratio of Fe to S, in other words, the most iron deficient, has monoclinic symmetry while the least iron deficient or metal-rich forms have hexagonal and orthorhombic structures (Janzen et al., 2000; Thomas et al., 2001).

Pyrrhotite rarely exists as a single phase and intergrowths of coexisting monoclinic and hexagonal pyrrhotite are common (Arnold, 1966). Belzile (2004) suggest that monoclinic pyrrhotite is less reactive than the hexagonal variant. But Vanyukov and Razumovskaya (1979) reported that monoclinic pyrrhotite with higher sulphur to iron ratio tends to have a higher oxidation rate than hexagonal pyrrhotite. Studies by Janzen et al. (2000) suggested that pyrrhotite crystal type did not have a consistent effect on pyrrhotite oxidation rate.

Pyrrhotite is more susceptible to weathering processes compared to other sulphide minerals. It is generally agreed that pyrrhotite is the most serious offender in the self-heating process (Ninteman, 1978). The order of decreasing susceptibility to weathering

13

for some sulphide minerals is: pyrrhotite, sphalerite, pentlandite, pyrite, chalcopyrite (Gunsinger et al., 2006). It is well documented that pyrrhotite is one of the most unstable mineral phases in sulphide mine wastes (Jambor, 1994). The study of oxidation of sulphide minerals conducted by Steger (1979) found that the total iron in the water-soluble oxidation products of pyrrhotite, chalcopyrite and pyrite is 1.7 mg Fe/g, 1.2 mg Fe/g and 0.65 mg Fe/g, respectively, after 4 hrs at pH 2.8 in hydroxylamine hydrochloride solution, indicating that pyrrhotite was much more reactive than pyrite.

2.2.2 Moisture and Oxygen

Past investigations have shown that moisture content plays a critical role in the self-heating of sulphides. A moisture content from 3 to 8 percent has been found to be the ideal condition for self-heating (Ninteman, 1978). The effect of moisture content on the rate constant of oxygen consumption per unit weight of a copper concentrate, that was used to evaluate self-heating (Appendix A3) is summarized in Table 2.1.

Table 2. 1 Rate constant for oxygen consumption per unit weight of copper concentrate at 60°C

moisture content (w %)	rate constant (min^{-1})
0.37	$1.20*10^{-3}$
3.70	$1.05*10^{-2}$
8.70	$1.53*10^{-2}$
15.80	$8.30*10^{-3}$

The rate constant increased to a maximum when the moisture content was within the range 3.7 to 8.7% then decreased with higher moisture content. A moisture content below about 2 percent and the water will evaporate quickly; at a moisture content above 8 percent the water will absorb heat by evaporation and prevent heating. Generally, water is

used as a spray on sulphide concentrates during transportation to dissipate the heat (Ninteman, 1978). A study conducted by Gunsinger et al. (2006) of pyrrhotite-rich tailings found that higher moisture content close to the impoundment surface impeded the ingress of oxygen and limited sulphide oxidation. The effective oxygen-diffusion coefficient depends on the degree of water saturation, so a high water content can retard oxidation. In order to inhibit or slow the oxidation of sulphide tailings, maintaining water saturated conditions can be applied (Tremblay, 2007).

It is reported that the "bone dry" materials or those with moisture content higher than 26% will not self-heat (Rosenblum and Spira, 1981). Figure 2.4 (Rosenblum and Spira, 1981) indicates that the self-heating rate of the sulphide tailings reached the highest point at about 3% moisture although the oxygen consumption rate remained constant over the range 1 to 13% moisture.
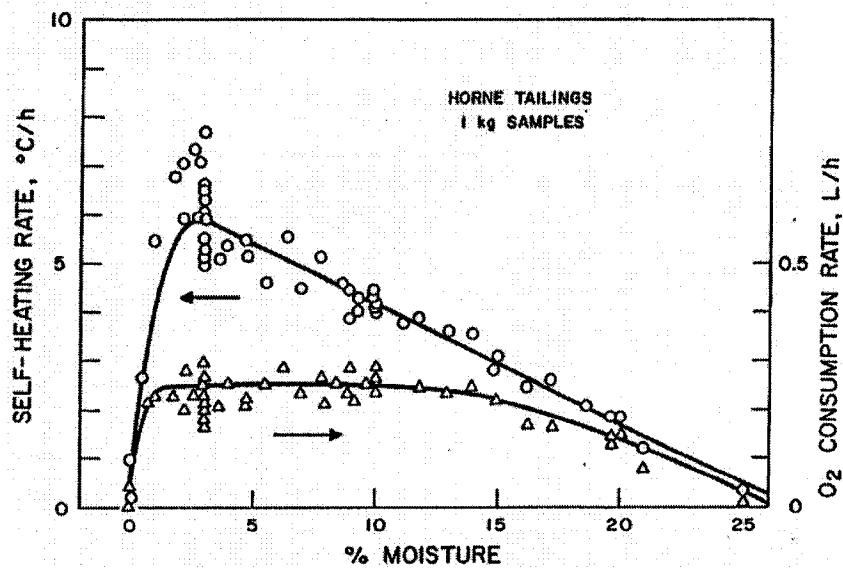
Figure 2. 4 Effect of moisture content on the self-heating rate and oxygen consumption of sulphide tailings (Rosenblum and Spira, 1981)

Steger (1982) studied the effect of humidity on the oxidation of monoclinic pyrrhotite at 50°C in a humidity controlled chamber and the results (Table 2.2) showed that the reaction rate, based on the release of iron and sulphate, increased at the higher relative humidity.

Table 2. 2 Oxidation rate of monoclinic pyrrhotite at 50°C (Steger, 1982)

relative humidity %	rate(mol/m²/s) based on the release of	
	Iron	Sulphate
37	$3.2*10^{-9}$	$8.0*10^{-10}$
50	$4.4*10^{-9}$	$9.1*10^{-10}$
55	$5.2*10^{-9}$	$9.1*10^{-10}$
75	$1.1*10^{-8}$	$9.0*10^{-10}$

Besides moisture, oxygen is the other vital factor in self-heating. No heat was generated if the sulphides were exposed to nitrogen during self-heating tests on pyrrhotite-rich materials performed by the author (see later). Compacting sulphides and covering stockpiles with plastic sheeting can suppress self-heating by preventing the ingress of air (Rosenblum et al., 2001).

Good (1977) had shown in ignition tests that reaction rate was lowered when an oxygen atmosphere was replaced by air although it did not apparently change the ignition temperature.

2.2.3 Temperature

Temperature plays an important role in the self-heating process. Data collected in self-heating tests on sulphide waste rock (Figure 2.5) (Rosenblum and Spira, 1995) showed that self-heating rates increased from below the detection limit at low temperature to 35°C/h at 70°C in stage A. There was a dramatic increase in self-heating rates when the

temperature was increased from 99°C to 110°C, just below the melting point of elemental

sulphur.
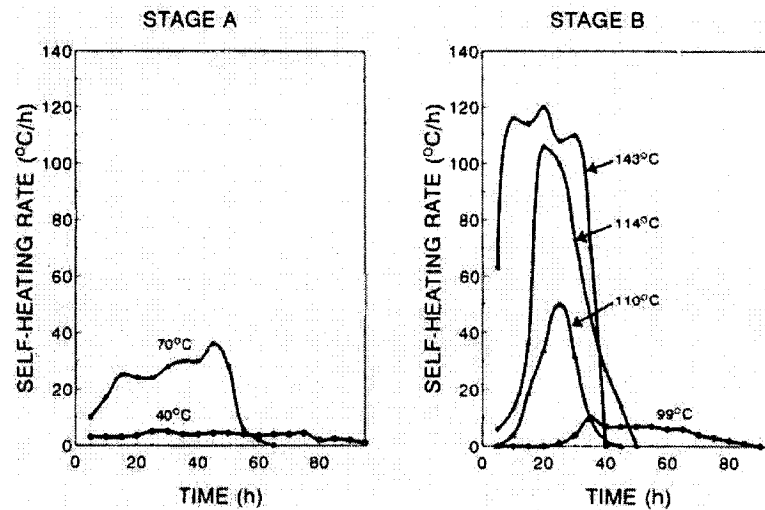
Figure 2. 5 Effect of temperature on self-heating of sulphide rock in stage A and B

(Rosenblum and Spira, 1995)

Tests on the effect of temperature on spontaneous heating of a copper concentrate (Appendix A3) indicated the rate constant of oxygen consumption per unit weight of concentrate increased from $2.2*10^{-3}$ at 30°C to $1.53*10^{-2}$ at 60°C.

Self-heating tests on sulphide waste rock conducted by Rosenblum and Spira (1995) (Figure 2.6) have shown that the rate of elemental sulphur formation increases with temperature. At 10°C, little sulphur was detected but rapid formation occurred above 30°C.
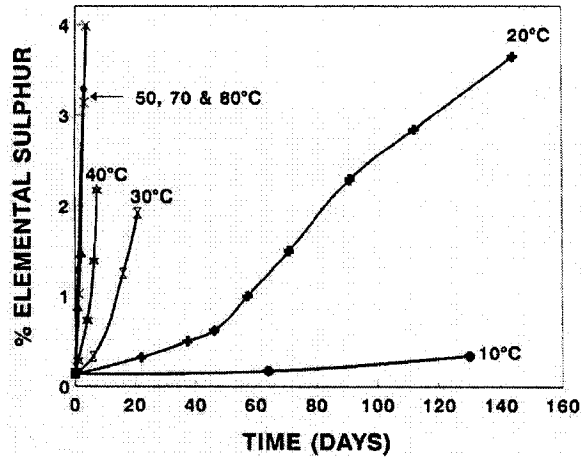
Figure 2. 6 Effect of temperature on rate of sulphur formation during weathering in stage A (Rosenblum and Spira, 1995)

The effect of ambient temperature on the oxidation rate of monoclinic pyrrhotite was studied by Steger (1982) at 62% relative humidity in a temperature controlled chamber and the results (Table 2.3) showed that the reaction rate based on the release of iron and sulphate increased with increasing temperature.

Table 2. 3 Oxidation rate of monoclinic pyrrhotite at 62% relative humidity (Steger, 1982)

temperature °C	rate(mol/m^2/s) based on the release of	
	Iron	Sulphate
28	$3.9*10^{-9}$	$6.5*10^{-10}$
35	$5.0*10^{-9}$	$7.1*10^{-10}$
43	$6.3*10^{-9}$	$7.8*10^{-10}$
50	$8.9*10^{-9}$	$8.4*10^{-10}$

2.2.4 Particle Size and Specific Surface Area

Coarse particles can be vulnerable to oxidation because they allow ready oxygen access (Gunsinger et al., 2006). However, reactivity will increase as particle size decreases

18

(Figure 2.6) (Lukaszewski, 1973): the finer the particle, the more surface area and, therefore, the more heat that is generated. The coarser the particle, the higher the ignition temperature.
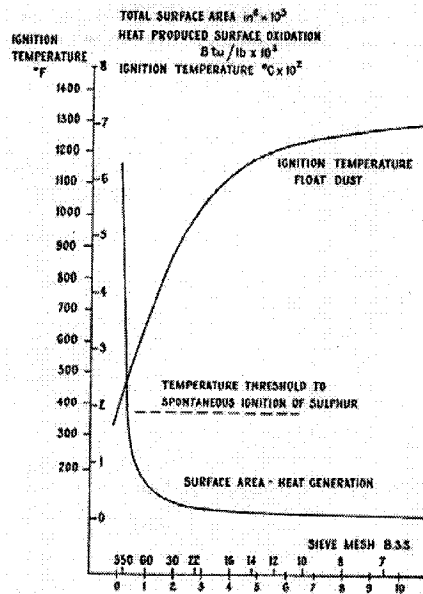
Figure 2. 7 Relationship between surface area, particle size, heat generated by oxidation and ignition temperature of pyritic float dust (Lukaszewski, 1973)

The ignition tests conducted by Good (1977) indicated that the ignition point increased from 400°C for -200 mesh pyrrhotite to 480°C for a -35+48 mesh sample. The self-heating tests conducted by Rosenblum and Spira (1981) showed that the self-heating rates of -325 mesh sulphide tailings was double that of the +325 fraction. Compacting sulphides can limit self-heating by reducing voidage and permeability of oxygen.

Thermal gravimetric analysis of pyrrhotite conducted by Reimers and Hjelmstad (1987), had shown that the ignition point lowered by about 50°C when particle size was made finer by increasing the milling time from 15 min to 120 min.

Janzen et al. (2000) claimed that surface roughness and fractures lead to higher specific surface areas and pyrrhotite with extensive fractures oxidized rapidly in their study of the effect of surface area on the oxidation rate. Farnsworth (1977) stated that irregular particle shape and small particle size increased the surface area and therefore increased the vulnerability to self-heating.

The effect of particle size on self-heating shown in Figure 2.8 (Rosenblum and Spira, 1995) indicates that the smaller the particles the higher the self-heating rates especially in stage B. Heat was not generated in stage A with particles larger than 0.5 mm, while particles coarser than 1.4 mm produced some heat in stage B.
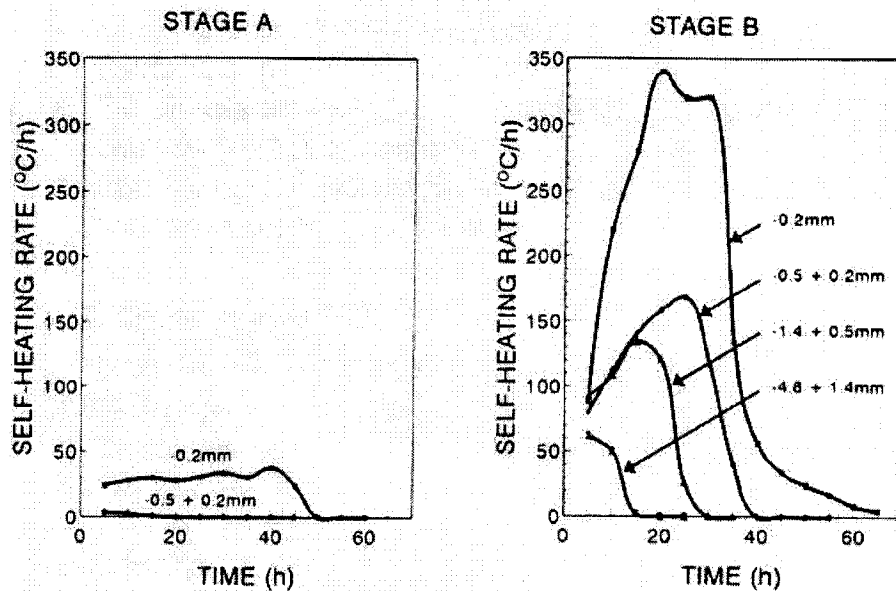
Figure 2. 8 Effect of particle size on self-heating rate in stage A and B (Rosenblum and Spira, 1995)

2.2.5 Galvanic Effects

Galvanic effects arise when two or more minerals are in contact with each other that differ in electrochemical properties. As a result electrons transfer from a less cathodic mineral to a more cathodic one (Rao, 2003). The role of galvanic effects on the flotation of sulphides has been studied; however, its effect on self-heating has not been well documented. The self-heating potential of mixtures of two or more sulphides is much higher than a single sulphide due to the galvanic effects according to Ninteman (1978). Cruz et al. (2001) claimed in their study of pyrite leaching, that at the beginning of the weathering process, the existence of other sulphides, for instance, galena, sphalerite and chalcopyrite, will affect pyrite reactivity, either promoting oxidation or passivation.

The rest potential values vs. standard hydrogen electrode (SHE) at pH 4 for common sulphide minerals are: pyrite (FeS_2), 0.66; marcasite (FeS_2), 0.63; chalcopyrite ($CuFeS_2$), 0.56; sphalerite (ZnS), 0.46; covellite (CuS), 0.42; pentlandite (NiFeS), 0.35; pyrrhotite (0.31); chalcocite (Cu_2S), 0.31 and galena (PbS), 0.21 (Rao, 2003). Mehta and Murr (1983) and Nowak et al. (1984) observed that the mineral with highest rest potential (typically pyrite) is galvanically protected while the ones with lower rest potential (most minerals relative to pyrite) are oxidized when the minerals are in contact. Pyrrhotite with a relatively low rest potential is one of the fastest minerals to oxidize. Nowak et al. (1984) performed experiments using acidic solutions of pH 2 saturated with oxygen and gave the following order of the magnitude of galvanic effect, galena-pyrite > chalcocite-pyrite>> chalcocite-chalcopyrite> galena-chalcopyrite> chalcopyrite-pyrite.

2.2.6 Ferric Iron

Ferric iron can have the same function as oxygen, i.e., can oxidize pyrrhotite. Janzen et al. (1996) claimed that oxidation rates were dramatically increased with the presence of ferric iron and that the oxidation rate with ferric iron was the most rapid of all reactions. A fractional reaction order from 0.45 to 0.66 was found by Janzen et al. (2000) in their study of the dependence of pyrrhotite oxidation on ferric iron at 25°C, pH 2.75 with initial ferric concentration $2*10^{-4}$ mol/L.

2.2.7 Trace Elements

The effect of trace elements on oxidation of pyrrhotite has been little studied thus far. Kwong (1995) (after Belzile et al., 2004) noted that pyrrhotite with high trace metal content oxidized slower than the ones with lower trace metal content. Although Janzen et al. (2000) noticed a trend of decreasing oxidation rate (at pH 2.75 and 25°C) with increasing trace metal content on 12 pyrrhotite samples, no dramatic effect was found.

2.2.8 Bacteria

The importance of micro-organisms, for instance Acidithiobacillus ferrooxidans, in the oxidation of sulphides has been considered by several authors. Schippers et al. (2007) reported in their geomicrobiological and geochemical studies of pyrrhotite containing tailings that the ratio of biological to chemical oxidation was about 50:50. Gunsinger et al. (2006) noted that sulphide-oxidizing bacteria from groups such as Acidithiobacillus can catalyze the weathering process and Acidithiobacillus ferrooxidans is an effective catalyst of the oxidation process (Biglari et al., 2006). Nordstrom and Southam (1997) (after Schippers et al., 2007) stated that the existence of metal sulphide oxidizing micro-organisms accelerated the kinetics of pyrite oxidation 30-300 fold. Mielke et al. (2003)

claimed that the presence of bacteria under acidic conditions promoted the oxidation of sulphides and generation of ferric iron.

2.3 Reaction Mechanisms

The chemical aspects of the self-heating of sulphide materials are not well understood. Spontaneous heating takes place through a series of steps and forms several intermediate species like ferrous and ferric ions, and solid products, for instance elemental sulphur, ferrous and ferric hydroxides, and goethite. Evaluation of the oxidation of sulphides based on the total metal or sulphate in the oxidation products can indicate the extent of reaction. Knowledge of the chemical composition of the oxidation products may help to better understand the reaction mechanisms. The following discusses possible mechanisms involved in the self-heating of pyrrhotite-rich materials.

It is generally believed that the overall oxidation process of pyrrhotite follows equation 2.1 (Shaw et al., 1998; Buckley and Woods, 1987; Janzen et al., 2000) and equation 2.2 (Shaw et al., 1998; Janzen et al., 2000) when oxygen and ferric iron are the oxidants, respectively.

$$Fe_{1-x}S + (2 - 1/2x)O_2 + xH_2O = (1 - x)Fe^{2+} + SO_4^{2-} + 2xH^+ \qquad (2.1)$$

$$Fe_{1-x}S + 4(2 - x)Fe^{3+} + 4H_2O = 3(3 - x)Fe^{2+} + SO_4^{2-} + 8H^+ \qquad (2.2)$$
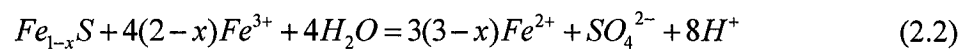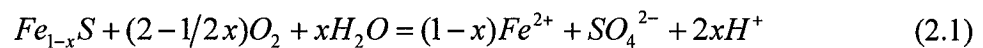
Gunsinger et al. (2006) considered that at pH below 4, the dominate mechanism follows equation 2.2 and that pyrrhotite will be oxidized by ferric iron. Low pH means ferric ion does not precipitate while above pH 3.0 ferric ion will precipitate as ferric hydroxide (Janzen et al., 2000). Mycroft et al. (1990) found that the oxidation mechanism did not

show a significant change between pH 4.6 and 13 in their study of pyrite oxidation. But, at low pH, more elemental sulphur was produced.

Pyrrhotite usually experiences partial oxidation with the formation of ferrous, elemental sulphur, goethite and ferric according to Shaw et al. (1998) and Janzen et al. (2000).

$$Fe_{1-x}S + 1/2(1-x)O_2 + 2(1-x)H^+ = (1-x)Fe^{2+} + S^0 + (1-x)H_2O \tag{2.3}$$

$$Fe_{1-x}S + Fe^{3+} + 3/4O_2 + 5/2H_2O = 2FeOOH + S^0 + 3H^+ \tag{2.4}$$

$$Fe_{1-x}S + 3/4(1-x)O_2 + 3(1-x)H^+ = (1-x)Fe^{3+} + S^0 + 3/2(1-x)H_2O \tag{2.5}$$

$$Fe_{1-x}S + 2(1-2)Fe^{3+} = 3(1-x)Fe^{2+} + S^0 \tag{2.6}$$
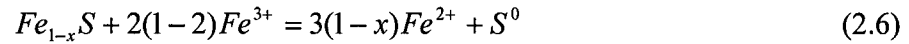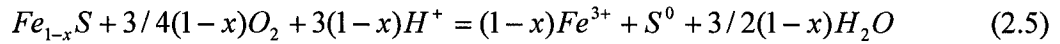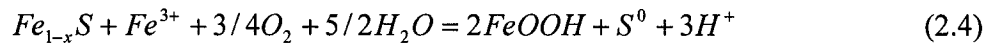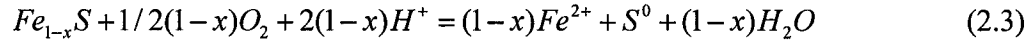
The oxidation of pyrrhotite can proceed by different pathways depending on conditions to yield different kinds of products. Lukaszewski (1973) claimed that under conditions of low aeration, ferrous sulphate and sulphur are the principal oxidation products of pyrrhotite while ferric sulphate and sulphuric acid are formed under high aeration.

Steger (1981) described pyrrhotite oxidized at 50°C and 37% relative humidity by equation 2.7.

$$Fe_7S_8 + O_2 = xFeS_2O_3 + (1-x)FeSO_4 \tag{2.7}$$

Subsequently, FeS_2O_3 might oxidize to $FeSO_4$ or $Fe_2(SO_4)_3$ through equations 2.8 and 2.9 accompanied by the formation of sulphate and elemental sulphur.

$$FeS_2O_3 + O_2 = FeSO_4 + S \tag{2.8}$$

$$2FeS_2O_3 + 3O_2 = Fe_2(SO_4)_3 + S \tag{2.9}$$
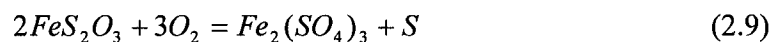
Steger found at 50% relative humidity, the oxidation and/or hydrolysis of $FeSO_4$ and $Fe_2(SO_4)_3$ formed an insoluble compound, possibly following equation 2.10.

$$Fe(SO_4) + (2x+1)H_2O + O_2 = 2Fe(OH)(SO_4) \cdot xH_2O \qquad (2.10)$$
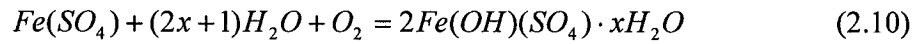
Ferric oxide and sulphuric acid were formed by the hydrolysis of $Fe(OH)(SO_4)$. xH_2O via equation 2.11

$$Fe(OH)(SO_4) + H_2O = FeO(OH) + H_2SO_4 \qquad (2.11)$$
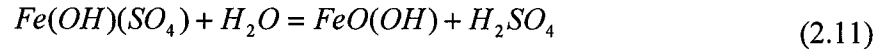
and sulphuric acid reacted via equation 2.12.

$$Fe_7S_8 + 7H_2SO_4 + O_2 = 7FeSO_4 + 7H_2O + 8S \qquad (2.12)$$
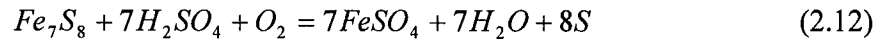
Shaw et al. (1998) stated that dissolved Fe^{2+} may be oxidized and hydrolyzed and form ferric hydroxide precipitate and acid via equation 2.13.

$$Fe^{2+} + 1/4O_2 + 5/2H_2O = Fe(OH)_3 + 2H^+ \qquad (2.13)$$
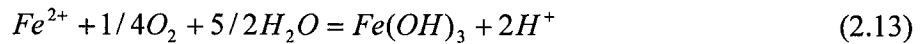
Marcasite (a form of FeS_2) observed as initial phase in the oxidation of pyrrhotite-rich tailings (Gunsinger et al., 2006) can be formed and suggested equation 2.14 (Shaw et al., 1998).

$$2Fe_{1-x}S + (1/2 - x)O_2 + 2(1-2x)H^+ = FeS_2 + (1-2x)Fe^{2+} + (1-2x)H_2O \qquad (2.14)$$

At low pH, pyrrhotite can be non-oxidatively dissolved by acid with generation of Fe^{2+} and H_2S (Good 1977; Belzile et al., 2004; Gunsinger et al., 2006; Thomas et al., 2000) according to equation 2.15.

$$Fe_{1-x}S + 2H^+ = H_2S + (1-x)Fe^{2+} \qquad (2.15)$$
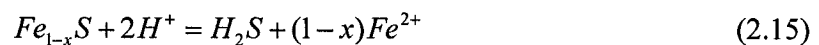
Steger (1977) stated that pyrrhotite is more readily attacked by acid with the liberation of H_2S than pyrite and chalcopyrite. The liberated H_2S might be oxidized in the presence of

25

oxygen by equation 2.16 (Filippou et al., 1997; Bukhtiyarova et al., 2000; Good, 1977) to form elemental sulphur (enthalpy of -297kJ/mol) (Somot and Finch, 2006).

$$H_2S + 1/2O_2 = S^0 + H_2O \qquad (2.16)$$

Elemental sulphur was detected by Rosenblum and Spira (1995) in their self-heating study of sulphide waste rock at 70°C. They found that the self-heating rates were closely related to the sulphur formed and reached zero when no sulphur was left. Farnsworth (1977) claimed that free sulphur can lower the ignition temperature and contribute to spontaneous reactions.

A significant emission of SO_2 was noticed by Good (1977) between 150°C and 220°C and he claimed that initial emission of sulphur dioxide resulted from the burning of elemental sulphur formed as an oxidation product of pyrrhotite. Sulphur dioxide as exit gas was detected by Rosenblum and Spira (1995) in their study of sulphide waste rock at 120°C and the heat generation followed the sulphur dioxide evolution. The presence of free sulphur might contribute to sulphide self-heating by equation 2.17 (Somot and Finch, 2006).

$$S + O_2 = SO_2 \qquad (2.17)$$

The liberated H_2S can also be oxidized to sulphur dioxide and generate more heat with enthalpy of -562 kJ/mol (equation 2.18) (Somot and Finch, 2006; Bukhtiyarova et al., 2000).

$$H_2S + 3/2O_2 = SO_2 + H_2O \qquad (2.18)$$

The reaction mechanism of oxidation, or self-heating of pyrrhotite is complex and different products will be generated depending on conditions. As mentioned, several variables affect self-heating and make it hard to control.

Chapter 3 Experimental

3. 1 Self-heating Apparatus, "Weathering" Apparatus and Sample Preparation

3.1. 1 Self-heating Apparatus

The self-heating apparatus (Figure 3.1) used in this research program was developed by Mr. Frank Rosenblum and co-workers at the Noranda Technology Centre (Rosenblum and Spira, 1995; Rosenblum et al., 2001; Somot and Finch, 2006). With the closure of the research center in 2002, this facility was relocated to the Department of Mining and Materials Engineering, McGill University. The basic self-heating apparatus consists of a 2L Pyrex vessel surrounded by a thermocouple controlled heater. The sample in the vessel is kept at a target temperature by the heater. Air is blown through the sample at a rate controlled by a mass flow meter in a set series of pulses controlled by a timer. The air (from a cylinder) is pre-heated to the sample temperature by passing through a heated copper coil. Upon air injection, an active sample reacts releasing heat and increasing temperature while a passive sample shows minimal response. The temperature increase is recorded by the thermocouple and analyzed to yield self-heating rate data. Other gases can be substituted for air (e.g., nitrogen). A pool of water can be introduced at the bottom reservoir to help maintain moisture levels (typically 6% w/w initially) and extend the reaction (weathering) period.
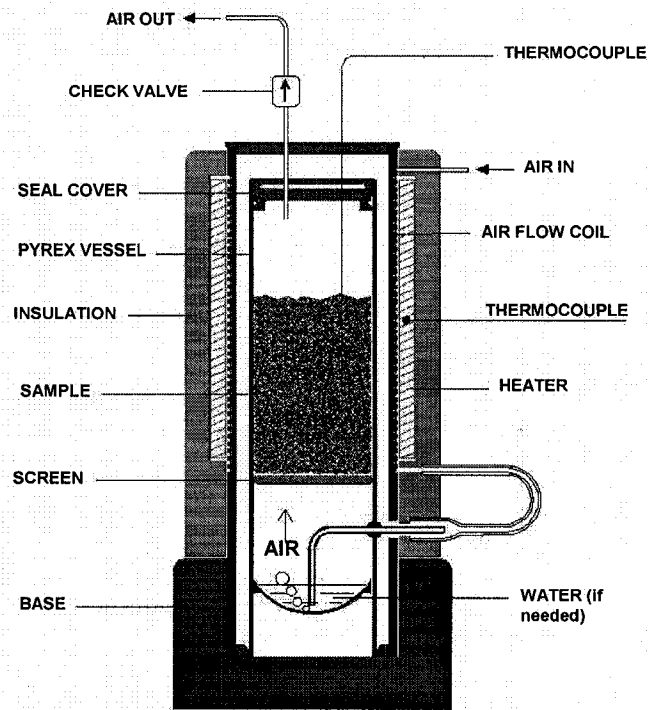
Figure 3. 1 Self-heating apparatus for Stage A and B (Rosenblum et al., 2001)

The self-heating process is considered in three stages (Rosenblum et al., 2001), stage A, B and C (Figure 3.2). Stage A initiates at ambient temperature and ends at 100°C (or when there is no moisture left in the system) and is associated with the formation of sulphur. Stage B follows and finishes at around 350°C with the liberation of sulphur dioxide. Stage C is extremely exothermic and temperatures reach more than 500°C and can lead to ignition and uncontrolled fires.
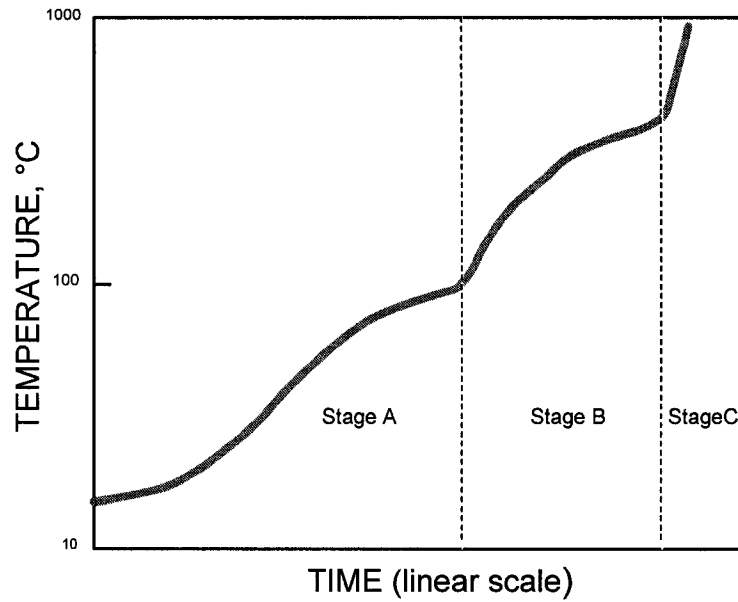
Figure 3. 2 Schematic representation of temperature rise at three stages of self-heating (Rosenblum et al., 2001)

Stage A and stage B are simulated using the apparatus in Figure 3.1. The temperature of a standard stage A test is maintained at 70°C. Air is injected at a flow rate of 100 mL/min for a period of 15 minutes at 5 hour intervals for a total of ten cycles or cycles. A 30 second vacuum is applied to drive out the condensates collected in the bottom reservoir into a trap. Air is then replaced by nitrogen (260 mL/min) to dry the sample and the temperature is increased to 140°C. This drying period lasts 9.5 hours. The standard stage B is then initiated with an air flow rate of 250 mL/min for 15 minutes each 5 hours for a total, again, of 10 cycles. The sequence for a standard stage A, B test is shown in Figure 3.3.
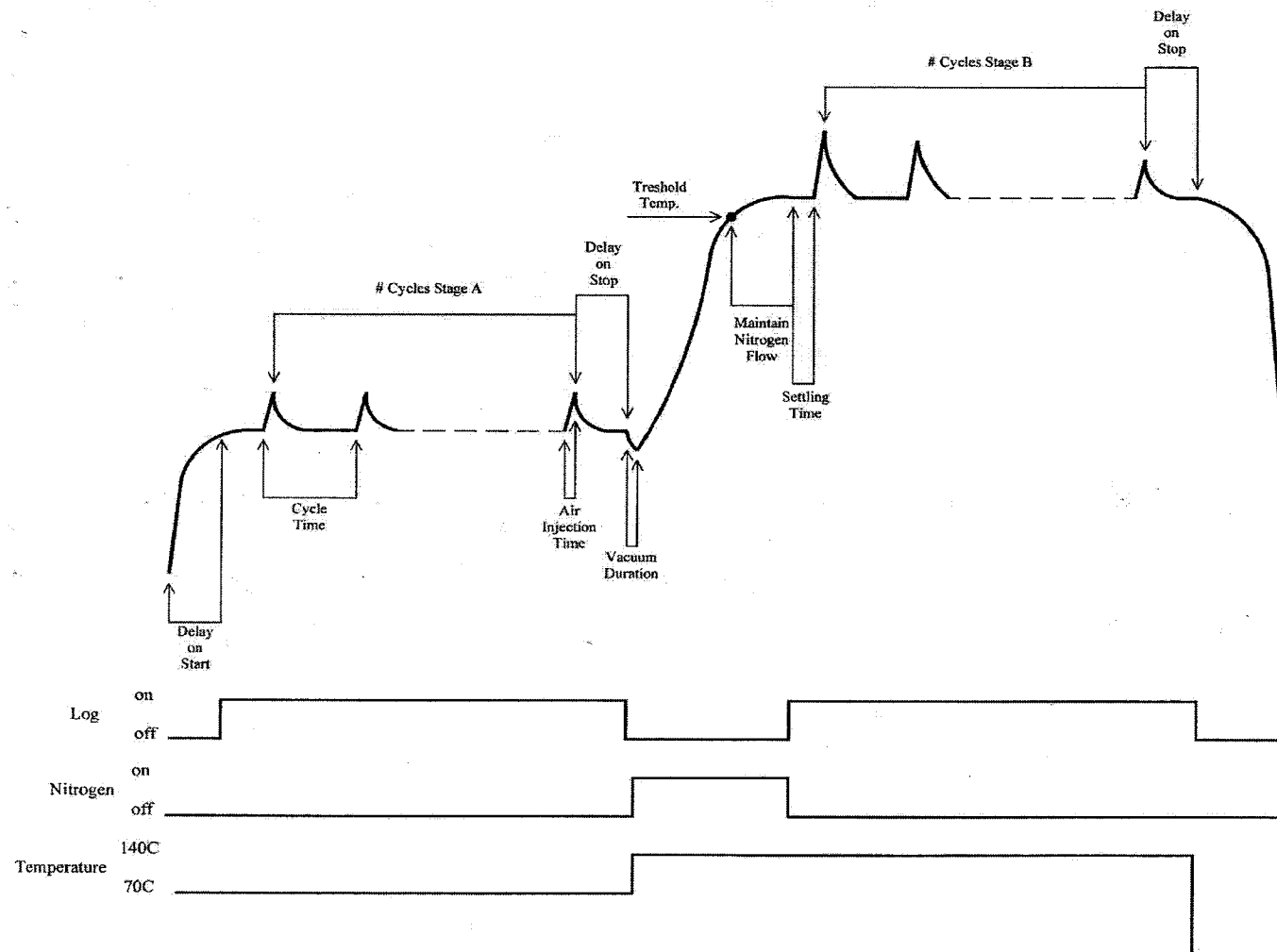
Figure 3. 3 Schematic representation of a self-heating plot showing all the operation (courtesy F. Rosenblum)

The output of a reactive sample is a series of temperature spikes corresponding to the air injections (Figure 3.4). The SELFHEAT software developed by Mr. Frank Rosenblum is used to process the data. The slope of the temperature increase part of the spike defines the self-heating rate. The total self-heating rate of a stage is the summation for each spike in the stage. Figure 3.4 includes the self-heating rates associated with each peak (units, °C/hr) for a specimen run.
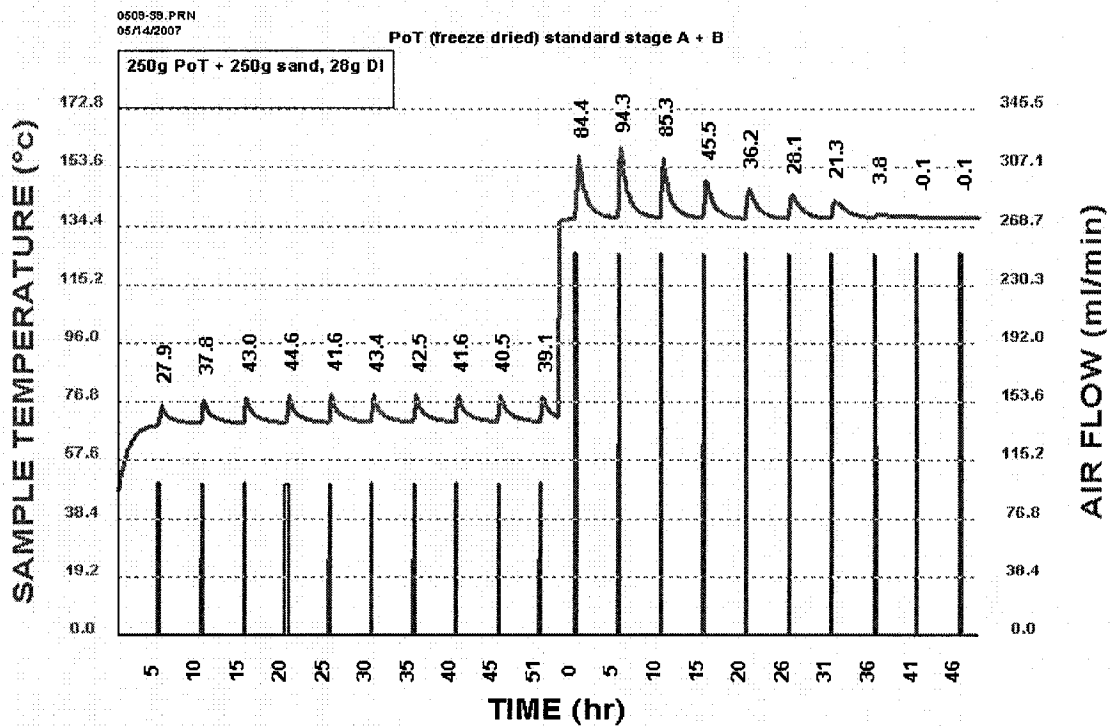
Figure 3. 4 Typical self-heating test response of stage A and B

Another mode of operation apart from the standard 10 air injection cycle is a so-called full cycle (Figure 3.5). This means the sample is run till it no longer shows a temperature increase with air injection. In other word, the self-heating capacity of the sample is exhausted under full cycle operation.
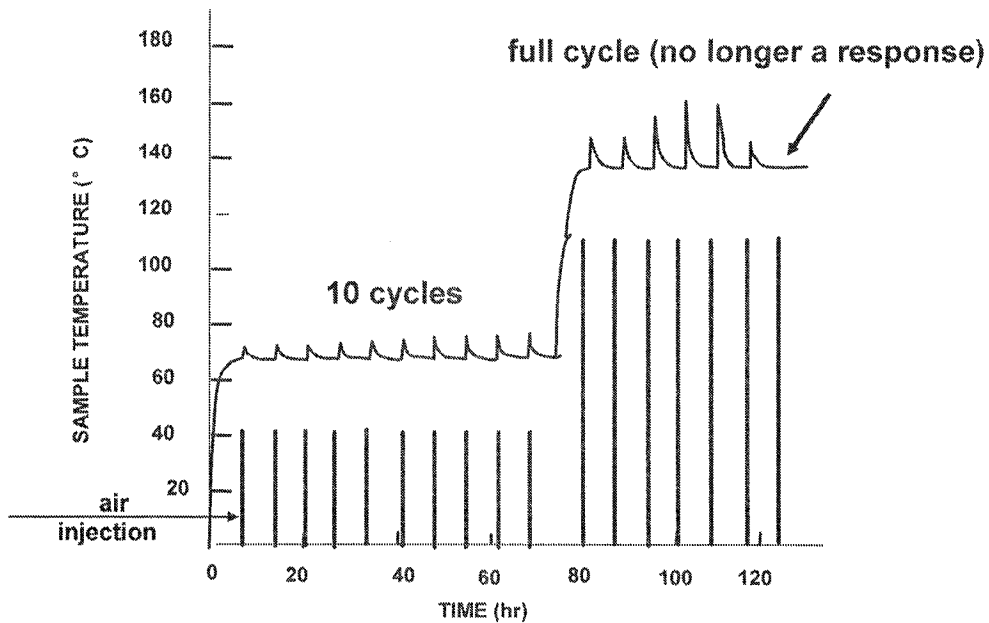
Figure 3. 5 Self-heating showing standard stage A and nonstandard stage B

operation

3.1. 2 "Weathering" Apparatus

Testing pyrrhotite-rich samples in the standard self-heating apparatus gave rise to the hypothesis that H_2S maybe a factor (Somot and Finch, 2006). There was some concern that the standard test procedure by employing periodic air injection may create the conditions promoting H_2S formation. That is, H_2S could be an artifact of the test procedure. Alternative procedures were required. Two were devised, generically referred to as "weathering tests".

The weathering apparatus (Figure 3.6) consists of a 1L reaction vessel, a transparent (microwave) bowl or a stainless steel bowl, placed in a 2.1L chamber containing water at the bottom.

polypropylene
filter

copper
piece

reaction
vessel

chamber

sample

water
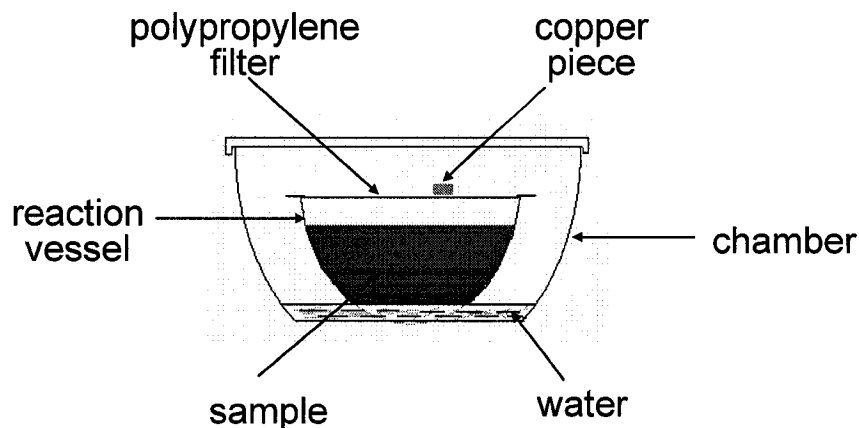
Figure 3. 6 Schematic picture of "weathering" apparatus

The initial use was to detect H_2S. A 500 gram freeze-dried PoT sample was placed in the reaction vessel. The chamber was closed, placed in an oven and the temperature set at 40°C. The purpose of using a transparent vessel was to detect the colour evolution of the sample. A grease-free, cleaned copper piece was placed on the acid-resistant polypropylene filter to detect liberated H_2S. The chamber was opened every two days to check the colour change of the copper piece and the sample.

The weathering apparatus was also used to test the effect of oxidation level. To vary the level, the exposure to air was regulated by three covers: no holes, three holes and 128 holes (Figure 3.7). Otherwise the set-up was as described previously. The chamber was placed in the oven set at 40°C and every two days, the chamber was opened to measure weight gain and assess colour change of the sample.
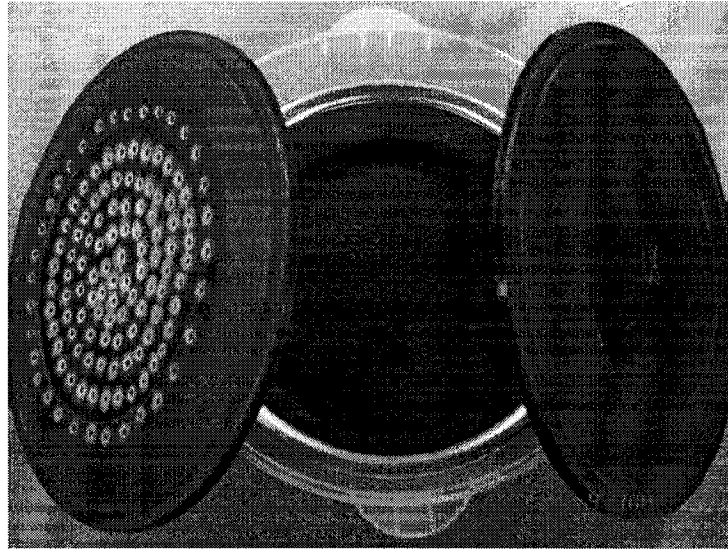
Figure 3. 7 Weathering apparatus showing two covers, 128 holes (left) and no holes (right)

3.1. 3 Sample Preparation

Samples used in this research were pyrrhotite-rich tailings (PoT) obtained from Falconbridge's (now Xstrata Nickel) Strathcona mill (Sudbury). The Po content is about 69% (Somot and Finch, 2006). The tailings product is the result of a series of operations (Figure 3.8) including grinding, regrinding, and mineral separation by magnetic and flotation processes. The monoclinic form of pyrrhotite may dominate in the PoT because of the magnetic concentration step.
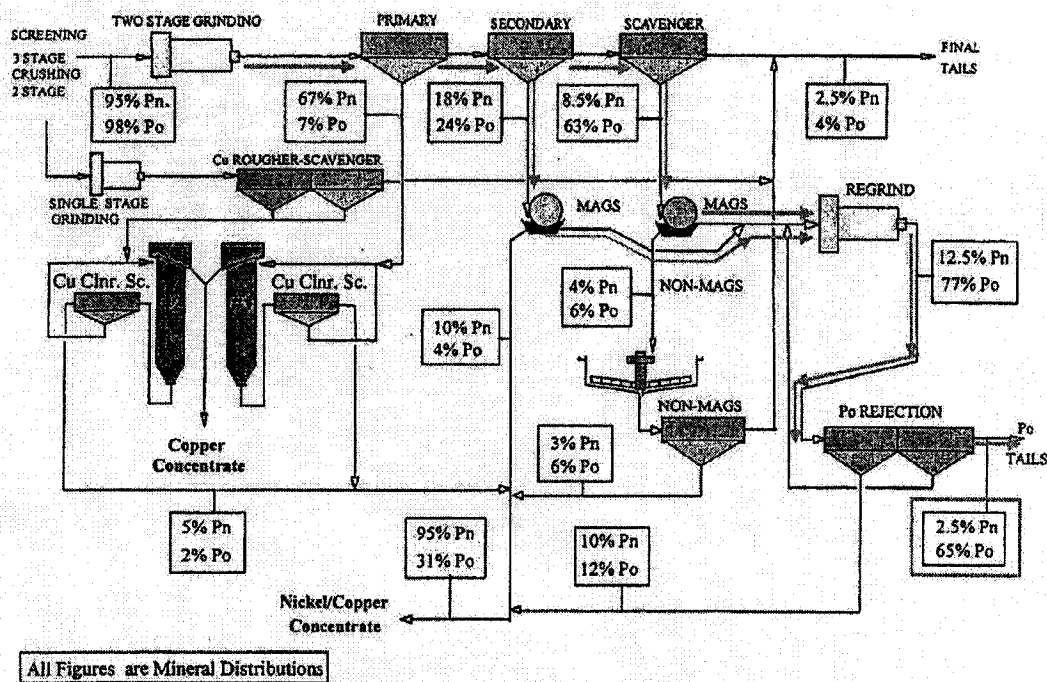
Figure 3. 8 Strathcona Concentrator Flowsheet (after Wells et al., 1997)

The samples were kept under water (i.e., as slurry) in a sealed plastic bag for transportation to McGill. They were split (sub-sampled) as slurry after mixing to approach homogeneity. The sub-samples were pressure filtered and the filter cakes were sealed immediately in plastic bags for storage in a freezer.

Samples used in all the experiments were prepared in two ways according to the purpose. Samples used in Chapter 4.1, Chapter 4.2 and Chapter 4.3 were freeze dried at -40°C (Chemical Engineering Department) before the experiment. The purpose of freeze drying is to limit the effect of sample preparation on the results. Samples used in Chapter 4.4 to establish the effect of oxygen level on self-heating were dried in an oven at 60°C for 4 hours. This was done due to the limited freeze drying capacity (50g per day) and large

amount of sample (about 20kg) needed. Once dried, the samples were rolled and mixed. The dried samples were sealed in plastic bags and stored in the freezer.

Samples tested in the self-heating apparatus were prepared as follows: 250g dried PoT powder was mixed with the same weight of coarse silica sand (80% passing 2.36mm) in a plastic bag; 28g deionised water was introduced by repeated spraying to achieve the target moisture content of 5.6%; and the sample in the bag was mixed thoroughly by hand to make it homogeneous.

3. 2 Characterization Methods

3.2. 1 Particle Size Distribution

A Laser Scatter Particle Size Analyser Model LA-920 (Horiba) was used for particle size distribution determination. The detection limit is quoted by the manufacturer as 0.020 μm.

3.2. 2 Atomic Absorption

Nickel in the PoT sample was determined by acid digestion (HCl/HNO_3) followed by Atomic Absorption Spectroscopy (AA). The assay is expressed as weight percent (the detection limit for Ni is 0.50 ppm). The content of other metals in the sample was below their detection limit for this method of analysis.

3.2. 3 X-Ray Fluorescence

An automated X-ray fluorescence (XRF) spectrometer (Philips PW 2440 4kW) with a rhodium 60kV end window X-ray tube was used for element analysis (Earth and

Planetary Sciences Department). The instrument precision is 0.12% relative. The detection limits are quoted as: Fe, S, Si, Mg, Al, Ca, Ni, Na, K and Ti, 0.01% weight; Cu, Co, Mn, Ba, Cl, P, Zn, Cr and Sr, 20ppm.

3.2. 4 X-Ray Diffraction

A Philips PW1710 with a rotating Cu anode was used for X-ray diffraction (XRD) measurements. The wave length was λ 1.54060Å (CuKα) with the X-ray tube set at 40 kV and 20 mA. The software used was 'Expert Quantify' for data acquisition and 'X'Pert High Score' for phase analysis.

3.2. 5 Scanning Electron Microscope

The JEOL JSM 840-A scanning electron microscope (SEM) with Everhart-Thornley secondary electron detector and solid state back scatter electron (BSE) detector was used. The EDAX Phoenix system was used for image acquisition with EDS (Energy Dispersive Spectrometer) for microanalysis. The EDS detector has a "Sapphire" window to permit analysis of elements down to boron.

3.2. 6 Raman Spectroscope

The Raman Spectroscopy (Brand: inVia Renishaw Spectrometer, Laser 514 nm Argon ion laser, CCD detector, Leica microscope, Chemistry Department) was used to check for the sulphur trapped inside the self-heating test apparatus and sulphur precipitates on the top of the silica sand.

3.2. 7 Electron Microprobe

The JEOL JXA-8900 Electron Microprobe with WDS (Wavelength Dispersive Spectrometer) detector (Earth and Planetary Sciences Department) was used to

characterize the weathering products at different oxygen levels. The operating conditions were: Accelerating voltage 20 kV, beam current 30 nA, beam size minimum. Synthetic and natural minerals were used as standards for calibration. The correction method is ZAF for oxides and CITZAF for sulphides. The counting time was 20s on peaks and 10s on background.

3.2. 8 Ion Chromatograph

Dionex DX-100 Ion Chromatograph was used to test the type of acid in the condensates derived from PoT samples in section 3.4. The detection limit for sulphate is 5 ppm. The system is equipped with an anion separation column NS-12 and the eluent solution is a mixture of carbonate and bicarbonate.

3. 3 Detecting H₂S

In the first attempt to detect H$_2$S, a copper piece was placed on top of the silica sand in the self-heating apparatus (Figure 3.9). The purpose was to isolate the copper from direct contact with the pyrrhotite sample. Any H$_2$S formed will react with copper through equation 3.1 (Karchmer, 1970) and form black copper sulphide.

$$4(Cu^o)_s + (O_2)_g + 2(H_2S)_g = 2(Cu_2S)_s + 2(H_2O)_{aq} \qquad (3.1)$$
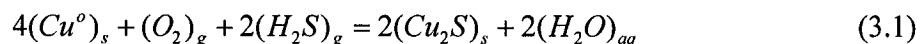
The coatings formed on the copper pieces were collected for XRD and SEM analysis.
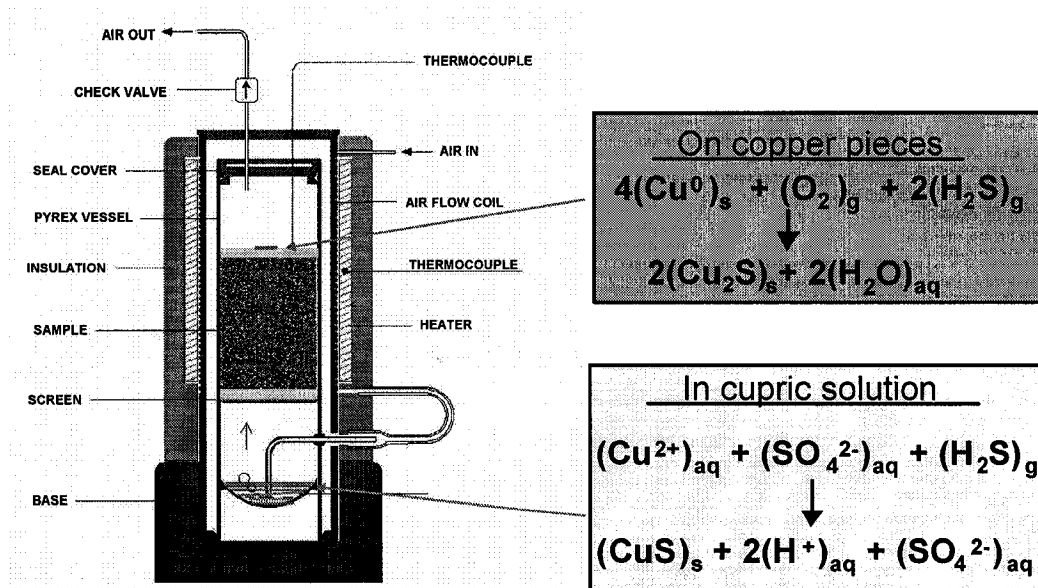
Figure 3. 9 Detecting of H₂S: copper pieces and cupric solutions

In a second procedure, a cupric solution was introduced into the bottom reservoir of the self-heating apparatus. The concentration was 0.5mol $(CuSO_4)/L$. The H_2S will be captured through reaction 3.2 (Karchmer, 1970), forming copper sulphide precipitates.

$$(Cu^{2+})_{aq} + (SO_4^{2-})_{aq} + (H_2S)_g = (CuS)_s + 2(H^+)_{aq} + (SO_4^{2-})_{aq} \qquad (3.2)$$
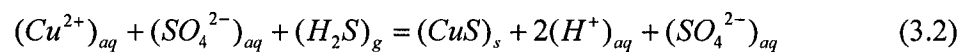
The black precipitates were pumped out of the vessel, cleaned with deionised water and centrifuged. The moist precipitates were stored in a Petri dish for air drying and XRD and SEM analysis was performed on the dried samples.

It was observed that some yellow precipitates formed on top of the silica sand and some were trapped in the check valve of the self-heating apparatus. These were suspected as being sulphur possibly resulting from partial oxidation of H_2S (Equation 3.3). That is, they could offer another 'detector' of H_2S. The samples were collected for XRD, SEM and Raman Spectroscopy analysis.

$$H_2S + 1/2 O_2 = S + H_2O \qquad (3.3)$$

The liberation of H_2S was also tested using the weathering apparatus (Figure 3.6) (details were discussed in section 3.1.2).

3. 4 Tracking the Source of Acid Needed for H_2S Liberation

Liberation of H_2S implies a reaction of sulphide with an acid under weakly oxidizing conditions (Good, 1977; Thomas et al., 2000; Belzile et al., 2004; Gunsinger et al., 2006). To track the source of acid pH was measured on the condensates derived from the PoT sample in a modified self-heating test. The condensates were further characterized by Ion Chromatography (IC).

The modified set-up was as follows. The tubing and connections in the self-heating apparatus were cleaned using 1:5 HNO_3 to remove any contaminants and then cleaned using deionised water five times. A 250g freeze dried PoT sample was diluted with 250g coarse sand and 28g DI water was introduced as spay to achieve 5.6% moisture content. A copper ($Cu°$) piece was added on top of sand to check liberation of H_2S.

The test itself was divided into three steps. In the first step, N_2 was blown at 100 mL/min for 1 hour before starting the experiments to expel trapped oxygen inside the vessel. Heating at 70 °C for 26 hours was used as the weathering period. The test was stopped and the $Cu°$ checked for colour change. The second step started by heating at 120 °C and blowing N_2 at 200 mL/min for 26 hours in order to expel the moisture in the sample and

condensates in the bottom reservoir. The resulting solution was collected in a trap. The solution was tested for pH and acid type (IC). A standard stage B test was conducted to check if there was a heating response resulting from the weathering conditions. This is a way to indirectly test for sulphur formation.

3. 5 Testing Importance of Less Oxidative Conditions

3.5. 1 Tests in Self-heating Apparatus

Two groups of tests under different air flow rates were conducted using the self-heating apparatus. All the samples were diluted 50% with coarse silica sand and moisture content was 5.6%.

For the first group of tests, six samples were run under otherwise stage A conditions at air flow rates of 50, 100, 150, 200, 250 and 300 mL/min for standard ten cycles followed by stage B at 250 mL/min for full cycle (i.e., till no further heat response). The air flow choice was influenced by trying to simulate conditions inside a stockpile ('low air', 50 mL/min) and on the surface of the stockpile ('high air', 300 mL/min).

The above samples, after running stage A for ten cycles, still showed potential to generate heat with further air injection. Consequently, in a second group of tests, two samples were run to full cycle under air flow rates (stage A) of 50 and 300 mL/min followed by stage B at 250 mL/min for full cycle.

3.5. 2 Tests in "Weathering" Apparatus

Three tests were conducted to explore the role of oxygen level. The "weathering" apparatus with no hole, three hole and 128 hole covers were used, with the temperature set at 40 °C.

Weight gain was recorded every two days. The weathered samples were then subjected to a stage B test to full cycle and XRD and electron microprobe analyses were conducted on the samples.

Chapter 4 Results and Discussion

4. 1 Characterization of PoT

Particle size distribution, metal content and mineralogy all play a role in self-heating of sulphide materials. Thus, characterizing the sample will help in the study of mechanisms of self-heating. The effect of sample preparation on self-heating will be included.

4.1. 1 Particle Size Distribution

The particle size distribution of the original PoT sample dried in the oven at 60°C was measured using the Laser Scatter Particle Size Analyser. Figure 4.1 shows that the particle size distribution ranges from about 0.16 to 175 μm with three modes, ca 0.5, 12 and 50 μm. Particle size or more precisely specific surface area is reported to be an important factor in the oxidation of sulphides as discussed in the literature review. Investigating a particle size effect on the self-heating of PoT was not part of this research.
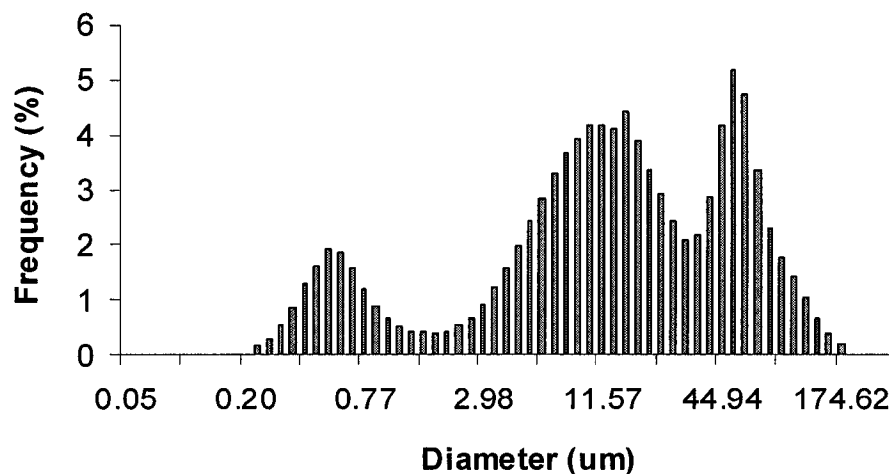
Figure 4. 1 Particle size distribution of PoT sample

4.1. 2 Metal and Sulphur Analysis by Atomic Absorption (AA) and X-ray Fluorescence (XRF)

Major and trace elements results are summarized in Tables 4.1 and 4.2 in weight percent and ppm units, respectively.

Table 4. 1 Major elements analysis by X-ray Fluorescence

Element	Fe	S	Si	Mg	Al	Ca	Ni	Na	K	Ti
Weight %	47.25	17.64	14.61	4.79	3.74	2.67	1.25	1.19	0.29	0.27

Table 4. 2 Trace elements analysis by X-ray Fluorescence

Element	Cu	Co	Mn	Ba	Cl	P	Zn	Cr	Sr
ppm	2270	850	600	480	470	420	350	320	170

The content of Ni by Atomic Absorption (AA) is 1.11 weight%, a result in good agreement with the XRF data. Most of the Ni is from pentlandite that was detected by electron microprobe (see section 4.1.3). Due to the low content of other metals and small amount of test sample, the atomic absorption method is not generally suitable. The trace Cu and Zn detected (Table 4.2) suggest chalcopyrite and sphalerite are present, but with regard to self-heating this is not expected to be important.

4.1. 3 XRD and Electron Microprobe Analysis

Richard and Watkinson (2001) report that Sudbury (Ontario) area ores are composed of variable proportions of monoclinic and hexagonal pyrrhotite, chalcopyrite and pentlandite (as the principal sulphide minerals). Electron microprobe analysis of a polished section of

the PoT sample readily identified pyrrhotite and pentlandite (Figure 4.2) and also pyrite and magnetite (Figure 4.3). Quartz (Figure 4.4) and several kinds of silicates were found by electron microprobe (corresponding to Si in Table 4.1).
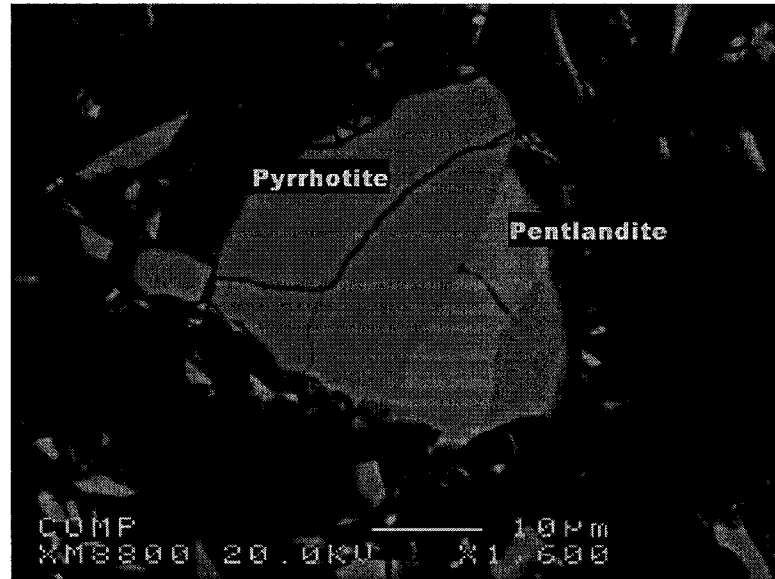
Figure 4. 2 Electron microprobe analysis of PoT sample showing pentlandite and pyrrhotite (a locked particle)
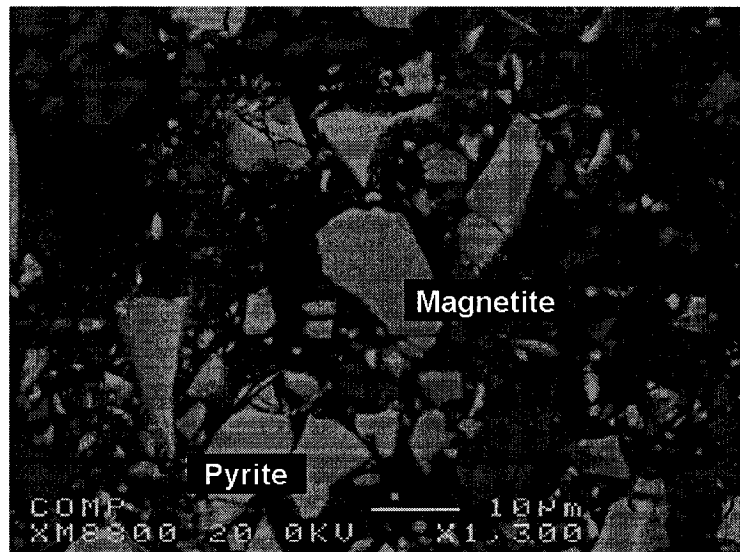
Figure 4. 3 Electron microprobe analysis of PoT sample with pyrite and magnetite
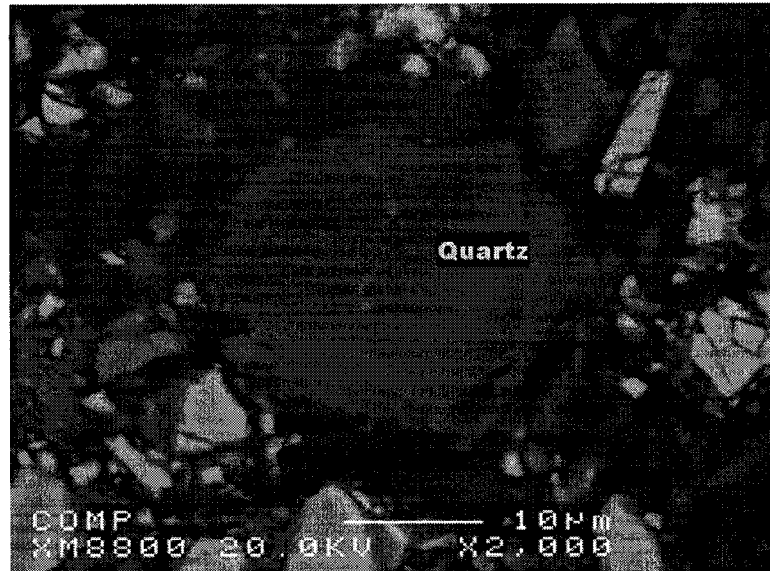
Figure 4. 4 Electron microprobe analysis of PoT sample with Quartz

The microprobe study on randomly chosen 100 points indicated 69 pyrrhotite points with a composition range of $Fe_{0.85}S$ to $Fe_{0.88}S$. According to this composition, the pyrrhotite is monoclinic.

The XRD spectra (Figure 4.5) confirmed that the original PoT sample contained monoclinic pyrrhotite (Fe_7S_8, reference code 24-79), along with hexagonal pyrrhotite ($Fe_{0.95}S_{1.05}$, reference code 01-75-600) and magnetite (Fe_3O_4, reference code 19-629). The mineral processing flow sheet (Figure 3.8) identifies that PoT enrichment with monoclinic species is due to the magnetic separation step.
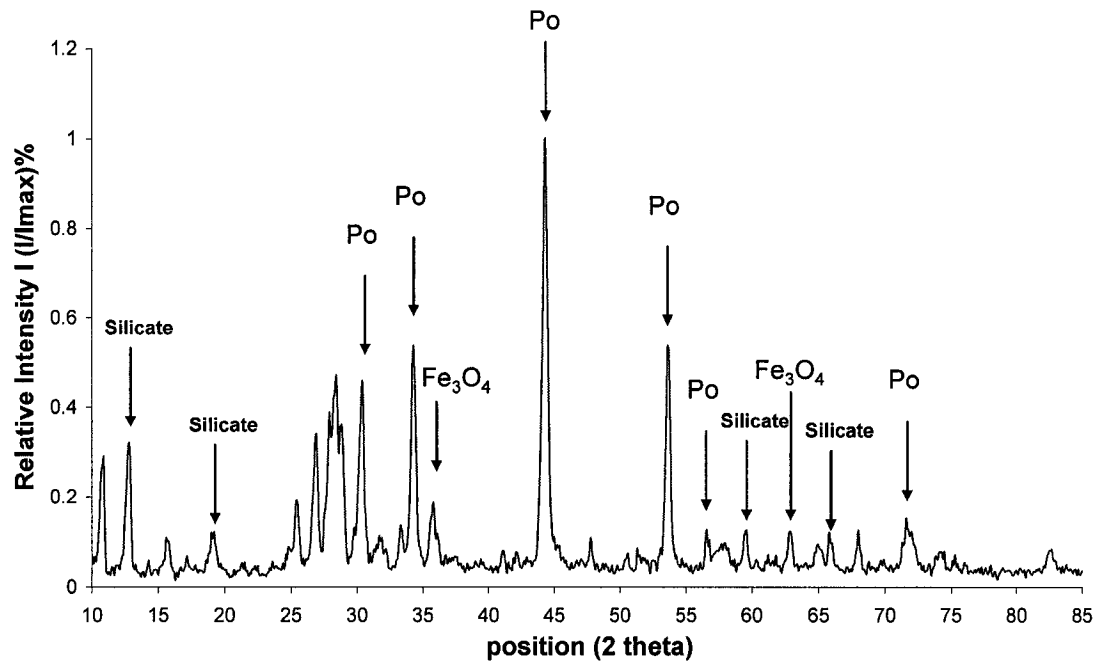
Figure 4. 5 XRD analysis of the original PoT

4.1. 4 Effect of Sample Preparation: Comparison of Freeze Dried and Oven Dried

Two tests were conducted to address a concern over a possible sample preparation effect on the self-heating response. One sample was freeze dried and another was oven dried at 60°C, as described in section 3.1.3. The results of standard self-heating tests are summarized in Figure 4.6. The Figure shows that the sample dried at 60°C gave slightly higher self-heating rate in stage A and B than the freeze dried sample, but the difference is within the repeatability of the self-heating test (Bournival 2006). As shown in the flowsheet (Figure 3.8), the PoT sample has experienced grinding, magnetic separation, flotation processes and storage, therefore, it is possible that the pyrrhotite surface has been contaminated by chemicals or partially oxidized. This history probably is more significant than the different sample preparation procedures. Based on the results of

Figure 4.6, it can be concluded that the drying process in a 60°C oven for 4 hours, no notable effect on Po is detected.
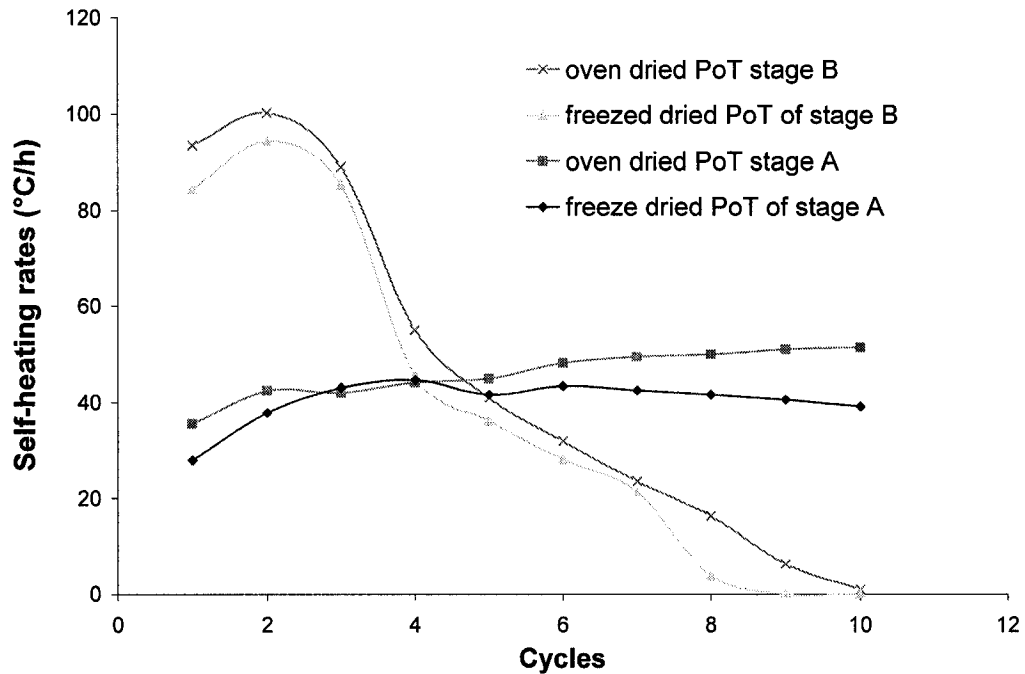
Figure 4. 6 Comparison of the effect of freeze dried and oven dried sample on self-heating response

4. 2 Testing Hypothesis of H₂S Liberation

4.2. 1 Coatings on Cu Pieces: XRD and SEM

One method employed to test for H_2S release was addition of copper metal on top of the silica sand (Figure 3.9). After the self-heating test, the original bright copper pieces became totally blackened indicating reaction with H_2S (Figure 4.7). The coatings were scraped from the surface of the copper pieces for examination.
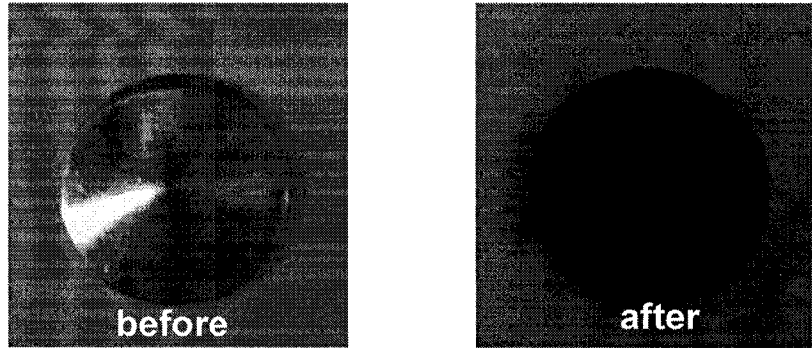
Figure 4. 7 The copper pieces before and after the self-heating test, stage A

X-ray diffraction (Figure 4.8) showed that the coatings were formed of well-defined crystals of covellite (CuS, reference code 00-024-0060) and chalcocite (Cu$_2$S, reference code 04-007-2389).
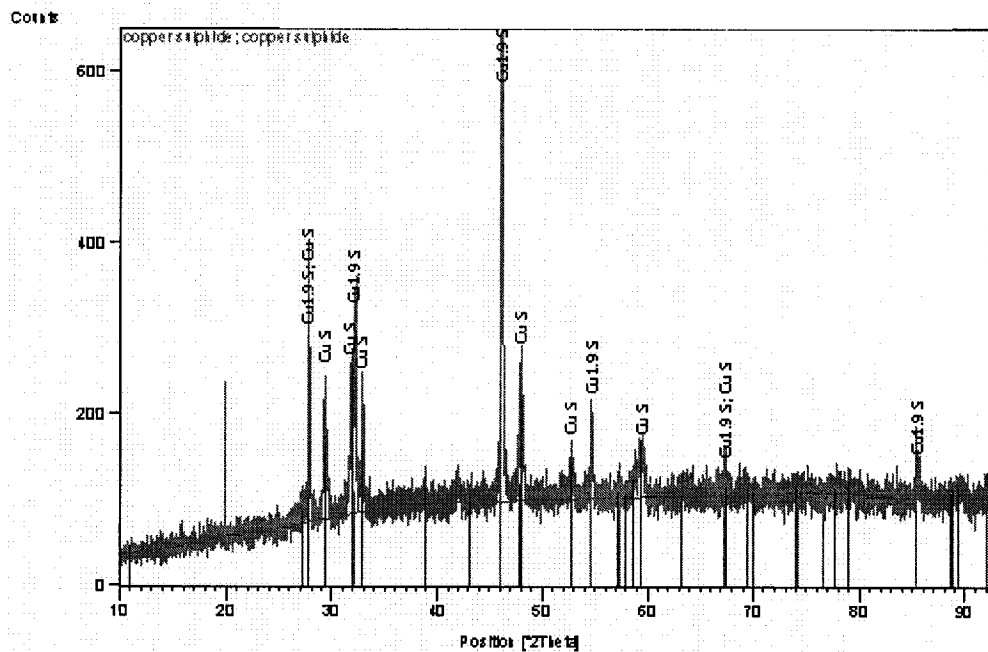
Figure 4. 8 XRD pattern of coatings on copper pieces: the CuS and Cu$_2$S lines are noted

Scanning electron microscopy (accelerating voltage 10 KeV) micrographs (Figure 4.9) showed dendritic crystals ranging from 2 to 5 μm in length. Elemental analysis (SEM-EDAX) identified copper and sulphur peaks.

At this juncture, no further investigation has been done into the reaction mechanism of H_2S formation. It was assumed that the well crystalline coatings on the copper pieces shown by XRD and SEM indicate that the reaction between H_2S and copper was slow under the self-heating test conditions (Kim, 2005). If there was ready availability of H_2S, reaction would be fast to form copper sulphides with more amorphous morphology. One reason the supply of H_2S may be restricted is the reaction with oxygen every 15 min when air is injected in the test procedure; the H_2S would oxidize giving the sharp temperature increase seen in the standard self-heating thermograms, which is indicative of gas phase reaction.
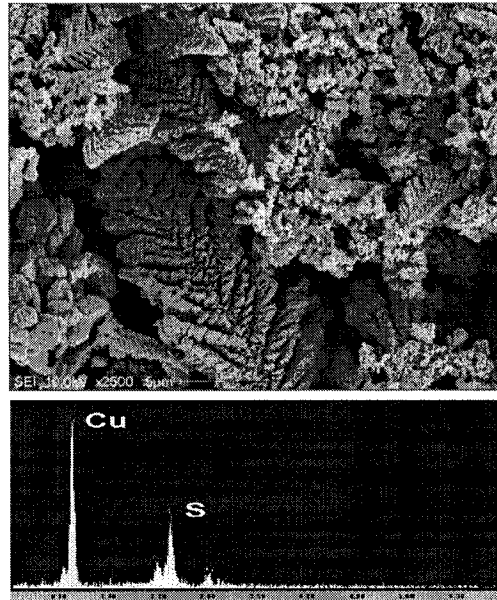
Figure 4. 9 SEM with EDAX analysis of coatings on copper pieces

51

4.2. 2 Precipitates from Cupric Solution: XRD and SEM

Another way to indicate the liberation of H_2S was to introduce cupric solution into the bottom reservoir. After the self-heating test, a web-like black film appeared on the surface of the solution and dispersed into aggregated precipitates on disturbing when taking the solution out of the reaction vessel (Figure 4.10). These black precipitates were recovered, cleaned using DI water, centrifuged five times, and transferred to a Petri dish to dry. X-ray diffraction and SEM examinations were conducted on the air-dried precipitates and the results are presented in Figures 4.11 and 4.12, respectively.
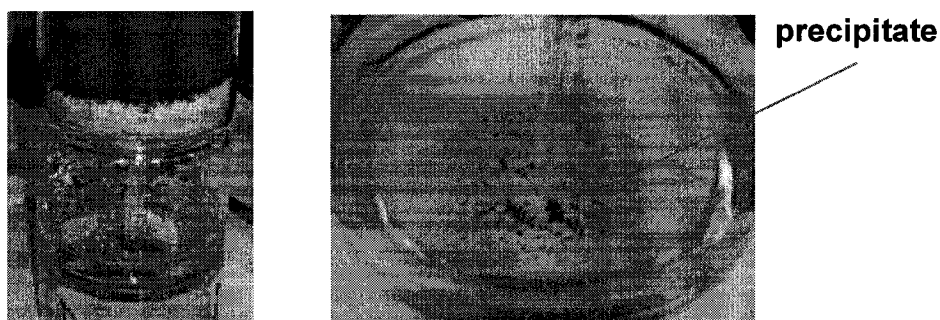
precipitate

Figure 4. 10 Black precipitates on the surface of cupric solution held in bottom reservior

The "noisy" XRD pattern (Figure 4.11) shows that the precipitates are not crystalline; however, the pattern is consistent with covellite (CuS, reference code 01-078-2391).

Counts

Position [? Theta]
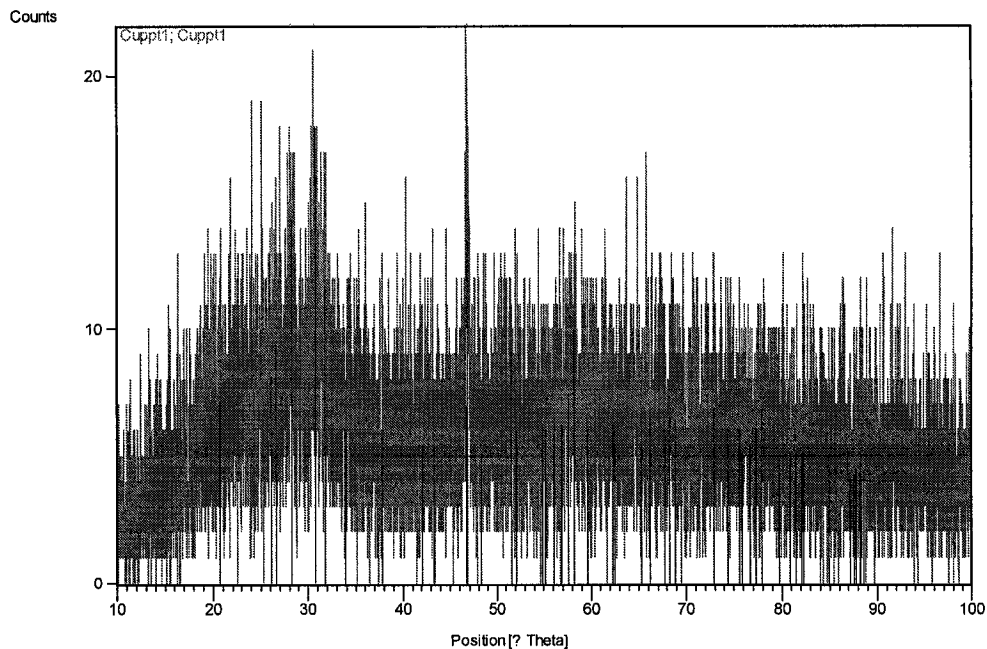
Figure 4. 11 XRD patterns of black precipitates of cupric solutions

The SEM data (Figure 4.12) showed that the precipitate had a range of morphologies. Some of the copper sulphide formed elongated or needle-like (acicular) particles about 5 μm long and appeared amorphous. This supports the XRD results. Regardless of where the sample was tested, the ratio between the Cu and S peaks (SEM-EDAX) was almost the same, which means the precipitates are homogeneous.
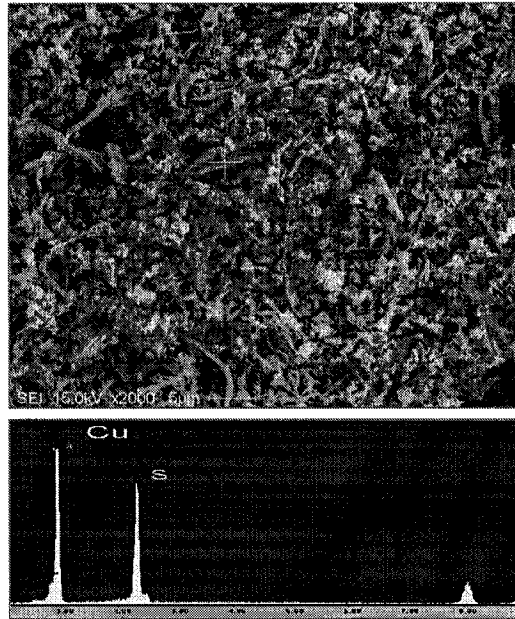
Figure 4. 12 SEM (with EDAX analysis) of precipitates of cupric solution

The presence of copper sulphide in the bottom reservoir suggests the released H_2S from the self-heating of pyrrhotite either diffused there as a gas or dissolved in sample moisture and dripped into the reservoir. In solution, the H_2S reacted with Cu^{2+} to form the copper sulphide precipitates. The reaction of H_2S in solution with cupric ions is affected by temperature, H_2S partial pressure and Cu concentration. Carroll and Mather (1989) reported that the solubility of hydrogen sulphide in water at 1 atm is about 0.06 mol% at 70 C° and the solubility decreased with increasing temperature. Supersaturation is the driving force for crystallization and the formation of a precipitate out of a solution involves nucleation, growth and aggregation of particles. The poor crystallinity suggests homogeneous nucleation is favored over growth (Demopoulos, 2006).

4.2. 3 Sulphur Precipitates: XRD, SEM and Raman Spectroscopy

Yellow particles, evidently sulphur, a possible partial oxidation product of H_2S, were found in various locations, notably: the wall of the reaction vessel, on top of the sand, on the cover of self-heating apparatus, and inside the check valve connecting to the gas exhaust system. The particles were collected for analysis. Figure 4.13 is the XRD pattern of particles recovered from the top of the sand. The peaks are indicative of sulphur with reference code of 00-008-0247 and 00-024-0733.
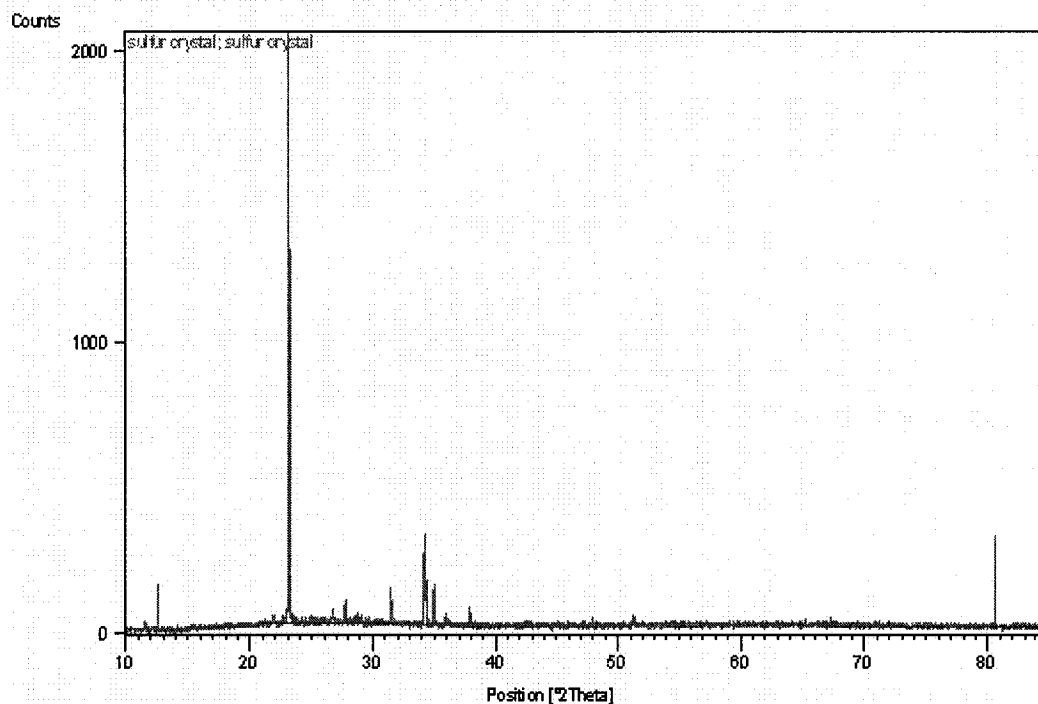
Figure 4. 13 XRD pattern of sulphur collected from the top of the sand

Figure 4.14 is the SEM (with EDAX analysis) of the particles formed on top of the sand. The particles showed dendritic crystals with a length around 100 μm which were clearly sulphur.
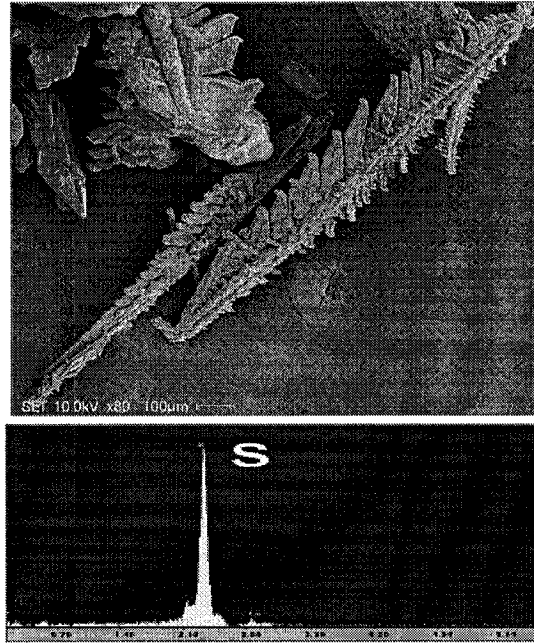
Figure 4. 14 SEM (with EDAX analysis) of sulphur formed on top of the sand

Raman Spectroscopy was conducted on particles collected from the check valve and from the top of the sand. The pattern (Figure 4.15) overlaps that of commercial S (Scientific Fisher) with characteristic sulphur peaks at wave numbers 216 and 470 cm^{-1}. The spectrum indicates that the sulphur produced in the self-heating process is elemental S (Ahmed et al., 1996).
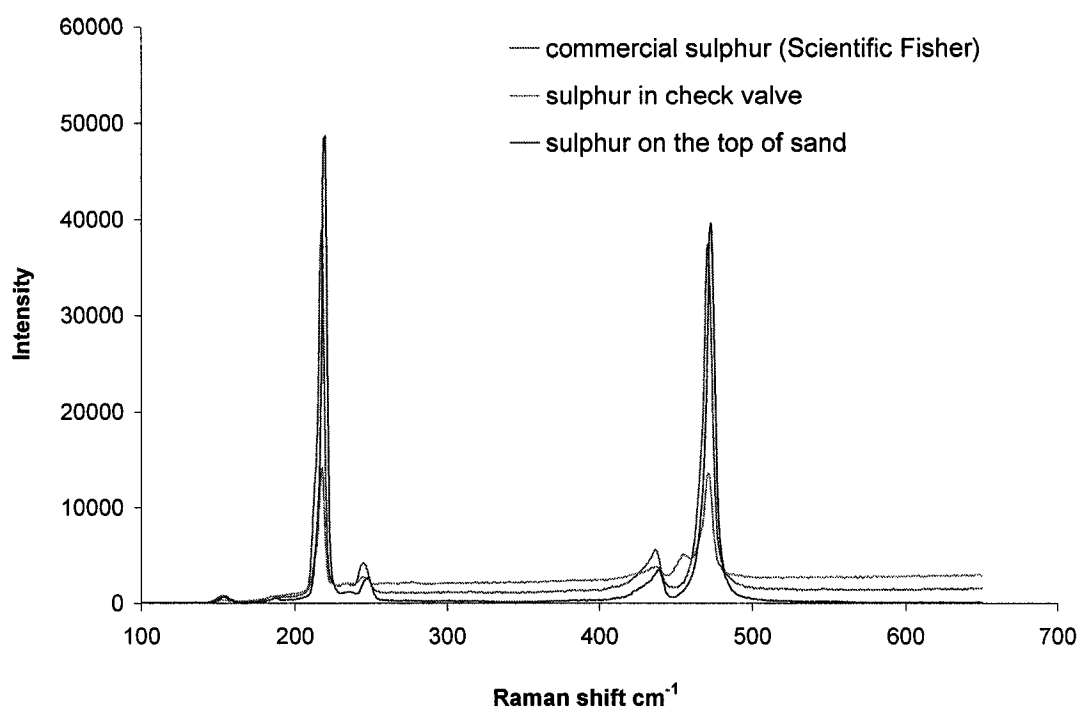
Figure 4. 15 Raman spectrum of sulphur deposited in the check valve

4.2. 4 Test Liberation of H₂S in "Weathering" Apparatus at 40 °C

The release of H₂S below the S° dew point was effectively what had been tested using the self-heating apparatus. The formation of copper sulphide as black coatings on copper pieces and black precipitates in copper sulphate solution indicated the production of H₂S during stage A of the self-heating test. The test employs periodic air injection which raised the concern that this may induce H₂S formation; i.e., H₂S may be an artefact of the procedure. Thus an alternative procedure was conducted in the weathering apparatus.

The weathering apparatus (Figure 3.6) consists of a reaction vessel placed in a 2.1L chamber with water at the bottom. A copper piece was introduced and the chamber was closed with the no-hole plastic cover. Every two days, the cover was opened, the sample

weighed and the colour of a copper piece and the sample were recorded. The visual results and the weight gain are shown in Figures 4.16 and 4.17, respectively.
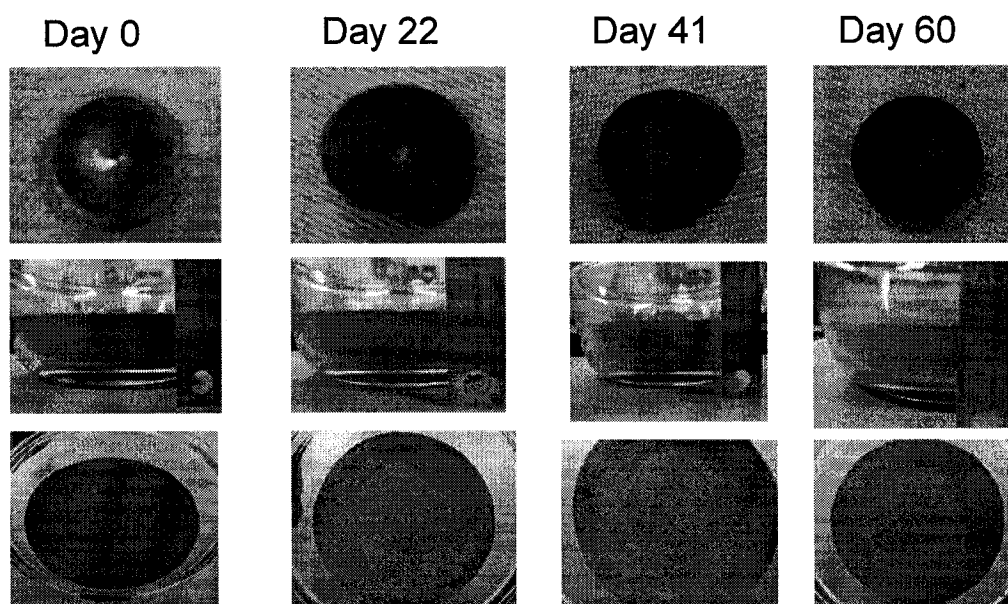
Figure 4. 16 Copper piece and PoT colour changes with time in sealed weathering apparatus

At day 0, the copper piece was bright and untarnished and the PoT sample was the original grey. After 22 days of weathering, the copper piece showed evidence of blackening and the surface of the sample changed to a light yellow. From the side view, a shallow reaction (yellowish) layer was noted. After 41 days, the copper piece was uniformly black and the reaction layer had deepened. At 60 days, the copper piece became totally black and side view showed that almost the entire sample had become yellow. Sulphur precipitates were also detected on the surface of the PoT sample after the 60 days of weathering.
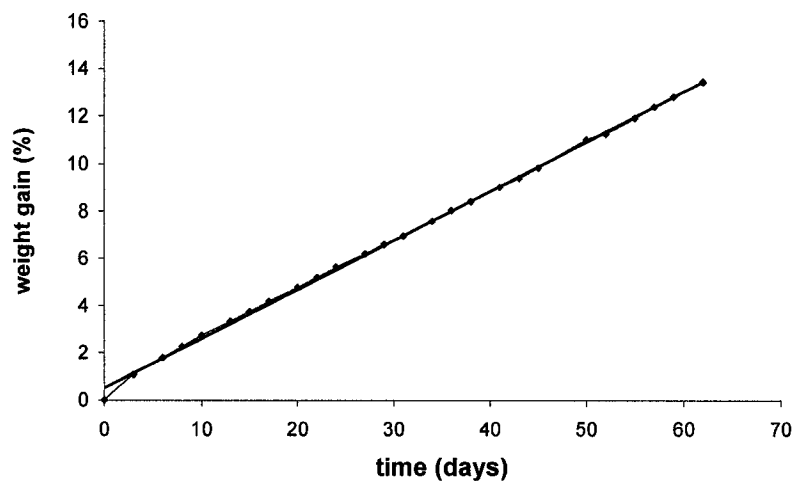
Figure 4. 17 Weight gain of PoT sample in the weathering apparatus (temperature 40°C)

The weight gain vs. time shows a linear relationship over the 60 days of weathering at 40°C. The detected liberation of H_2S did not show as a weight loss which means either the quantity of the released H_2S was small or the H_2S was adsorbed by the minerals and possibly transformed to polysulphides or elemental sulphur. The colour change (to yellow) of the PoT sample indicated the sample underwent chemical reactions and did not just absorb water. The surface of the sample became hard after weathering indicating that the sample had been hydrated. After the weathering test, the sample was taken out of the reaction vessel and ground to make homogeneous for XRD analysis. Figure 4.30 shows that reaction products maghemite (γ-Fe_2O_3), goethite ($FeO(OH)$) and elemental sulphur were formed. Thus uptake of both water and oxygen account for the weight gain.

The following sequence of reactions is proposed based on the observations.

1. H_2S gas is liberated via equation 4.1,

$$Fe_{1-x}S + 2H^+ = H_2S + (1-x)Fe^{2+}$$ (4.1)
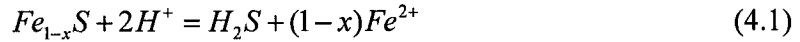
This reaction is exothermic with enthalpy -11.77 kJ/mol calculated using software of HSC Chemistry 5. It is well known that pyrrhotite is unstable under acidic conditions and can be non-oxidatively dissolved by acid with generation of Fe^{2+} and H_2S (Good, 1977; Belzile et al., 2004; Gunsinger et al., 2006; Thomas et al., 2000). Nonoxidative dissolution of pyrrhotite seems to be a notable contributor to ferrous iron release during the weathering of pyrrhotite in acidic solutions (Janzen et al., 2000).

2. The ferrous donates electrons to become ferric by equation 4.2,

$$Fe^{2+} = Fe^{3+} + e^-$$ (4.2)

3. Oxygen accepts the electrons and is reduced to OH⁻ through equation 4.3 (Habashi and Bauer, 1966; Pratt et al., 1994; Kalinnikov et al., 2001),

$$1/2O_2 + H_2O + 2e^- = 2OH^-$$ (4.3)
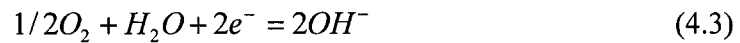
4. Ferric iron reacts with OH⁻ to form goethite by equation 4.4,

$$Fe^{3+} + 3OH^- = 1/2Fe_2O_3 + 3/2H_2O = FeO(OH) + H_2O$$ (4.4)
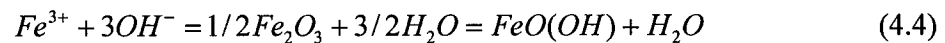
5. Liberated H_2S might be partially oxidized to elemental sulphur or fully oxidized to sulphur dioxide via equations 4.5 and 4.6 (Bukhtiyarova et al., 2000), respectively,

$$H_2S + 1/2O_2 = S + H_2O$$ (4.5)

$$H_2S + 3/2O_2 = SO_2 + H_2O$$ (4.6)

The iron oxy-hydroxides formed may actually catalyze the reaction between H_2S and oxygen (Steijns and Mars, 1974). Hydrogen sulphide can be oxidized by Fe (III) oxy-oxides, for example Fe_2O_3, FeOOH and Fe_3O_4 (Yao et al., 1996), to form elemental sulphur. Both reactions 4.5 and 4.6 are exothermic with enthalpy -264.6 kJ/mol and -562

kJ/mol, respectively (Somot and Finch, 2006). The sulphur precipitates formed on top of the PoT sample were very likely the oxidation product of H_2S. Buckley and Woods (1984) detected no significant amount of elemental sulphur when pyrrhotite was exposed to air or aqueous solution. Filippou et al. (1997), Bukhtiyarova et al. (2000) and Good (1977) state that sulphur may be formed by the oxidation of H_2S.

The melting point of elemental sulphur is around 112.8 to 118.9°C (Elving and Kolthoff, 1970) compared to the experiment set at 40°C. From the evidence of the blackened copper pieces and sulphur particles, both in the weathering and self-heating tests, strongly suggests oxidation of H_2S. Steijns and Mars (1974) stated that at temperatures below 100°C, the oxidation of H_2S may proceed in the liquid (water) phase.

There are other possible ways that elemental sulphur can be produced. For example, it may be produced by direct partial oxidation of pyrrhotite by oxygen (equations 4.7 and 4.8), by ferric iron (equation 4.9) and by both (equation 4.10).

$$Fe_{1-x}S + 1/2(1-x)O_2 + 2(1-x)H^+ = (1-x)Fe^{2+} + S^0 + (1-x)H_2O \qquad (4.7)$$

(Janzen et al., 2000)

$$Fe_{1-x}S + 3/4(1-x)O_2 + 3(1-x)H^+ = (1-x)Fe^{3+} + S^0 + 3/2(1-x)H_2O \qquad (4.8)$$

(Shaw et al., 1998)

$$Fe_{1-x}S + 2(1-2)Fe^{3+} = 3(1-x)Fe^{2+} + S^0 \qquad (4.9)$$

(Shaw et al., 1998)

$$Fe_{1-x}S + Fe^{3+} + 3/4O_2 + 5/2H_2O = 2FeOOH + S^0 + 3H^+ \qquad (4.10)$$
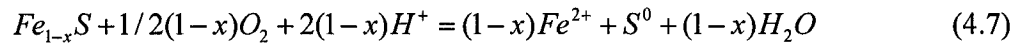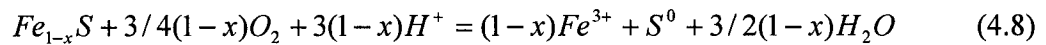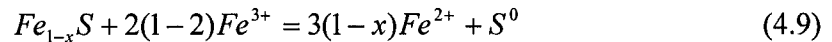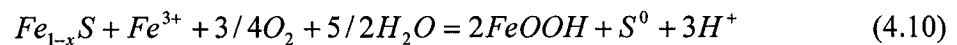
(Janzen et al., 2000)

The generation of H_2S from pyrrhotite has been noted in leaching experiments. Gerlach et al. (1965) (after Filippou et al., 1997) reported formation of H_2S gas in their study on pyrrhotite pressure oxidative leaching and concluded that the presence of H_2S was the result of direct acid attack on pyrrhotite. Filippou et al. (1997) noticed H_2S in pressure oxidation experiments in the initial stage of the overall leach reaction.

Hydrogen sulphide liberation was detected by the copper piece after more than 20 days of weathering at 40°C in the sealed weathering apparatus; in other words, under low oxidative conditions. The presence of 'reaction' layers due to previous exposure to air and water during the mining and milling processes may act to slow non-oxidative and oxidative dissolution and result in an 'induction period'. An induction period before the liberation of H_2S was found by Thomas et al. (2000) using pyrrhotite reacted with perchloric acid.

Thomas et al. (1998) reported that H_2S was produced by an acid-consuming reaction under non-oxidative or reductive conditions and the production of H_2S can increase the rate of oxidative dissolution by three orders of magnitude, from 10^{-8} to 10^{-5} mol m^{-2} s^{-1}. When the experiment was conducted with air purging rather than an inert gas (Ar), there was evidence that dissolution rate was suppressed (Thomas et al., 2000). The amount of surface oxidation products on the mineral surface, the acid strength and the temperature determine the length of the induction period.

The differential thermal analysis of pyrrhotite conducted by Reimers and Hjelmstad (1987) in the temperature range 100°C to 500°C and an atmosphere of dry air suggested

that the self-heating of pyrrhotite may not be triggered because of sulphate formation from oxidation by air, because pyrrhotite needed to be heated to 140°C to 150°C before the required exothermic reaction was initiated. In other words, direct oxidation of pyrrhotite dose not appear to be the source of self-heating and, indeed, a prior history leading to sulphate formation may suppress H_2S generation and self-heating.

4. 3 Tracking the Source of Acid Needed for H_2S Liberation

4.3. 1 pH Test on Condensates

Generation of H_2S requires acidic conditions. A modified self-heating test was performed to track the source of acid, following the procedure described in section 3.4. In the first step, the oxygen trapped inside the reaction chamber was purged by pure nitrogen; therefore a non-oxidative reaction (equation 4.1) with pyrrhotite occurred. The results (Figure 4.18) show the condensates had a pH 2.9 (and again the copper piece turned black).

It can be concluded that the acid was not from the reactions in the self-heating test as no oxygen was introduced but arose from previous "weathering" of the PoT sample that had already generated acidic moisture. This is most likely a common situation, that moisture in sulphide materials becomes acidic.

4.3. 2 Acid Species Characterization by Ion Chromatography

Ion chromatography on the collected condensates identified the anionic species as SO_4^{2-}, as anticipated. Pyrrhotite readily undergoes oxidation, a product of which is sulphuric acid (Nicholson et al., 1994). Pratt et al. (1996) note that pyrrhotite, as one of the solid

wastes from mining operations, oxidizes to produce highly acidic, sulphuric acid-bearing water, and demonstrated that the pressures and stresses of milling sharply increases the susceptibility of pyrrhotite to oxidation.
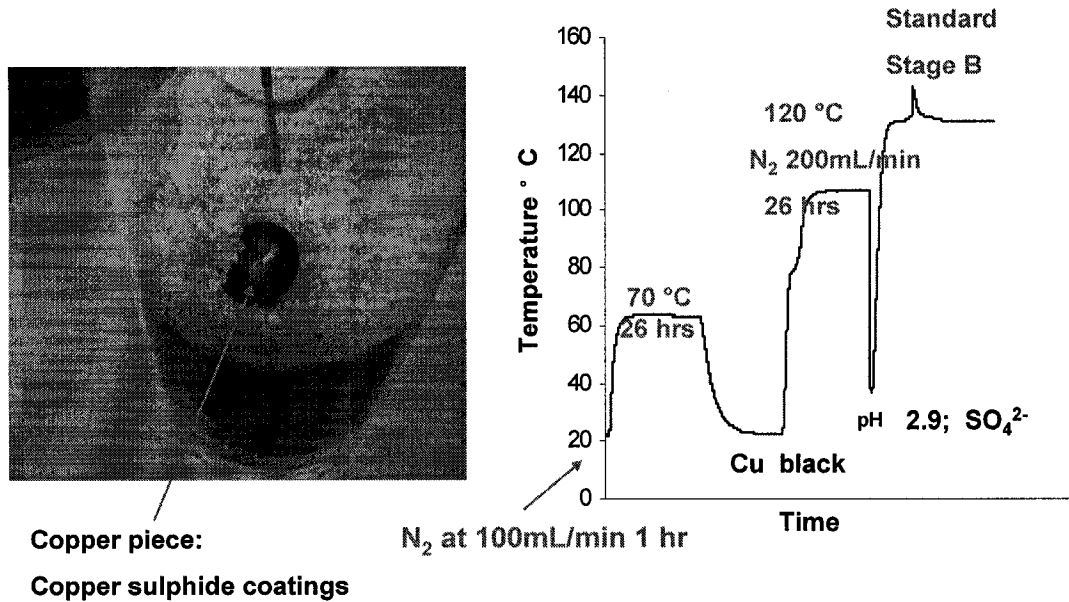
Figure 4. 18 pH and temperature response

4.3. 3 Self-heating of Stage B Test

Stage B test is used to evaluate the effect of weathering on the sample. For the sample used to track acid, Figure 4.18 shows only a single small peak in stage B then no further response. A direct stage B test (Appendix Figure A1-2) on an as-received sample showed a similar single peak which infers that the sample tested in Figure 4.18 was essentially the same as the original; i.e., the original sample carried acidic moisture. The single peak may come from sulphur (Rosenblum and Spria, 1995) formed during previous oxidative processes and the lack of further peaks indicates that no sulphur was produced during the weathering stage conducted here.

4. 4 Importance of Less Oxidative Conditions in Self-heating of Pyrrhotite-Rich Materials

There is evidence from field studies that the temperature at a certain distance inside a stockpile, typically about 0.5 m in from the surface, is much higher than either at the surface or further inside the stockpile. Figure 4.19 (Rosenblum et al., 2001) is a sulphide concentrate stored at Port of Montreal waiting for shipment to a Noranda smelter. The temperature in the 'hot region' inside the stockpile reached more than 71°C. The layer had a colour change to orange or brown. In this layer, the oxygen concentration in the pore water is assumed to be lower than that available in the surface moisture and higher than that in moisture further inside. The high temperature and colour change suggested that the apparently low oxidative conditions that encourage self-heating occur at this specific layer, which coincidentally favours production of H_2S. Lukaszewski (1969) stated that hot spots in piles were characterized by a rapid evolution of heat.

Reacted layer inside stockpile

Hot region   Stockpile at Port of Montreal
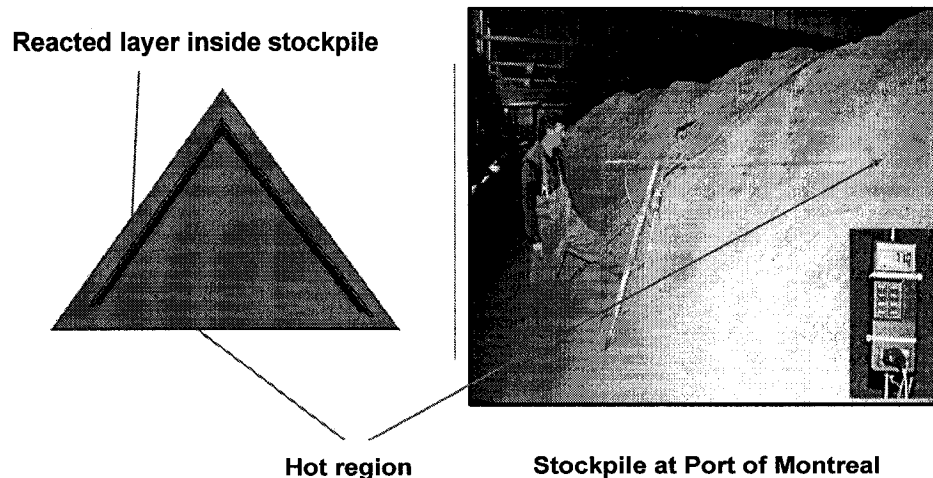
Figure 4. 19 Reacted layer and hot spot inside the stockpile (Rosenblum et al., 2001)

4.4. 1 Tests in Self-heating Apparatus under Different Air Flow Rates of Stage A

Two groups of tests were conducted using the self-heating apparatus. The results of the first group, tests at different air flow rates (AFR) of stage A, are summarized in Figure 4.20.
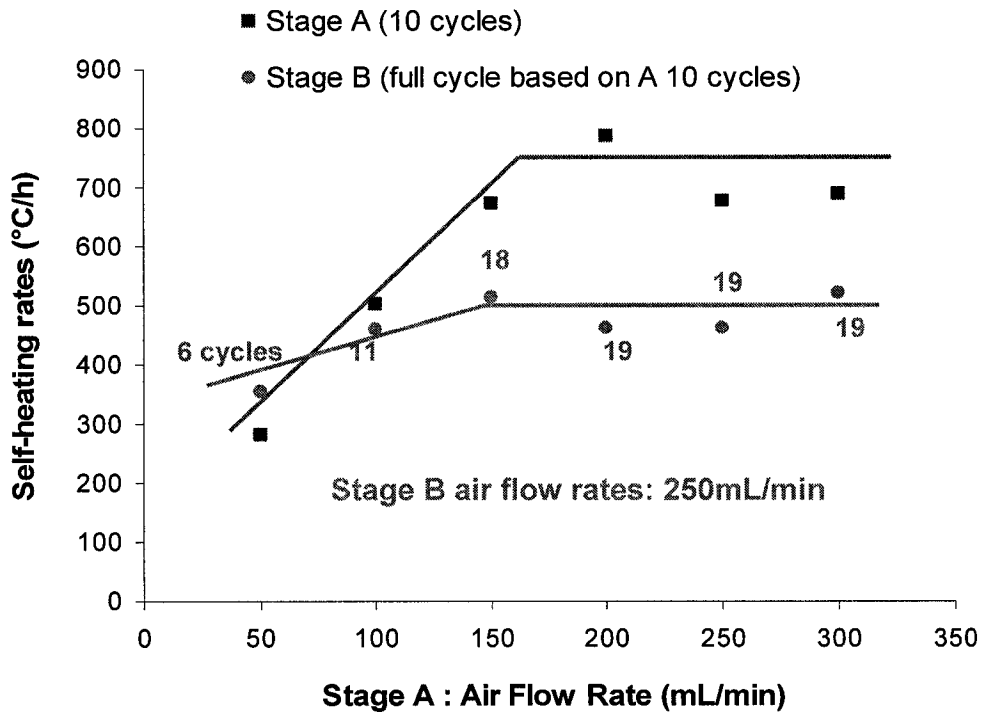
Figure 4. 20 Self-heating rates of stage A (10 cycles) and B (full cycle)

For stage A, initially, the self-heating rate increased with increasing AFR till it reached a 'saturation' point around 150 to 200 mL/min and then the response became constant. The plateau means any higher AFR for stage A will not promote self-heating but suppress it. The response of stage B showed a similar trend to stage A although the experiments lasted for different cycles (till exhaustion), indicated by the number beside each datum.

Analysing the self-heating response of Stage A cycle by cycle (Figure 4.21), it can be seen that for the first five cycles the self-heating responses increased with increasing AFR but the response dropped quickly after the fifth cycle at high AFR while the response continued to increase slowly at low AFR. That means samples weathered under low AFRs (50 and 100 mL/min) still have strong potential to generate heat after ten cycles.
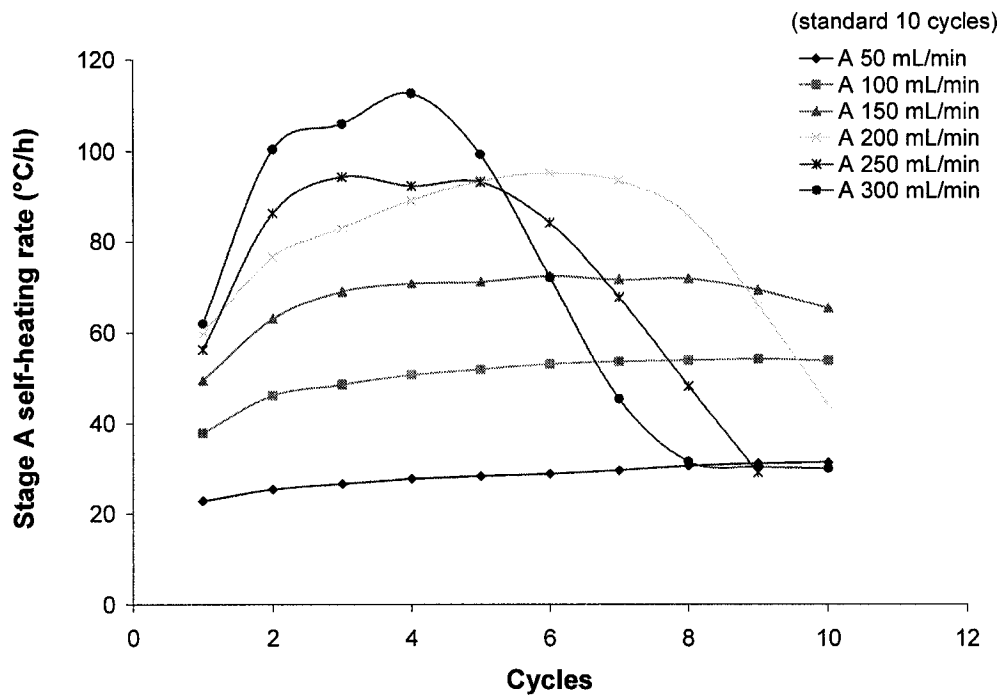
Figure 4. 21 Cycle by cycle self-heating response of stage A (standard 10 cycles)

Rosenblum and Spira (1995) reported that elemental sulphur was formed during weathering in Stage A and continued to build up till there was no moisture left in the sample. The self-heating of Stage B depended on the sulphur formed in Stage A. Therefore, the heating response in stage B gradually decreased and reached zero when all the free sulphur was consumed. The full cycle response of Stage B (Figure 4.22) showed that for the first two cycles, higher self-heating rates were generated by the samples

weathered under low AFRs (50 and 100 mL/min). Based on the study of Rosenblum and

Spira (1995), the results of stage B indicate that sulphur produced after weathering under

low AFR was more reactive and yielded high heating response, especially for the initial

two cycles. The sulphur produced under weathering at high AFR may be covered or

coated and thus gave low heating response. Rosenblum and Spira reported the sample

recovered some heat response after washing, which suggests that soluble coatings (e.g.

sulphates) had been removed.
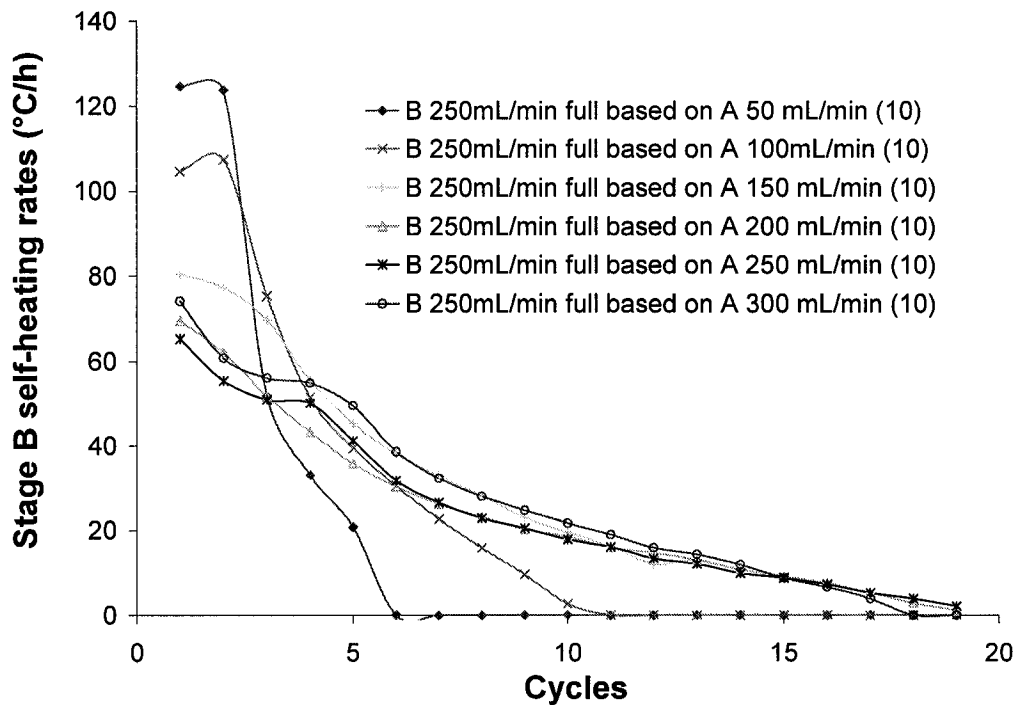
Figure 4. 22 Cycle by cycle self-heating response of stage B (full cycle)

based on stage A (10 cycles)

The self-heating tests of stage A were run for the standard ten cycles prior to stage B. In

order to investigate the full potential of the samples weathered under stage A, the

following group of tests was performed.

For this group of tests, two samples were run under stage A air flow rates of 50 and 300 mL/min to full cycle (i.e., till no further heat response) and stage B at 250 mL/min also to full cycle. Self-heating results are summarized in Figure 4.23.
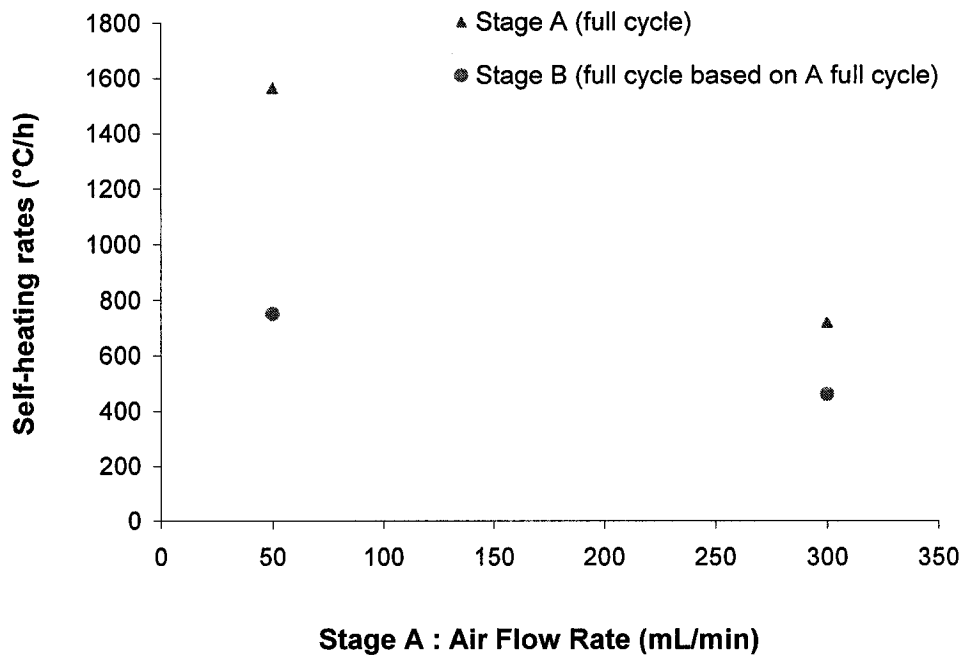
Figure 4. 23 Self-heating rates of stage A (full cycle) and B (full cycle)

The self-heating rates of stage A decreased significantly going from AFR of 50 mL/min to 300 mL/min, dropping from 1560 to 720°C/hr and in stage B from 750 to 460°C/hr. The sample weathered at 50 mL/min lasted 107 cycles while the other sample was exhausted after 24 cycles at 300 mL/min (Figure 4.24). Although the sample showed higher heating rates in the first seven to eight cycles, after that the response decreased sharply, and cumulatively the sample was less reactive.
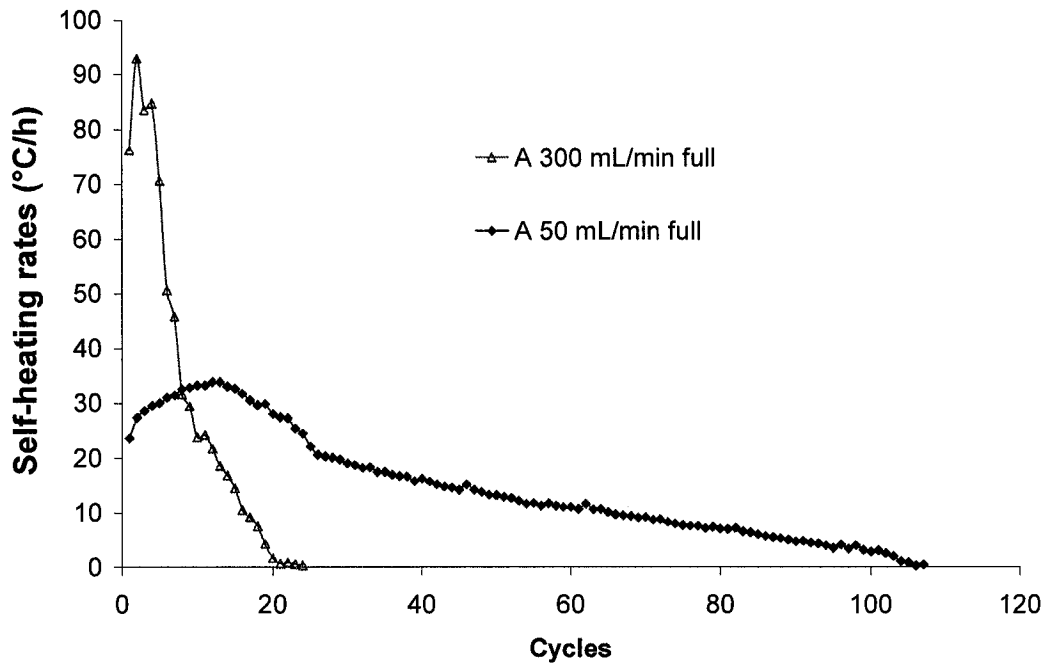
Figure 4. 24 Cycle by cycle self-heating response of stage A (full cycle)

The oxidation of sulphides will consume water according to equations 2.1 and 2.2. The PoT samples will not heat when no moisture is left. Under low AFR, water might be formed via the oxidation of hydrogen sulphide (equation 2.16). The newly generated water will extend the weathering period and therefore more heat will be produced. However, under high AFR (higher oxidizing conditions), little or no hydrogen sulphide is formed and the surface of the PoT sample might be covered or coated by oxidation products, for instance goethite or maghemite, that prevent further reaction.

The cycle response of Stage B (Figure 4.25) can be revealing. Commonly, the heating response of Stage B decreases with number of air cycles and goes to exhaustion slowly with little sulphur remaining. However, for the one weathered under low ARF (50

mL/min) to full cycle the curve went up and reached its highest point at the 23rd cycle then went to zero after 30 cycles. This atypical behaviour of stage B under low AFR conditions confirms that self-heating is promoted under low oxidative conditions and that either larger amounts of sulphur are formed or the sulphur is more reactive (e.g., finer), and therefore gives higher heating response. It is hypothesized that the sulphur formed at low AFR was dominantly the oxidation product of hydrogen sulphide (equation 4.5) while that formed at high AFR was dominantly the oxidation product of pyrrhotite (equations 4.7, 4.8, 4.9 or 4.10).
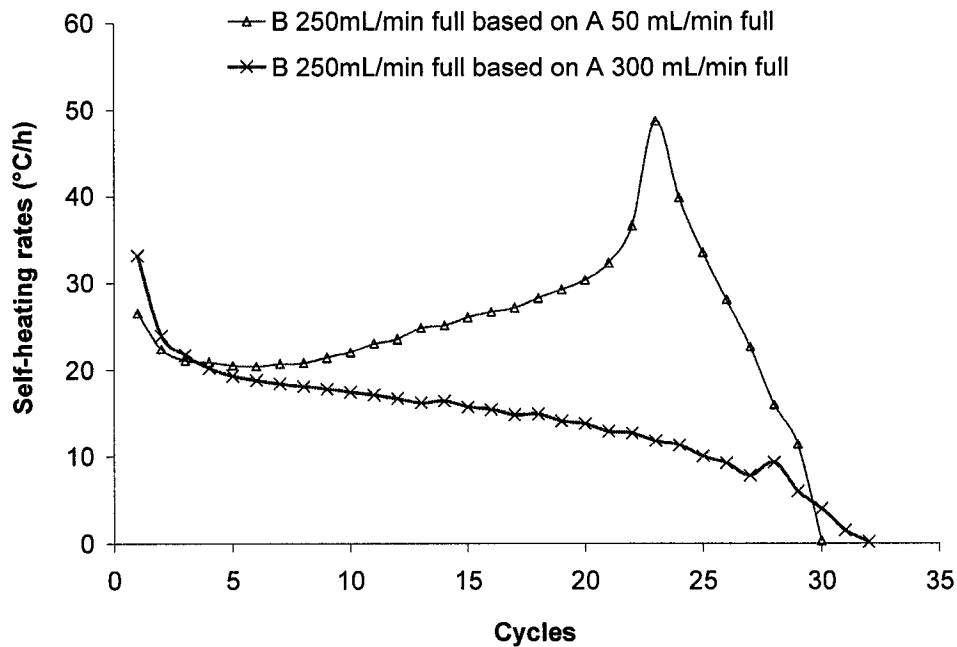
Figure 4. 25 Cycle by cycle self-heating response of stage B (full cycle)

based on stage A (full cycle)

Comparing all the tests conducted, Figure 4.26 shows that the heat produced at high AFR (300 mL/min) did not show much difference between standard (ten cycles) and full cycle

while a large difference can be seen under low AFR (50 mL/min). Pyrrhotite showed much higher self-heating potential weathered at low AFRs (less oxidative conditions). The less oxidative conditions, it is argued favour H_2S liberation which plays an important role in the self-heating of pyrrhotite-rich materials.
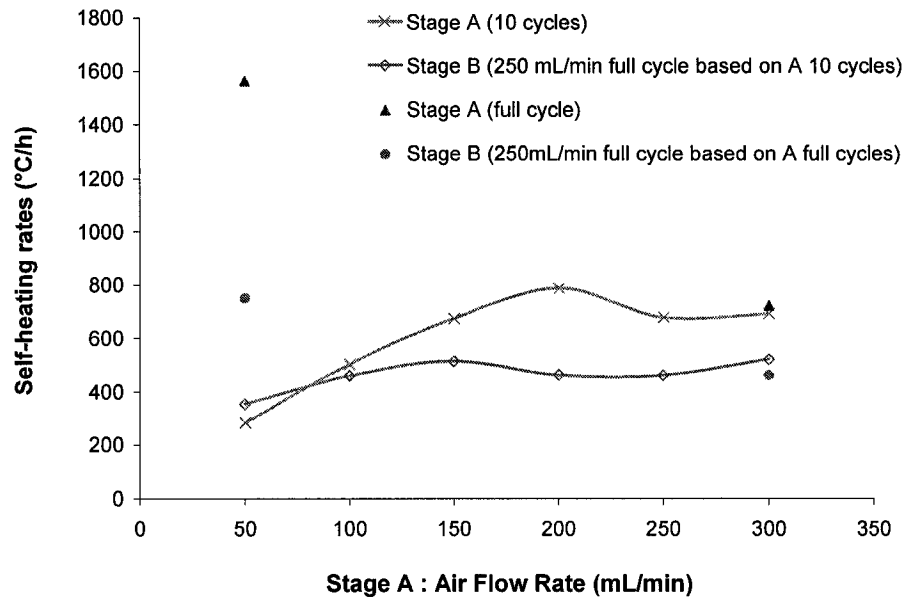
Figure 4. 26 Self-heating response of stage A and B (full cycle)

4.4. 2 Weight Gain at 40 °C in Weathering Apparatus

4.4.2.1 Weight gain test

Three tests were conducted to explore the role of oxygen level in self-heating of pyrrhotite-rich materials using the weathering apparatus with no hole, three hole and 128 hole covers set at 40°C (Figure 3.7).

The weight of the sample was recorded every two days over 27 days (Figure 4.27). Under limited air access conditions (no hole and three hole covers), the weathered samples

showed higher weight gain, 15.3% and 22.4%, and higher degree of oxidation (by colour change) compared with that under the 128 hole cover. The results indicated that oxygen (and probably humidity) level in the weathering apparatus control the weight gain and degree of reaction.
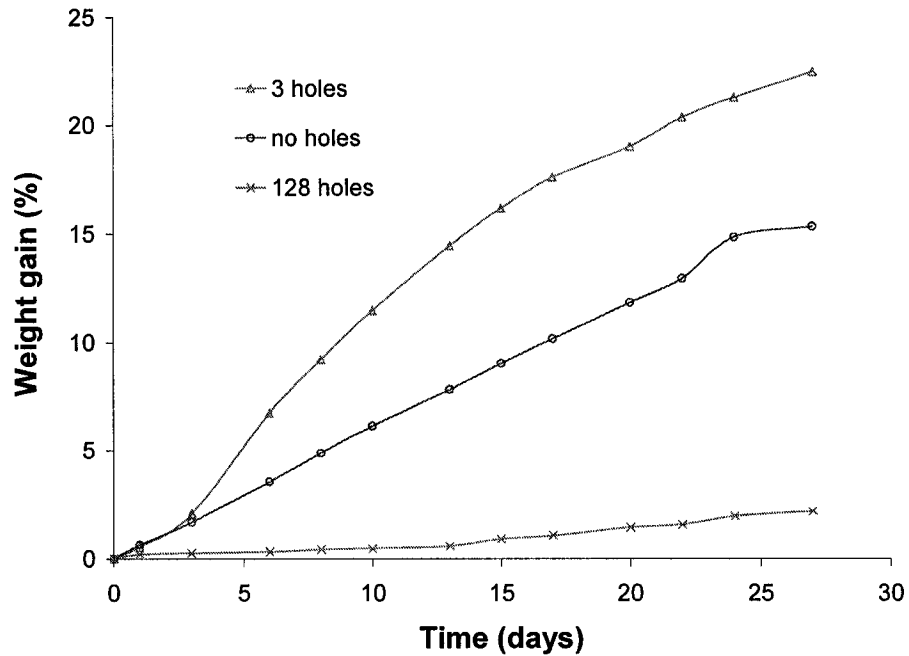
Figure 4. 27 Weight gain curves of PoT sample weathered under three conditions after 27 days

Figure 4.28 shows the colour change after weathering under the three conditions. The PoT sample under limited air conditions changed to yellowish brown while the one in the 128 holes weathering apparatus with ready air access, remained the original grey. A colour change due to oxidation of pyrrhotite containing ore from bronze to brown was observed by Good (1977).
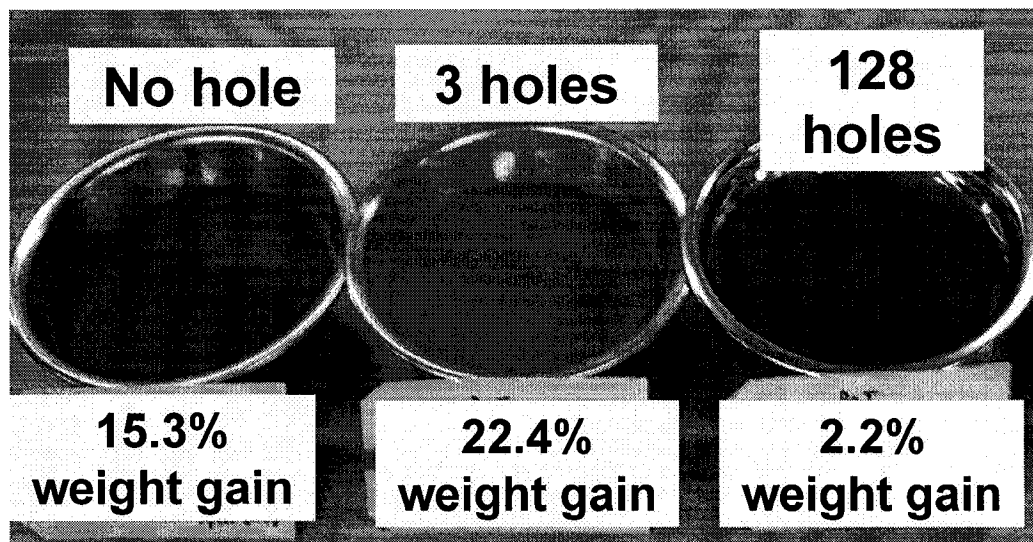
Figure 4. 28 Visual evidence of PoT sample weathered under three conditions after 27 days

It was reported by Wu and Li (2005) that a linear relationship existed between the quantity of oxygen absorbed and the weight increment of sulphides at ambient temperature. That means the more reactive the sulphides are, the higher the weight gain. The limited air conditions (no hole and three hole covers), under which PoT had the higher weight gain after weathering, favour reaction while conditions with high exposure to air (128 hole cover) suppress it.

4.4.2. 1 Stage B self-heating test on products

To evaluate the self-heating potential of the weathered samples under the three conditions, stage B self-heating tests were applied. The samples were taken out of the weathering apparatus, mixed to make homogeneous and diluted with 250 g coarse silica sand. Stage B tests were performed to full cycle. Figure 4.29 shows that the samples weathered under less oxidative conditions (no hole and three hole covers) lasted 43 and 41 cycles, respectively, with self-heating rates of 634°C/h and 570°C/h, respectively. In

contrast, the sample weathered under the 128 hole cover lasted only 3 cycles with a 68°C/h heating rate similar to the original PoT (1 cycle, self-heating rate 29°C/h). The results suggest that a larger amount of sulphur was produced by the PoT sample under restrictive conditions, giving the long time till exhaustion. In contrast, little sulphur was generated under high air exposure conditions and was rapidly depleted upon air cycle in stage B.
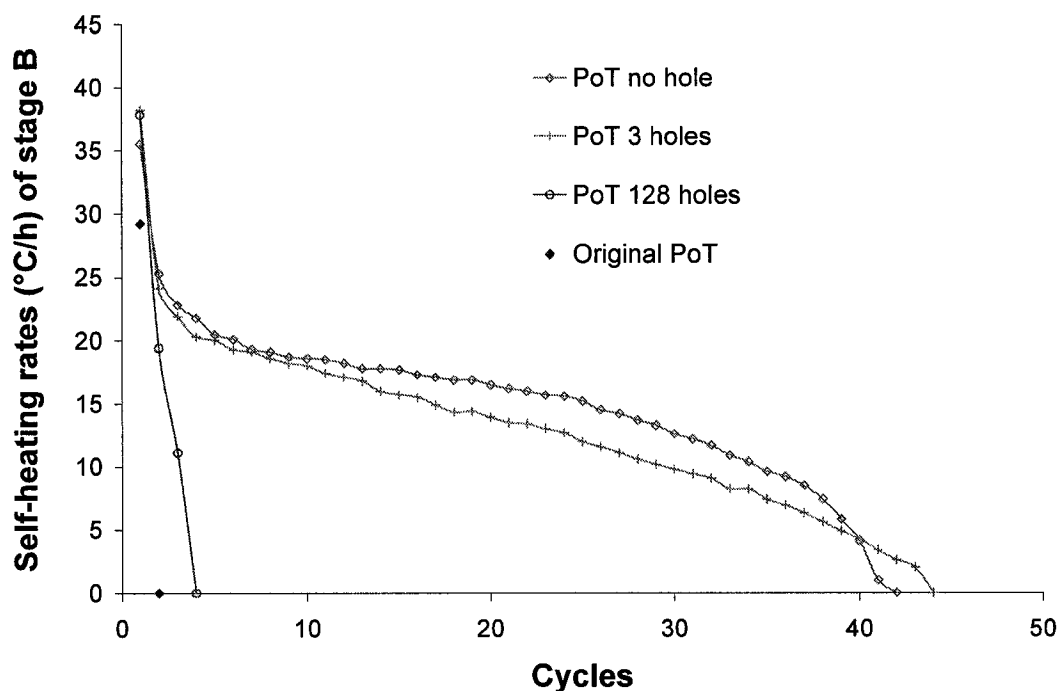
Figure 4. 29 Self-heating response of stage B (full cycle) of the weathered products

To summarize, the PoT sample with the higher weight gain and higher degree of oxidation (by colour change) weathered under the less oxidative conditions yielded higher stage B self-heating rates, indicative of favourable conditions to produce elemental sulphur.

4.4.2. 2 XRD and electron microprobe analysis on products

The characterization of the secondary mineral phases (Jambor, 1994) formed during pyrrhotite weathering was performed by X-ray diffraction (XRD) on whole powder and electron microprobe analysis on selected particles.

The XRD spectra (Figure 4.30) reveal the presence of reaction products maghemite (Fe_2O_3), goethite ($FeO(OH)$) and elemental S in the sample weathered in the no hole and three hole cover tests. The presence of Fe_2O_3 and $FeO(OH)$ corresponds to the colour of the weathered sample, and the elemental sulphur corresponds to the high self-heating rate of stage B (Figure 4.29). Elemental sulphur was observed by Janzen et al. (2000) and they estimated that ca. 85% of the oxidized sulphide had accumulated as elemental sulphur as the result of incomplete oxidation.

Comparing the XRD patterns of the three weathered samples and the original PoT sample, the three hole sample seemed to have reacted most with higher maghemite and elemental sulphur peaks. However, more goethite was identified in the no hole sample which might be due to the even less oxidative condition. The possible mechanism of goethite formation was discussed in section 4.2.4. Under the no hole condition, oxygen is easier to be reduced to OH⁻ than for the three hole case. The disappearance of magnetite in the samples weathered under restrictive air conditions indicates that maghemite was the oxidation product of magnetite. No clear alterations were found for the 128 hole weathered sample compared with the original sample. The phases identified from the XRD results are summarized in Table 4.3.

Both goethite and elemental sulphur were reported by several authors in their study of pyrrhotite-rich materials (Shaw et al., 1998; Janzen et al., 2000; Cruz et al., 2001).

Table 4. 3 XRD results of original and weathered PoT

Sample ID	pyrrhotite $Fe_{1-x}S$ 01-75-600 & 24-79	magnetite $FeFe_2O_4$ 19-629	maghemite Fe_2O_3 4-755	goethite FeO(OH) 29-713	S 72-2402	rosickyite S 13-141	sulphur S 1-478
PoT original	✓	✓	—	—	—	—	—
PoT 128 holes	✓	✓	✓	—	—	—	—
PoT 3 holes	✓	—	✓	✓	✓	✓	✓
PoT no hole	✓	—	✓	✓	✓	✓	✓

Figure 4. 30 XRD analysis of the original and the weathered PoT

Electron microprobe analysis was performed on polished sections of the original PoT sample and the weathered products. Ten spots were selected randomly to measure the Fe/O ratio to test for maghemite (Fe_2O_3, ratio 2/3) (Figure 4.31) and other iron oxides/hydroxides in the weathered products. The electron microprobe results are in agreement with the XRD data.

Figure 4. 31 Electron microprobe analysis of PoT sample weathered in no hole cover showing maghemite

X-ray diffraction and electron microprobe examination of the reaction products confirmed the presence of ferric oxide (maghemite, Fe_2O_3) and ferric oxy-hydroxide (goethite, $FeO(OH)$) in the no hole and three holes cases indicating that the restricted air condition promoted the oxidation of the PoT sample; or, conversely, high air conditions suppressed the oxidation process. The low self-heating rates of stage B for the sample weathered in 128 holes confirmed that no elemental sulphur was formed, as indicated by XRD.

It is postulated that a thin film of cemented material (for instance, ferrous or ferric sulphate) formed on the surface of pyrrhotite under rich air condition. The cemented layers locally decrease the porosity which decreases oxygen diffusivity and impedes the ingress of gaseous oxygen (Blowes et al., 1991). Thomas et al. (2000) observed that a barrier layer formed resulting from oxidative dissolution in their tests air purging

pyrrhotite suspended in perchloric acid ($0.1M$ $HClO_4$). Biglari et al. (2006) stated that the oxidation products may act as a barrier to oxygen transport. The oxidized layer provides a significant barrier to diffusive oxygen transport to the reactive surface. The space previously occupied by sulphide becomes filled with oxidation products, thus forming a barrier to oxygen diffusion. Ferric hydroxide formed a passive layer on the surface of the unreacted pyrrhotite core, which inhibited further oxidation of the mineral, in tests conducted by Lehmann et al. (2000).

Cruz et al. (2005) found that oxidation products that coated and passivated the pyrrhotite surface controlled pyrrhotite reactivity in their electrochemical studies of pyrrhotite under simulated weathering conditions at pH 5.5.

Although the oxidation products goethite and elemental sulphur were identified in the two samples weathered under limited air conditions, they did not seem to passivate further oxidation reactions. Mikhlin et al. (2002) also pointed out that the surface layer enriched in elemental sulphur and ferric oxyhydroxide did not inhibit sulphide oxidation and acid production when the pyrrhotite was leached in HCl and exposed to humid air.

The cementation by ferric oxy-hydroxide minerals ('hardpan') is evident as a hard layer formed after one month of weathering. It is assumed that the layer formed slowly due to low oxygen availability under the no hole and three hole conditions. With limited oxygen and high humidity, H_2S was liberated through non-oxidative dissolution. As the sulphide leaves as H_2S, the surface of pyrrhotite becomes relatively iron enriched. The oxidation of H_2S and partial oxidation of pyrrhotite contributes to the formation of elemental sulphur.

80

It was reported by McGregor et al. (2002) that goethite dominated cemented layers showed enrichment of total elemental sulphur compared to the surrounding uncemented tailings in their study of pyrrhotite-bearing mine tailings. The XRD and stage B self-heating test results are in good agreement with this enrichment of elemental sulphur argument. Hardpan layers with goethite-rich secondary mineralization have also been observed by Gunsinger et al. (2006) in their studies of pyrrhotite-rich tailings. Lukaszewski (1973) stated that the cementing of sulphide wastes is attributable to natural oxidation processes. The presence of pyrrhotite will make the cementing process more effective.

Wunderly et al. (1996) assumed that the oxidation process is controlled by oxygen diffusivity. First, the rate of oxygen diffusing downward through the pore spaces, and, second, oxygen diffusion through any secondary alteration coatings on the pyrrhotite grains.

Buckley and Woods (1985a) proposed that diffusion of iron from the outermost layers of the solid lattice occurred forming, sequentially, iron(II) oxide, iron(III) hydroxyl-oxide and hydrated oxides at the air/solid interface. Ferric oxy-hydroxide (goethite, FeO(OH)) is the oxidation product of ferrous ions by either equation (4.11), suggested by Janzen et al. (2000) and Belzile et al. (2004), or equation (4.12) suggested by Gunsinger et al. (2006).

$$Fe^{2+} + 1/4O_2 + 2H^+ = Fe^{3+} + 1/2H_2O \qquad (4.11)$$

$$Fe^{3+} + 2H_2O = FeOOH + 3H^+ \qquad (4.12)$$
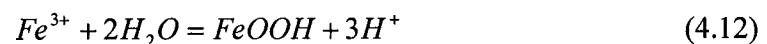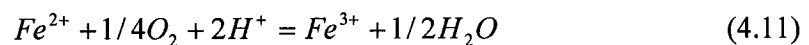
With the liberation of H_2S, suppressed under the high oxygen conditions (128 holes in weathering apparatus and high air flow rates in self-heating apparatus), oxidative dissolution will not proceed as fast as that initiated under restricted oxygen conditions; therefore, less heat will be generated. Both the process of liberation of H_2S and the oxidation of H_2S to sulphur or sulphur dioxide are exothermic. The initiation of H_2S formation under low oxidative conditions is a crucial step in self-heating.

Chapter 5 Conclusions

This thesis explores the conditions leading to self-heating of pyrrhotite-rich materials by testing for H_2S liberation, tracking the source of the acid required for H_2S generation and investigating the role of level of oxidation conditions.

Hydrogen sulphide was liberated in stage A in the standard self-heating test identified by the black copper sulphide coatings on copper and black copper sulphide precipitates in copper sulphate solution. Hydrogen sulphide was also detected in the "weathering" apparatus at 40 °C.

Hydrogen sulphide was produced by the reaction between pyrrhotite and acid under restricted oxidative conditions. The acid was identified as sulphuric acid and derived not from the reactions in the self-heating test but from previous "weathering" of the sample.

In the weathering apparatus tests, samples under limited exposure to air showed higher weight gain, higher degree of oxidation (by colour change and presence of oxy-hydroxides and elemental sulphur identified by X-ray diffraction) and higher stage B self-heating rates compared with the sample with high exposure to air. In the self-heating apparatus tests, samples under low air flow rates in stage A showed significantly higher self-heating rates in both stage A and B. Less oxidative conditions favouring the production of H_2S play a critical role in the self-heating of pyrrhotite-rich materials.

5.1 Recommendations

More controlled testing of oxidation and moisture levels. Samples can be weathered under different ratio of air/nitrogen conditions using the new weathering setup. Based on the weight gain, stage B self-heating rates and detailed characterization of the products, the critical conditions leading to self-heating can be defined.

Pyrrhotite as the most susceptible sulphide triggering self-heating can be mixed with concentrates such as sphalerite or galena at different ratios to evaluate the self-heating potential due to possible galvanic effects.

To test the existence of catalysts in the PoT sample and confirm the point that catalysts play a role in H_2S oxidation, EDTA extraction can be used to remove the iron oxides and test whether the self-heating potential is reduced. As an alternative, possible oxy-hydroxide catalysts could be tested to determine if H_2S oxidation is promoted.

References

Ahmed, A.A., Sharaf, N.A., and Condrate, R.A., "Raman microprobe investigation of sulphur-doped alkali borate glasses"; Journal of Non-Crystalline Solids 210 (1997) 59-69.

Arnold, R.G., "Mixtures of hexagonal and monoclinic pyrrhotite and the measurement of the metal content of pyrrhotite by X-ray diffraction"; The American Mineralogist, Vol. 51, July, 1966.

Belzile, N., Chen, Y., Cai, M., and Li, Y., "A review on pyrrhotite oxidation"; Journal of Geochemical Exploration 84 (2004) 65-76.

Biglari, M., Nicholson, R.V., Reilly, P.M., and Scharer, J.M., "Model Development and Parameter Estimation for the Oxidation of Pyrrhotite-Containing Rock Surfaces"; The Canadian Journal of Chemical Engineering, Volume 84, February 2006.

Blowes, D.W., Reardon, E.J., and Jambor, J.L., "The formation and potential importance of cemented layers in inactive sulfide mine tailings"; Geochimica Cosmochimica Acta, Vol. 55, pp. 965-978, 1991.

Bournival, G., "Sulphide Self-heating Project Report"; McGill University, Department of Mining, Metals and Materials Engineering, September 2006.

Bowes, P.C., "Spontaneous heating and ignition in iron pyrites"; The Industrial Chemist, January, 1954, pp. 12-14.

Buckley, A.N., and Woods, R., "X-ray photoelectron spectroscopy of oxidized pyrrhotite surfaces I. Exposure to air"; Applications of Surface Science 22/23 (1985) 280-287.

Buckley, A.N., and Woods, R., "X-ray photoelectron spectroscopy of oxidized pyrrhotite surfaces II. Exposure to aqueous solutions"; Applications of Surface Science 20 (1985) 472-480.

Bukhtiyarova, G.A., Bukhtiyarov, V.I., Sakaeva, N.S., Kaichev, V.V., and Zolotovskii, B.P., "XPS study of the silica-supported Fe-containing catalysts for deep or partial H_2S oxidation"; Journal of Molecular Catalysis A: Chemical 158 (2000) 251-255.

Carroll, J.J., and Mather, A.E., "The solubility of hydrogen sulphide in water from 0 to 90°C and pressures to 1 Mpa"; Geochimica Cosmochimica Acta, Vol. 53, pp. 1163-1170, 1989.

Cruz, R., Bertrand, V., Monroy, M., and Gonzalez, I., "Effect of sulfide impurities on the reactivity of pyrite and pyritic concentrates: a multi-tool approach"; Applied Geochemistry 16 (2001) 803-819.

Cruz, R., Gonza´lez, I., and Monroy,M., "Electrochemical characterization of pyrrhotite reactivity under simulated weathering conditions"; Applied Geochemistry 20 (2005) 109-121.

Demopoulos, G.P., "Aquesous Precipitation and Crystallization for the Production of Particulate Solids with Desired Properties"; Course MIME 652, Aqueous Processing 2006 Edition, pp 1-49.

Elving, P.J., and Kolthoff, I.M., "Analytical chemistry of sulphur and its compounds"; Volume 29, Interscience Publishers.

Farnsworth, D.J.M., "Introduction to and background of sulphide fires in pillar mining at the Sullivan mines"; CIM Bulletin, Vol. 70, 782, pp. 65-71, 1977.

Fierro, V., Miranda, J.L., Romero, C., Andres, J.M, Arriaga, A. and Schmal, D., "Model predictions and experimental results on self-heating prevention of stockpiled coals"; Fuel 80 (2001) 125-134.

Filippou, D., Konduru, R., and Demopoulos, G.P., "A kinetic study on the acid pressure leaching of pyrrhotite"; Hydrometallurgy 47 (1997) 1-18.

Good, B.H., "The oxidation of sulphide minerals in the Sullivan mine"; CIM Bulletin, Vol. 70, 782, pp. 83-88, 1977.

Gunsinger, M.R., Ptacek, C.J., Blowes, D.W., and Jambor, J.L., "Evaluation of long-term sulfide oxidation processes within pyrrhotite-rich tailings, Lynn Lake, Manitoba"; Contaminant Hydrology 83, 2006, 149-170.

Habashi, F., and Bauer, E., "Aqueous oxidation of elemental sulfur"; I&EC Fundamentals, Vol. 5, No. 4, November 1966, 469-471.

Headley, G.S., Bloomer, T.O., and Glennie, J.A., "Hot muck mining methods"; CIM Bulletin, Vol. 70, 782, pp. 72-78, 1977.

Interim report on the research in spontaneous heating of metal sulfide concentrates (II) 1976 (the reference has been lost, see Appendix A3).

Jambor, J.L., "Mineralogy of sulfide-rich tailings and their oxidation products"; Environmental Geochemistry of Sulfide Mine-Wastes Vol. 22, May 1994 Short Course Handbook.

Janzen, M. P., Nicholson, R.V., and Scharer, J.M., "Pyrrhotite reaction kinetics: Reaction rates for oxidation by oxygen, ferric iron, and for nonoxidative dissolution"; Geochimica et Cosmochimica Acta, Vol. 64, No. 9, pp. 1511-1522, 2000.

Jones, J.C., Henderson, K.P., Littlefair, J. and Rennie, S., "Kinetic parameters of oxidation of coals by heat-release measurement and relevance to self-heating tests"; Fuel Vol.77, No. 1/2, pp.19-22, 1998.

Jones, J.C.and Littlefair, J., "Novel behavior in the self-heating of coal filter cake"; Fuel Vol.76 No.12, pp. 1165-1167, 1997.

Kalinnikov, V.T., Makarov, D.V., and Makarov, V.N., "Oxidation sequence of sulfide minerals in operating and out of service mine waste storage"; Theoretical Foundations of Chemical Engineering, Vol. 35, No.1, 2001, pp. 63-68.

Karchmer, J.H. ed., "The analytical chemistry of sulphur and its compounds"; NY, Wiley-Interscience, pp. 289.

Lehmann, M.N., Kaur, P., Pennifold, R.M., and DunnA, J.G., "A comparative study of the dissolution of hexagonal and monoclinic pyrrhotite in cyanide solution"; Hydrometallurgy 55 (2000) 255-273.

Lukaszewski, G.M., "Natural oxidation and the reaction of AN-FO explosives in mineral sulphides at Mount Isa Mines Limited"; Ninth Commonwealth Mining and Metallurgical Congress 1969, Offices of the Congress and of the Institution of Mining and Metallurgy, pp. 1-17.

Lukaszewski, G.M.,"Sulphides in underground mine filling operations"; Jubilee Symposium on Mine Filling Mt Isa, 1973, pp. 87-96.

McGregor, R.G., and Blowes, D.W., "The physical, chemical and mineralogical properties of three cemented layers within sulfide-bearing mine tailings"; Journal of Geochemical Exploration 76 (2002) 195-207.

Mehta, A.P., and Murr, L.E.," Fundamental studies of the contribution of galvanic interaction to acid-bacterial leaching of mixed metal sulphides"; Hydrometallurgy, 9 (1983) 235-256.

Mielke, R.E., Pace, D. L., Porter, T., and Southam, G., "A critical stage in the formation of acid mine drainage: coloniuzation of pyrite by acidithiobacillus ferrooxidans under pH-neutral conditions"; Geobiology (2003), 1, 81-90.

Mikhlin, Y.L. , Kuklinskiy, A.V., Pavlenko, N.I., Varnek, V.A., Asanov, I.P., Okotrub, A.V., Selyutin, G.E., and Solovyev, L.A., "Spectroscopic and XRD studies of the air degradation of acid-reacted pyrrhotite"; Geochimica et Cosmochimica Acta, Vol. 66, No.23, pp. 4057-4067, 2002.

Mycroft, J.R., Bancroft, G.M., McIntyre, N.S., Lorimer, J.W., and Hill, I.R., "Detection of sulphur and polysulphides on electrochemically oxidized pyrite surfaces by X-ray photoelectron spectroscopy and Raman spectroscopy"; J.Electroanal.Chem., 292(1990) 139-152.

Nicholson, R.V., Scharer, J.M., and Charles, A.P., "Laboratory studies of pyrrhotite oxidation"; ACS Symposium Series (1994), 550 (Environmental Geochemistry of Sulfide Oxidation), 14-30.

Ninteman, D.J., "Spontaneous oxidation and combustion of sulfide ores in underground mines A literature survey"; Information Circular 8775, United States Department of the Interior Bureau of Mines

Nordon, P., "A model for the self-heating reaction of coal and char"; Fuel, 1979, Vol 58, June, pp. 456-464.

Nowak, P., Krauss, E., and Pomianowski, A., "The electrochemical characteristics of the galvanic corrosion of sulphide minerals in short circuited model galvanic cells"; Hydrometallurgy, 12 (1984) 95-110.

Orlova, T. V., and Stupnikov, V. M., and Krestan, A.L., "Mechanism of oxidative dissolution of sulphides"; Zhurnal Prikladnoi Khimii 61, 2172-2177.

Posfai, M., "Pyrrhotite varieties from the 9.1km deep borehole of KTB project, 2000"; http://www.minsocam.org/MSA/AmMin/TOC/Articles_Free/2000/Posfai_p1406-1415_00.pdf

Pratt, A. R., Muir, I. J. and Nesbitt, H. W., "X-ray photoelectron and Auger electron spectroscopic studies of pyrrhotite and mechanism of air oxidation"; Geochimica et Cosmochimica Acta, Vol.58, No.2, pp. 827-841, 1994.

Pratt, A.R., Nesbitt, H.W., and Muir, I.J., "Generation of acids from mine waste: Oxidative leaching of pyrrhotite in dilute H_2SO_4 solutions at pH 3.0"; Geochimica et Cosmochimica Acta, Vol. 58, No.23, pp. 5147-5159, 1994.

Pratt, A.R., Nesbitt, H.W., and Mycroft, J.R., "The increased reactivity of pyrrhotite and magnetite phases in sulphide mine tailings"; Journal of Geochemical Exploration 56 (1996) 1-11.

Rao, S.R., and Leja, J., "Surface Chemistry of Froth Flotation"; Kluwer Academic / Plenum Publishers, New York, 2004.

Reimers, G.W., and Hjelmstad, K.E., "Analysis of the oxidation of chalcopyrite, chalcocite, galena, pyrrhotite, marcasite, and arsenopyrite"; Bureau of Mines, U.S. Department of the Interior, 1987.

Research into the spontaneous combustion of sulphide lead, copper, and zinc concentrates; Laboratory 4.11, Diary No. 4-3602/1977 I BUNDESANSTALT FUR MATERIALPRUFUNG (BAM).

Richard, J.H., and Watkinson, D.H., "Cu-Ni-PGE Mineralization within the Copper Cliff Offset Dike, Copper Cliff North Mine, Sudbury, Ontario: Evidence for Multiple Stages of Emplacement"; Explo. Mining Geol., Vol. 10, Nos. 1 and 2, pp. 111-124, 2001.

Rosenblum, F., and Spira, P., "Evaluation of hazard from self-heating of sulphide rock"; CIM Bulletin, Vol. 88, No. 989, 44-49, 1995.

Rosenblum, F., and Spira, P., "Self-heating of sulphides"; The Thirteenth Annual Meeting of the Canadian Mineral Processors, 1981, 34-49.

Rosenblum, F., Nesset, J., and Spira, P., "Evaluation and control of self-heating in sulphide concentrates"; CIM Bulletin, Vol. 94, No. 1056, 92-99, 2001.

Sasaki, K., "Effect of grinding on the rate of oxidation of pyrite by oxygen in acid solutions"; Geochimica et Cosmochimica Acta, Vol. 58, 21, pp. 4649-4655, 1994.

Schippers, A., Kock, D., Schwartz, M., Bottcher, M.E., Vogel, H., and Hagger, M., "Geomicrobiological and geochemical investigation of a pyrrhotite-containing mine waste tailings dam near Selebi-Phikwe in Botswana"; Journal of Geochemical Exploration 92 (2007) 151-158.

Self-Heating Substances Test - DOT/UN Division 4.2,
http://www.chilworth.com/lab_trans.cfm

Shaw, S.C., Groat, L.A., Jambor, J.L., Blowes, D.W., Hanton-Fong, C.J., and Stuparyk, R.A., "Mineralogical study of base metal tailings with various sulfide contents, oxidized in laboratory columns and field lysimeters"; Environmental Geology 33 (2/3) 1998 209-217.

Somot, S., and Finch, J.A., "High Self-Heating Rate of Pyrrhotite-Rich Materials - H_2S as A Fuel?"; 38th Meeting of Canadian Mineral Processor, Proceedings 2006, pp. 83-92.

Stachulak, J.S., "Computerized fire monitoring, criteria, techniques and experience at Inco Limited"; CIM Bulletin, Vol. 83, 937, pp. 59-67, 1990.

Steger, H.F., "Oxidation of sulphide minerals - VI Ferrous and ferric iron in the water soluble oxidation products of iron sulphide minerals"; Talanta, Vol. 26, pp. 455-460, 1979.

Steger, H.F., "Oxidation of sulphide minerals -1 Determination of ferrous and ferric iron in samples of pyrrhotite, pyrite and chalcopyrite"; Talanta, Vol. 24, pp. 251-254, 1977.

Steger, H.F., "Oxidation of sulfide minerals VII. Effect of Temperature and Relative Humidity on the Oxidation of Pyrrhotite"; Chemical Geology, 35 (1982) 281-295.

Steijns, M., and Mars, P., "The Role of Sulfur Trapped in Micropores in the Catalytic Partial Oxidation of Hydrogen Sulfide with Oxygen"; Journal of catalysis 35, 11-17 (1974).

Thomas, J.E., Skinner, W.M., and Smart, R.St.C., "A mechanism to explain sudden changes in rates and products for pyrrhotite dissolution in acid solution"; Geochimica et Cosmochimica Acta, Vol. 65, No.1, pp. 1-12, 2001.

Thomas, J.E., Smart, R.St.C., and Skinner, W.M., "Kinetic Factors for Oxidative and Non-oxidative dissolution of Ion Sulfides"; Minerals Engineering, Vol. 13, No. 10-11, pp. 1149-1159, 2000.

Thomas, J.E., Jone, C.F., Skinner, W.M., and Smart, R.St.C., "The role of surface species in the inhibition of pyrrhotite dissolution in acid conditions"; Geochimica Cosmochimica Acta, Vol. 62, No. 9, pp. 1555-1566, 1998.

Tremblay, G., "Environmental Challenges and Opportunities for the Mining Industry"; Short Course on Mineral Processing Systems- McGill University May14-18, 2007.

Vanyukov, A. V., and Razumovskaya, N.N., "Hydrothermal oxidation of pyrrhotites"; Izv. Vyssh. Uchelon. Zaved., Tsvetn. Metall. 6, 605-610.

Wang, H., Dlugogorski, B.Z. AND Kennedy, E. M., "Coal oxidation at low temperatures: oxygen consumption, oxidation products, reaction mechanism and kinetic modelling"; Progress in Energy and Combustion Science 29 (2003) 487-513.

Wang, H., Dlugogorski, B.Z. AND Kennedy, E. M., "The decomposition of solid oxygenated complexes formed by coal oxidation at low temperatures"; Fuel 81 (2002) 1913-1923.

Vanyukov, A. V., and Razumovskaya, N.N., "Hydrothermal oxidation of pyrrhotites"; Izv. Vyssh. Uchelon. Zaved., Tsvetn. Metall. 6, 605-610.

Wells, P.F., Kelebek, S., Burrow, M.J., and Suarez, D.F., "Pyrrhotite rejection at Falconbridge's Strathcona Mill"; CIM, 36th Annual Conference, pp. 51-62, 1997.

Wu, C, and Li, Z., "A simple method for predicting the spontaneous combustion potential of sulphide ores at ambient temperature"; Mining Technology (Trans. Inst. Min. Metal. A) June 2005 Vol. 114, A125-A128.

Wunderly, M.D., Blowes, D.W., Frind, E.O., and Ptacek, C.J., "Sulfide mineral oxidation and subsequent reactive transport of oxidation products in mine tailings impoundments: a numerical model"; Water Resources Research, Vol. 32, No. 10, pp. 3173-3187, October 1996.

Yao, W., and Millero, J.F., "Oxidation of hydrogen sulfide by hydrous Fe(III) oxides in seawater"; Marine Chemistry 52 (1996) 1-16.

Appendix
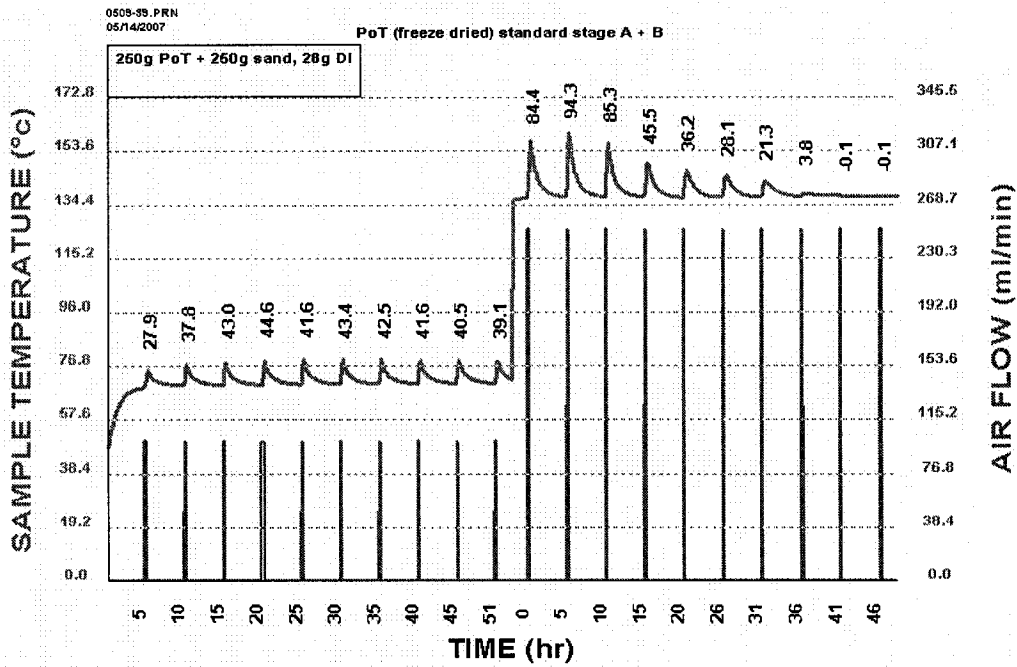
Figure A1- 1 Standard self-heating response of freeze dried PoT
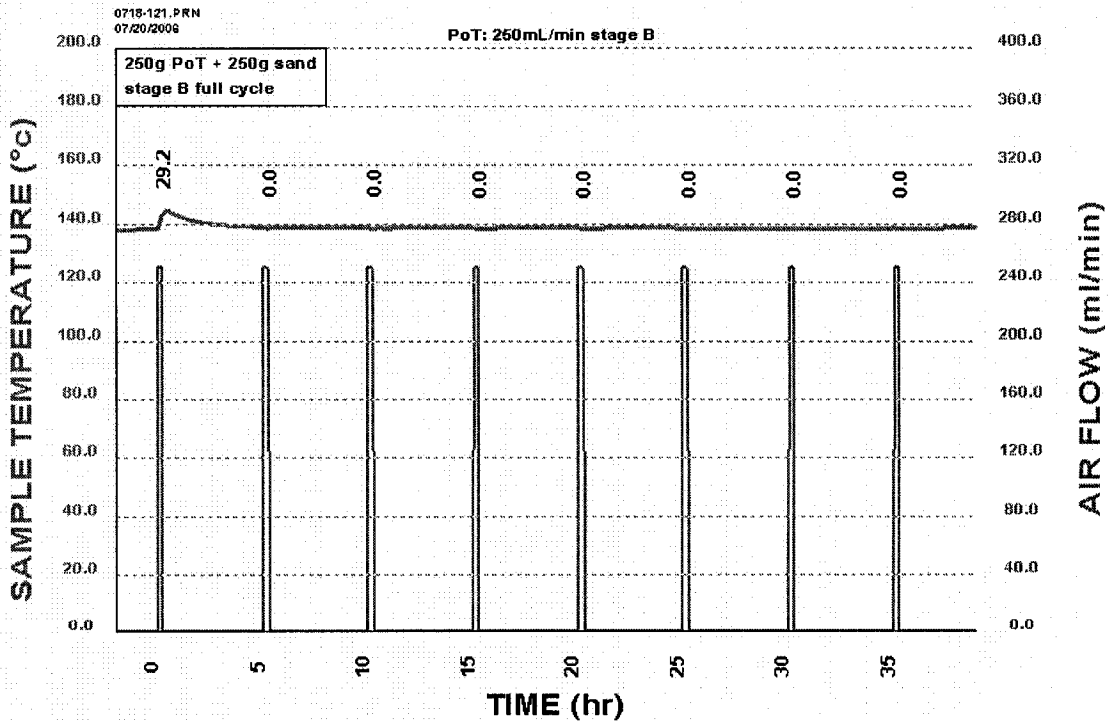
Figure A1- 2 Direct stage B self-heating response of PoT
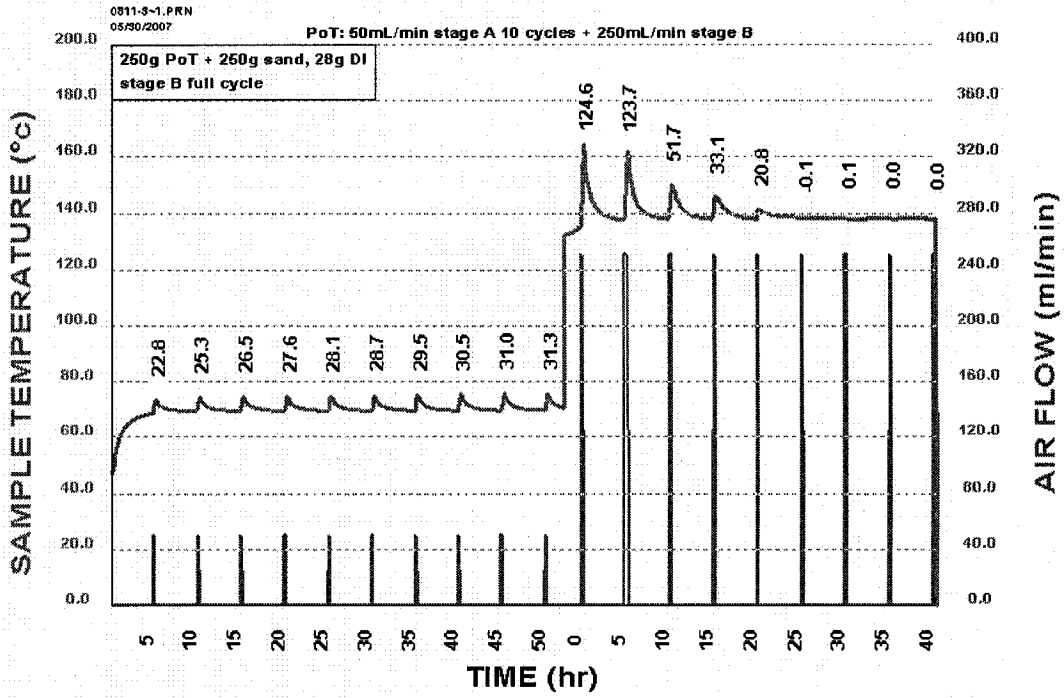
Figure A1- 3 PoT with AFR of stage A 50mL/min (ten cycles of A, full cycle of B)
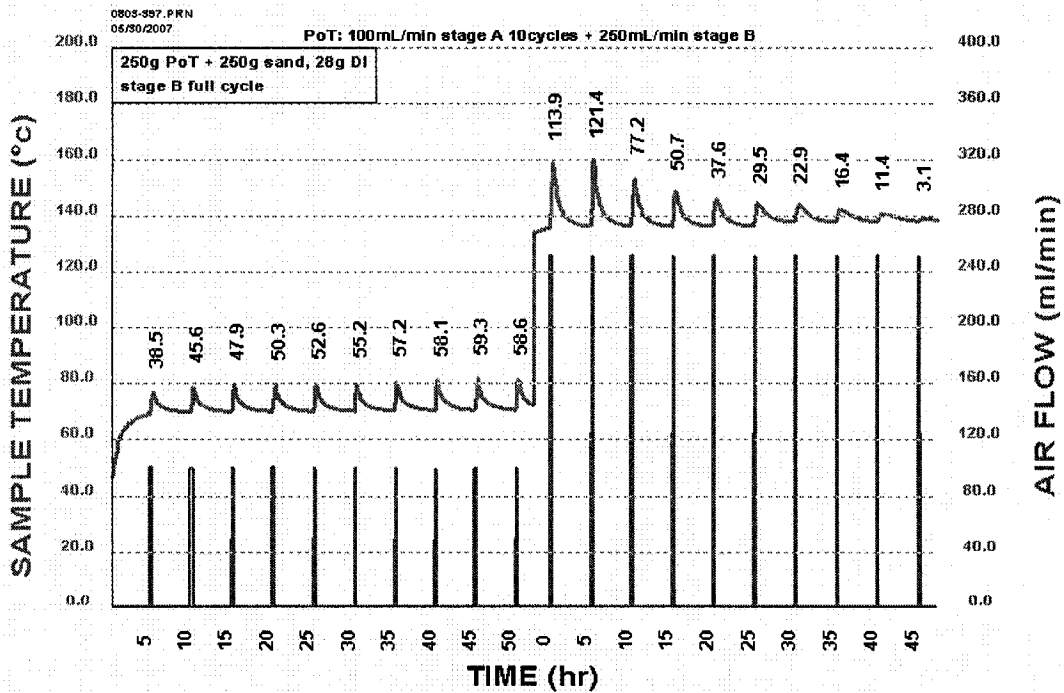
Figure A1- 4 PoT with AFR of stage A 100mL/min (ten cycles of A, full cycle of B)
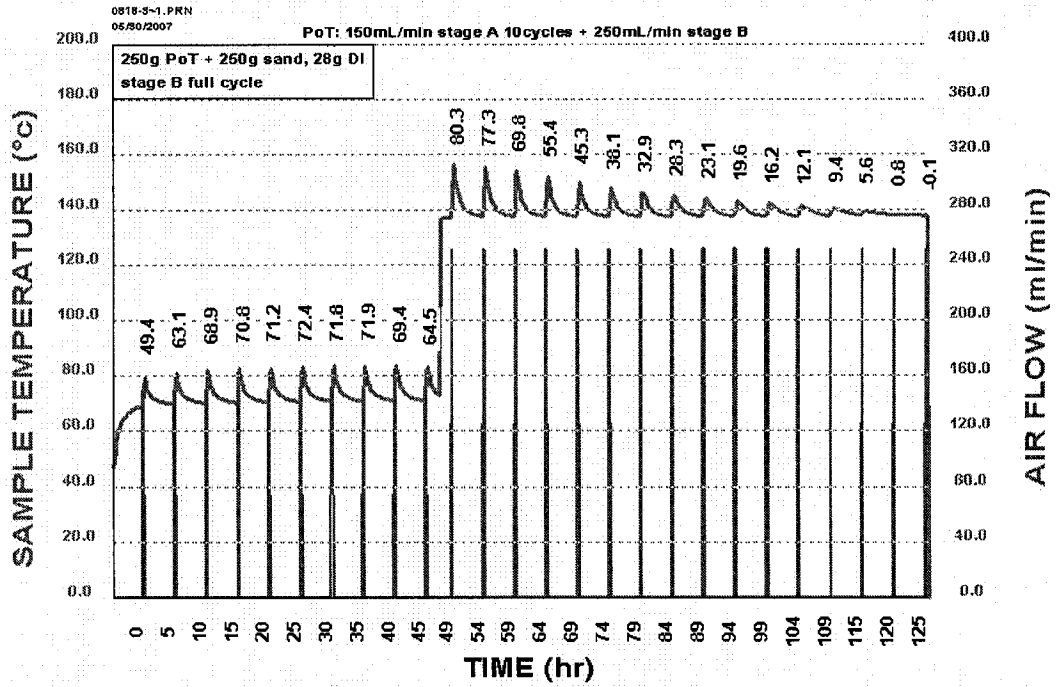
Figure A1- 5 PoT with AFR of stage A 150mL/min (ten cycles of A, full cycle of B)
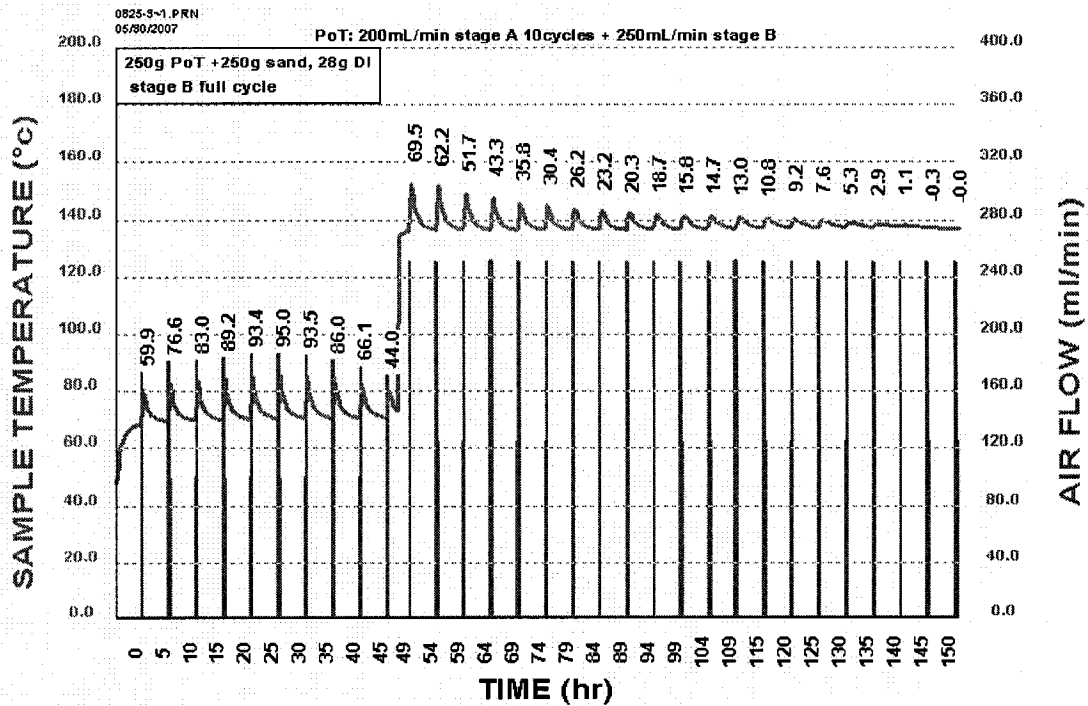
Figure A1- 6 PoT with AFR of stage A 200mL/min (ten cycles of A, full cycle of B)

94
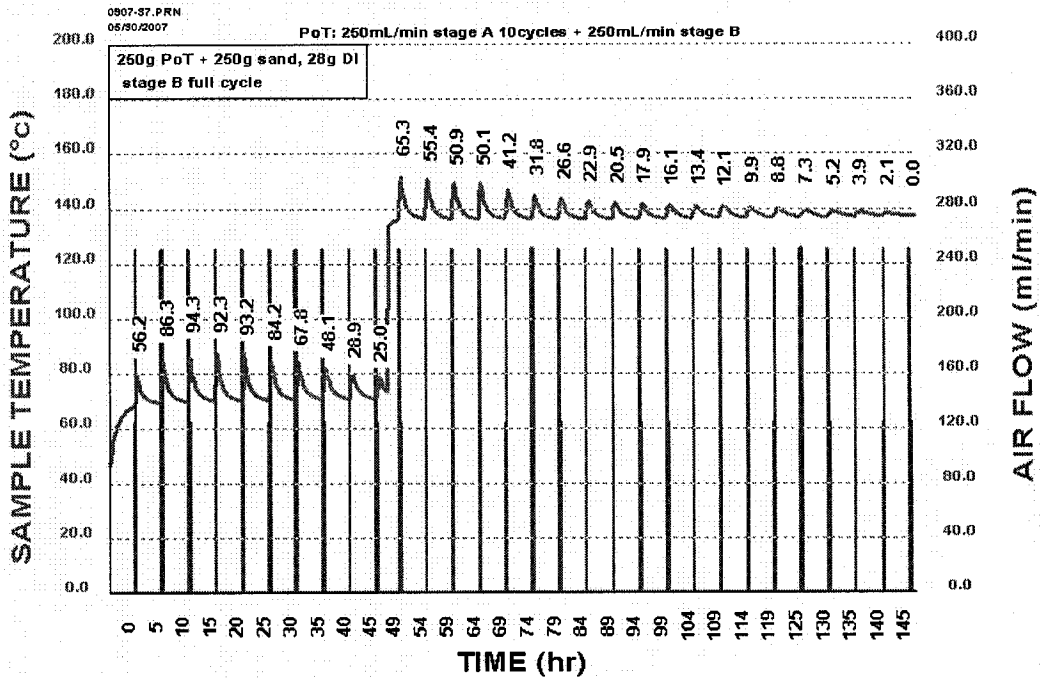
Figure A1- 7 PoT with AFR of stage A 250mL/min (ten cycles of A, full cycle of B)
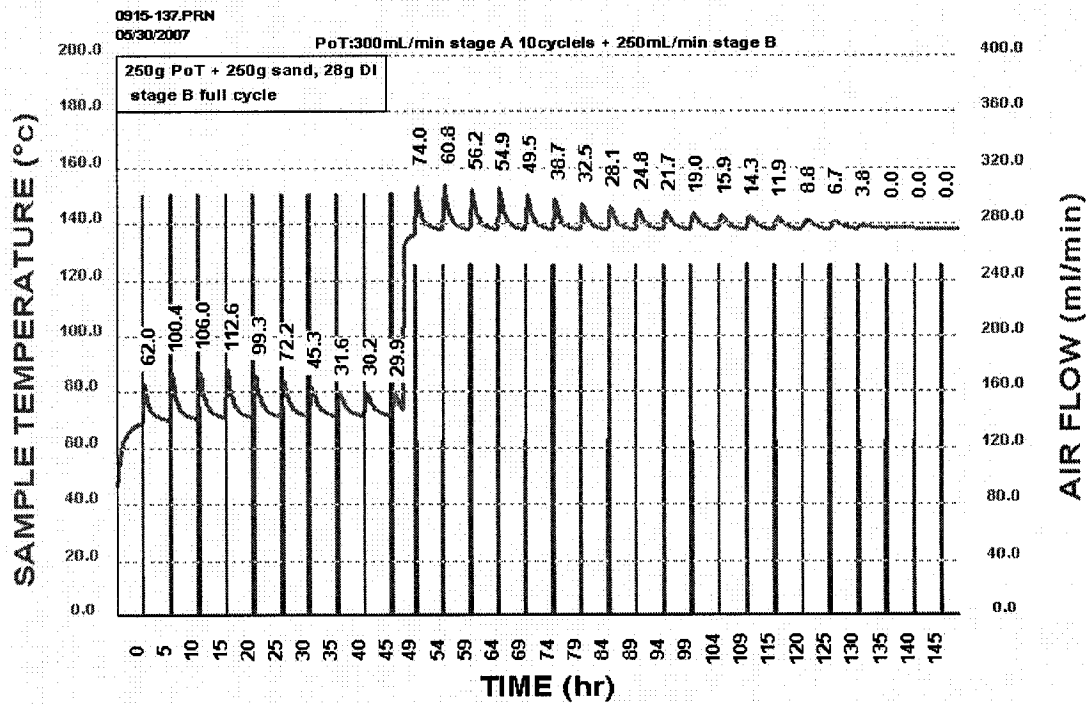
Figure A1- 8 PoT with AFR of stage A 300mL/min (ten cycles of A, full cycle of B)

95
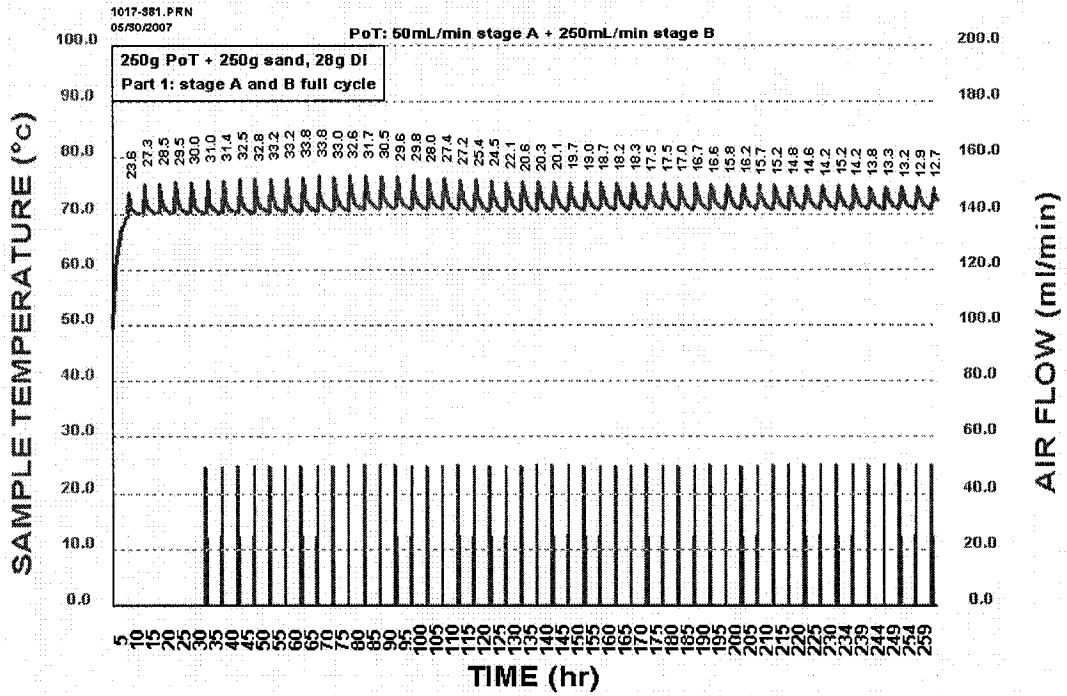
Figure A1- 9 PoT with AFR of stage A 50mL/min (full cycle of A and B) part 1
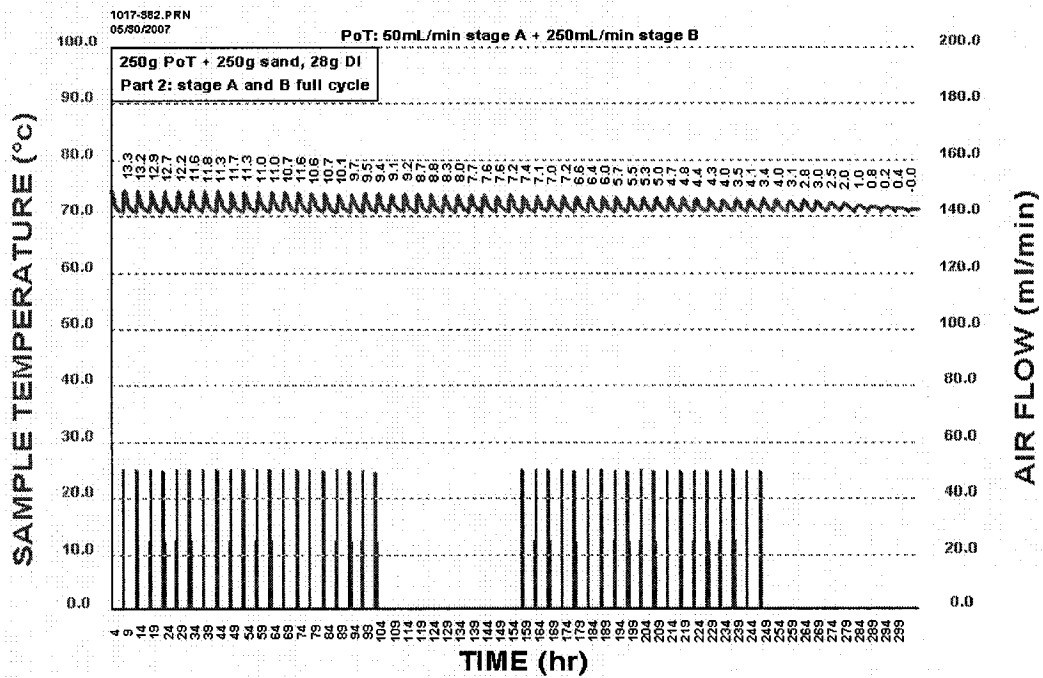
Figure A1- 10 PoT with AFR of stage A 50mL/min (full cycle of A and B) part 2
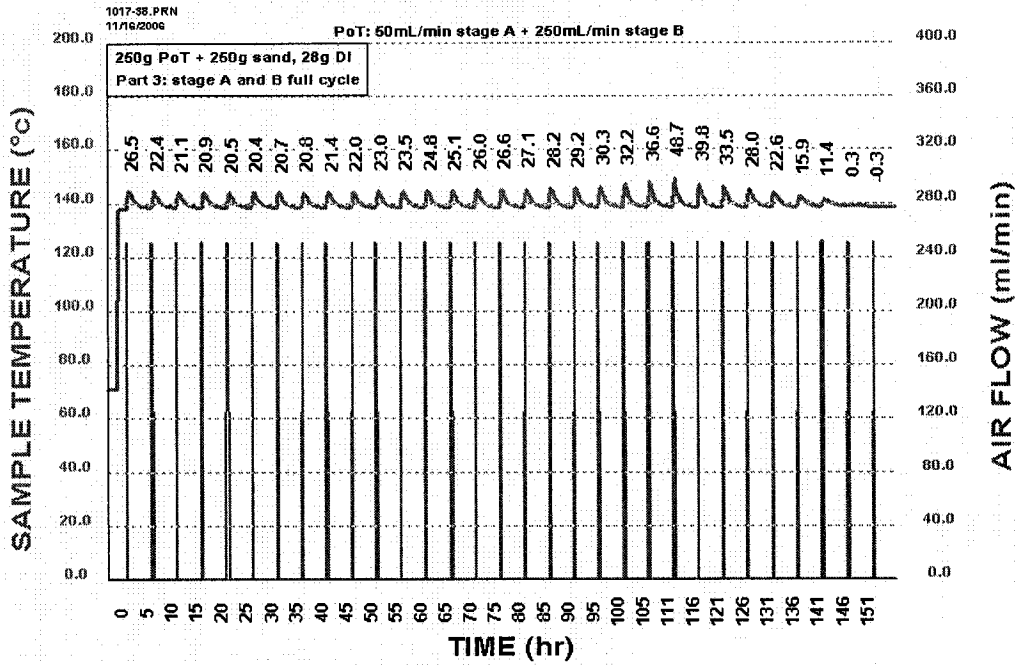
Figure A1- 11 PoT with AFR of stage A 50mL/min (full cycle of A and B) part 3
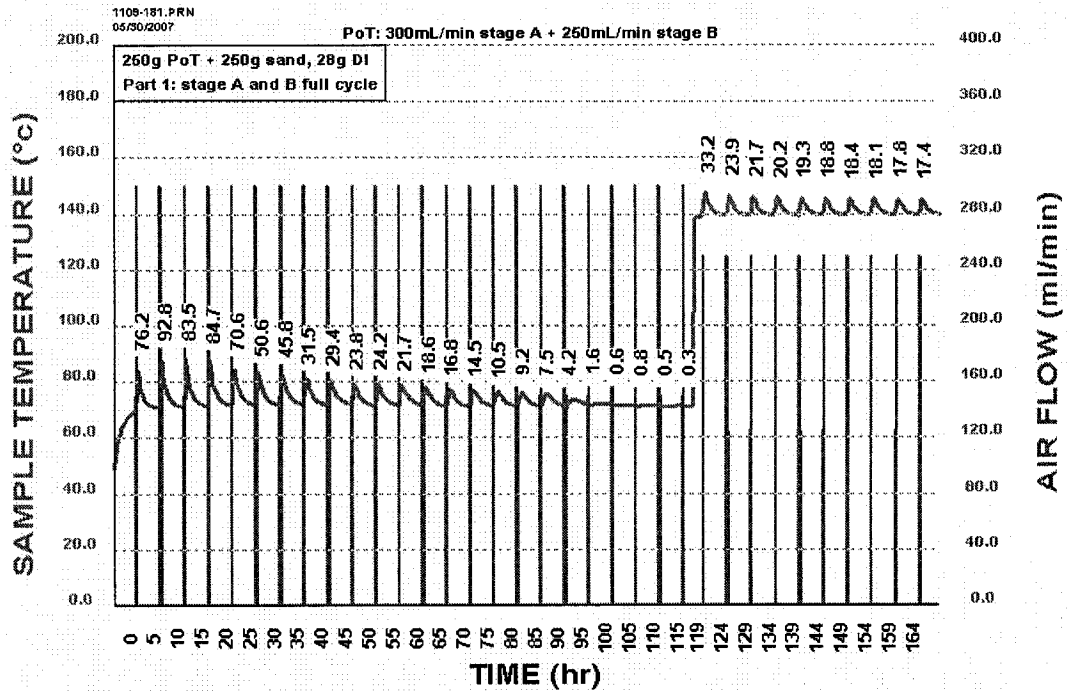
Figure A1- 12 PoT with AFR of stage A 300mL/min (full cycle of A and B) part 1

PoT: 300mL/min stage A + 250mL/min stage B

200.0

250g PoT + 250g sand, 28g DI
Part 2: stage A and B full cycle

180.0

160.0 18.8 18.4 18.1 17.8 17.4 17.0 16.7 16.2 16.4 15.7 15.4 14.8 14.9 14.1 13.7 12.9 12.7 11.8 11.3 10.0 9.2 7.7 9.3 6.0 4.0 1.6 0.2 0.1 -0.1 0.0 -0.1 -0.1 -0.0 0.0 -0.2

SAMPLE TEMPERATURE (°C)

AIR FLOW (ml/min)

TIME (hr)
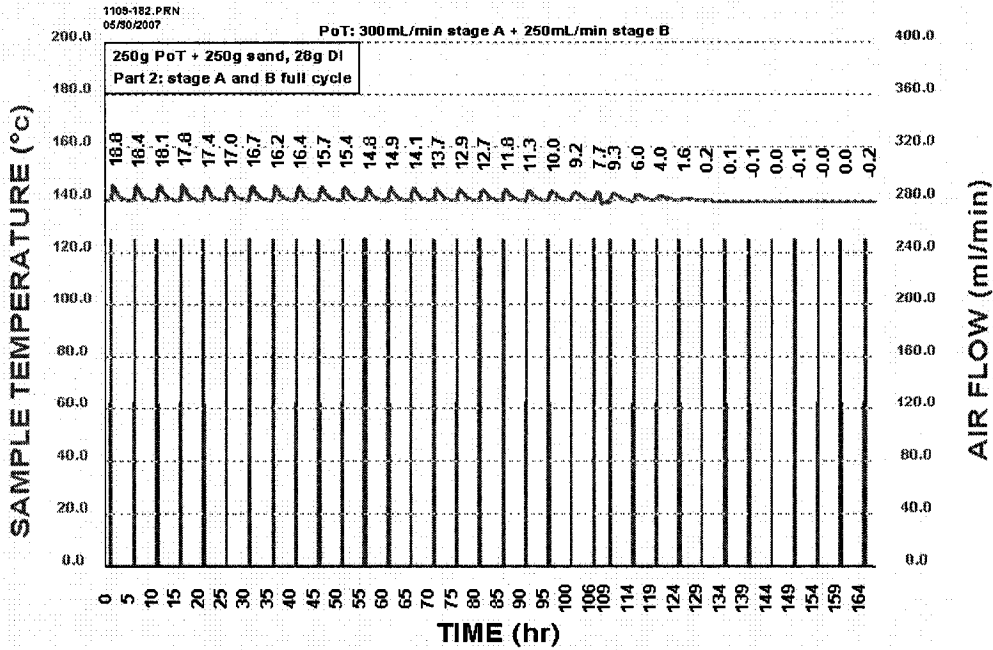
Figure A1- 13 PoT with AFR of stage A 300mL/min (full cycle of A and B) part 2

250 mL/min stage B: no hole "weathering" apparatus product

200.0

250g products + 250g sand
stage B full cycle

180.0

160.0 35.5 25.3 22.8 21.8 20.5 20.1 19.3 19.1 18.7 18.6 18.5 18.2 17.8 17.8 17.8 17.3 17.1 16.9 16.9 16.4 16.2 16.0 15.7 15.5 15.2 14.5 14.2 13.7 13.3 12.7 12.2 11.7 10.9 10.4 9.7 9.2 8.5 7.4 5.8 4.1 1.0 -0.1 -0.2 -0.1

SAMPLE TEMPERATURE (°C)

AIR FLOW (ml/min)

TIME (hr)
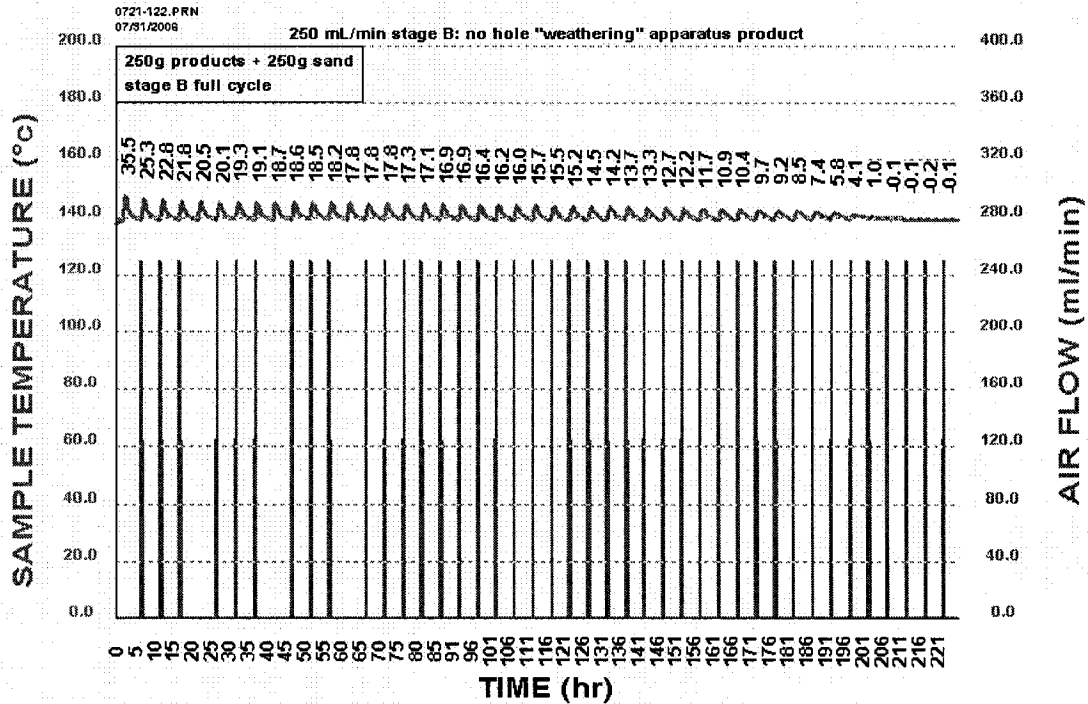
Figure A1- 14 Stage B self-heating response of PoT in no hole weathering apparatus
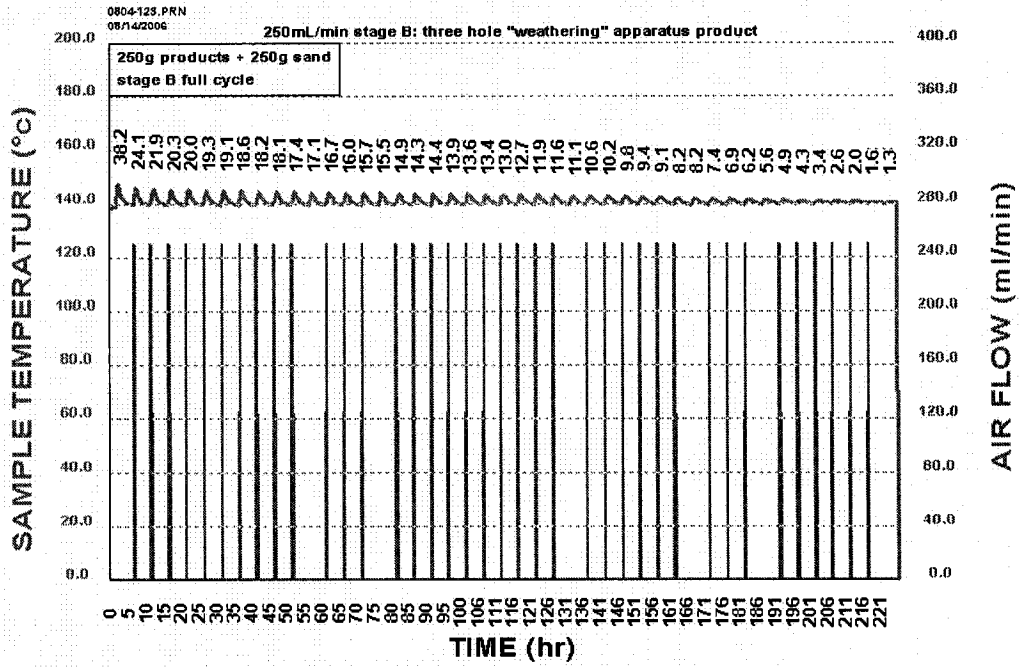
Figure A1- 15 Stage B self-heating response of PoT in three hole weathering apparatus
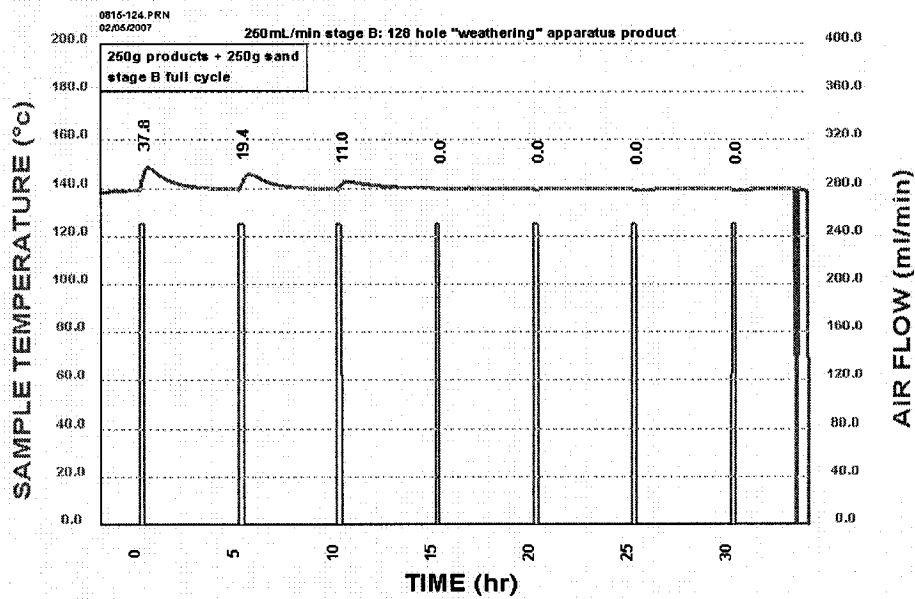
Figure A1- 16 Stage B self-heating response of PoT in 128 hole weathering apparatus

Table A2- 1 Weight gain test in weathering apparatus

Days	Weight gain (g)			Weight gain (%)		
	no hole	3 hole	128 holes	no hole	3 hole	128 holes
0	0	0	0	0	0	0
1	3.2	2.7	1	0.64	0.54	0.2
3	8.4	10.3	1.3	1.68	2.06	0.26
6	17.8	33.7	1.6	3.56	6.74	0.32
8	24.4	46.1	2.1	4.88	9.22	0.42
10	30.7	57.4	2.4	6.14	11.48	0.48
13	39.2	72.2	2.9	7.84	14.44	0.58
15	45.2	80.8	4.6	9.04	16.16	0.92
17	50.9	87.9	5.3	10.18	17.58	1.06
20	59.2	95.0	7.2	11.84	19	1.44
22	64.7	101.7	7.9	12.94	20.34	1.58
24	74.1	106.3	9.8	14.82	21.26	1.96
27	76.6	112.2	10.8	15.32	22.44	2.16

INTERIM REPORT ON THE RESEARCHES IN

SPONTANEOUS HEATING OF METAL

SULFIDE CONCENTRATES (II)

- 1976 -

INDEX

Introduction

I. Measurement of oxygen consumption

II. Storing test with a constant temperature and humidity chamber

III. Practical survey on transportation of Bougainville copper concentrate by the carrying vessel

Introduction

Conforming to the conclusion made at the 25th session of Sub-Committee on CDG, the further fundamental studies about the measurement of spontaneous heating of metal sulfide concentrates have been carried out, in Japan, with the view of establishing the practicable standard method to classify the hazard situation of sulfide concentrates.

The test by storing in laboratory chamber and the practical survey on sea transportation of Bougainville copper concentrate, which is liable to spontaneous heating, by the experts who boarded on the carrying vessel have been also progressed.

The results obtained from the above comprehensive investigation are compiled in this report.

For easy reference, the conclusions are presented firstly summerizing as following.

Conclusion:

(1) The procedure of the measurement and the analytical method of the data are covered, in which some of the results relating to the effect of moisture content, temperature and species of concentrates on the rate of oxygen consumption were explained in detail. For identifying of the reactivity of concentrates it is concluded as the superior method to calculate the rate constant of oxygen consumption per unit weight of concentrates from the experimental results.

This method will be available as a surpassing information when deciding the international standard method for identifying the hazard ranking of sulfide concentrates.

(2) It was re-confirmed that trimming and providing compaction to the stow surface after loading, effective covering by plastic sheets and no serving of ventilation to the holds during transportation could prevent the spontaneous heating adequately.

(3) The temperature of the concentrate during transportation rised locally in the case when performed in such a tentative method as no trimming thereon after loading and a substantical variation in temperature of the concentrate was also recorded as a result measured at the location in the hold.

The layer, where a high temperature was observed, positioned down to a certain depth from the stow surface, indicating the maximum temperature.

(4)* A formation of both water and acid soluble components was evidently
recognized at the very portion whereof a substantial rise in temperature
of the concentrate was observed.

I.   Measurement of oxygen consumption

1.   Apparatus

The schematic arrangement of measuring apparatus and the reaction vessel
are shown in Fig. 1.1 and 1.2. The sample of concentrates is put in the
reaction vessel (1) and the air in the closed system in the apparatus
are circulated over the surface of the sample in the reaction vessel at
a constant rate by the roller pump (6) and an oxygen pressure is measured
continuously by the oxygen meter (8). The pressure in the closed system
is kept constant at an atmospheric pressure for obtaining the rate
constant easily from the oxygen pressure. Platinum contact just upon
the mercury manometer (10) closes the circuit of relay (12) immediately
when the pressure in closed system is just below the atmospheric pressure
and the motor (14) lifts the water column (4) automatically, so the
pressure in the closed system is equal to the atmospheric pressure.
Copper pipe coil (5) acts as preheating air introduced in the reaction
vessel. The flow of air circulated by the roller pump becomes a pulsed
stream, so the motor (14) moves intermittently according to this pulsated
movement of the level of the mercury manometer (10), so it is difficult
to keep the pressure in the closed system constant. A capillary tube
(18) is used to prevent this pulsed stream of air. Water trap (7)
returns water, which is evapolated, to the sample. Accuracy of the
oxygen meter (8) is checked by chromatography during experiments.
About one cm^3 of gas is taken from the outlet for gas sampling (9) for
this check of the oxygen meter.

Oxygen consumption can be calculated from the data of oxygen concent-
ration, and the rate constant of the reaction for oxygen consumption is
obtained.

Instead of measurement of oxygen concentration, a volume change of gas
in the closed system may be measured in the same apparatus. The oxygen
meter and the outlet for gas sampling are not necessary in this case.

Leakage of gas in and from the apparatus diminishes the accurary of the results, so no existance of leakage must be confirmed before experiments The procedure of the measurement is explained in the following section.

2. Measurement of volume, mole amounts and an apparent temperature of air in the closed system

A volume, mole amounts and an apparent temperature of air in the closed system are necessary to calculate the rate constant for the oxygen consumption. These values must be measured before the measurement of the change of the oxygen pressure.

2.1 300g of a standard sample (true specific gravity ρ_s, moisture content w_s %) is packed in the reaction vessel under the constant weight.

2.2 Air in the whole system of the measurement is replaced to inert gas such as nitrogen or argon, and the reaction vessel is heated up to the reaction temperature, T, in a thermostatic vessel.

2.3 The level of the surface of water in the pressure regulator (3) is set to A of the scale attached to the pressure regulator by lifting the water column (4). The excess of inert gas in the measuring system is taken off from the stopcock (17). The pressure in the closed system is kept to an atmospheric pressure, and the volume V_t in the closed system at the level A of the pressure regulator is obtained by the following procedure.

2.4 The temperature of the measuring system is lowered to a room temperature T_R. The pressure in the closed system becomes lower than the atmospheric pressure.

2.5 By lifting the water column (4), the pressure in the closed system is maintained to the atmospheric pressure and the level of the surface of water in the pressure regulator goes to B as shown in Fig. 1-3. The volume, V_1, in the closed system in this case is

$$V_1 = V_t - S|A - B| \text{ cm}^3$$

where S is the area of the cross section of the pressure regulator, cm^2

(here, the diameter of the cross section is 2.8 cm, so S is 6.16 cm^2)

2.6 At a room temperature, the water column (4) is lowered and the difference between levels of water surfaces of the pressure regulator and the water column, that is, the pressure in the closed system is measured. The volume V_2 in the closed system is

$$V_2 = V_t + S|C - A| \, cm^3$$

These relations are shown in Fig. 1.3.

2.7 V_t is calculated from $P_1V_1 = P_2V_2$

2.8   Mole amounts of air, n, in this closed system can be calculated from the following relation.

$$P_1\{V_t - S|A - B|\} = nRT_R$$

where, $P_1 = 1030$ cm H_2O

R : gas constant, 821×10^2 cm $H_2O \cdot cm^3/K \cdot mole$

2.9   In the term 2.2, the sample is heated to T, but the temperature of air in the closed system is not T, because some parts of air in the closed system is kept at a room temperature. The average temperature T' of air in the system can be obtained from $P_1V_t = nRT'$, where $P_1 = 1030$ cm H_2O, R is gas constant, V_t and n are obtained in 2.7 and 2.8.

2.10   The volume V_{vt}, where a sample is not packed in the measuring system and the level of water surface in the pressure regulator is A, is

$$V_{vt} = V_t + \left\{ \frac{300 - 300 \times \frac{ws}{100}}{\rho s} + 300 \cdot \frac{ws}{100} \right\}$$

Notes:

(1) Nearly the same condition as the actual measurement for oxygen consumption is applied to the procedure for obtaining the mole fraction n, volume V_t and average temperature T'.

(2) The values of V_t and n, which are obtained by procedures 2.5, 2.6, and 2.7 at the reaction temperature T, are not accurate, because the mole amounts of air in the part of the closed system, which is kept at the reaction temperature, are different at each condition of the pressure and the volume in the closed system, so the average temperatures of air at each condition are not equal and the formula, $P_1V_1 = P_2V_2$, is not valid.

(3) Instead of this procedure, the other one can be applied to the measurement of the mole amounts of air, n, and the volume, V_t. The mole amounts of air, n, is obtained at the room temperature at first, then the air is heated to the reaction temperature T and the volume V_t at the mark A of the level of the water surface of the pressure regulator is measured. This

level A in the pressure regulator must be used for the actual measurement of oxygen consumption.

3. Measuring procedure of oxygen consumption

3.1 300g of the concentrate (true specific gravity ρ, moisture content w %), which is measured, is compacted in a reaction vessel under the constant weight.

3.2 The stopcock over the reaction vessel as shown in Fig. 1.4 is connected to a vacuum system and the air in the vessel is pomped off during about 30 second. Then the stopcock is closed and the reaction vessel is inserted in the thermostatic vessel and is kept during about 30 minutes. The temperature of the sample in the reaction vessel becomes equal to the reaction temperature.

3.3 Then the glass cap over the reaction vessel is taken off and the reaction vessel is connected to the measuring system and the stopcocks (15), (16), and (17) is opened and air is blowed into the measuring system by the outer pump through the stopcock (17). The water column is moved to adjust the level of the water surface of the pressure regulator to the mark A, which is determined in the item 2.3. The roller pump is moved in this procedure. Before starting the experiment, the concentration of oxygen in this closed system is kept at 20.5 % carefully.

3.4 The stopcocks (15) and (17) are closed and the oxygen concentration is measured by oxygen meter continuously and automatically.

3.5 1 cm^3 of the sample gas is taken off from the closed vessel by the outlet of gas sampler just after starting the experiment, and after 4 and 20 hours, and the gas is analysed by gas chromatography. This procedure is done to check the accuracy of the oxygen meter.

3.6 The measurement is stopped after 24 hours and the reaction vessel is taken out from the thermostatic vessel and the moisture content and chemical composition are measured if necessary.

4. Calculation of the rate constant

4.1 The initial mole amounts of air, n_i

The initial mole amounts of air in the measuring system with the sample (true specific gravity ρ, moisture content w %) before the experiment can be calculated by the following formula;

$$n_i = n + \frac{P \ (V_i - V_t)}{}$$

where P; one atmosphere, 1030 cm H_2O

R; gas constant, 821×10^2 cm $H_2O.cm^3/K.mole$

T; average temperature of air in the closed system, K, measured in the item 2.9.

V_i; the initial volume in the measuring system at the mark A of the pressure regulator

$$V_i = V_{vt} - \frac{300 - 300 \times \frac{w}{100}}{\rho} + 300 \times \frac{w}{100}$$

The mole amounts of oxygen, a, in the measuring system is

$$a = 0.205 \times n_i$$

4.2 Calculation of mole amounts, x, which is consumed, from the data of the oxygen pressure PO_2

From the formula, $PO_2 = \frac{a - x}{n_i - x} P$

$$x = \frac{n_i (0.205 - PO_2)}{1 - PO_2} \text{, where P is one atmosphere}$$

4.3 Reaction rate equation

The mole amounts of oxygen, which are consumed by concentrates per unit time, are proportional to the oxygen pressure[1],

$$\frac{dx}{dt} = m \cdot PO_2$$

and $PO_2 = \frac{a - x}{n_i - x} P$, where P is total pressure in the closed system and is one atm.

So, $\frac{dx}{dt} = m \frac{a - x}{n_i - x}$

By integrating this formula, the next equation can be formed,

$$(n_i - a) \cdot \ln (a-x) + (a-x) = -mt + c \dots \dots \dots \dots (1)$$

The left side term of the equation, $(n_i-a) \cdot \ln (a-x) + (a-x)$, is plotted against time and the inclination of this plotted line is the rate constant m.

4.4 The example of the experiment

Specie of the concentrate	Musoshi copper concentrate
true specific weight ρ	3.49
moisture content w %	8.70
measuring temperature °C	60

1) Hayase, Mariko; Journal of the Mining and Metallurgical Institute of Japan, V.73, No.825, P141 (1957)

rate of gas circulation cm^3/min.   110

initial volume of air V_i cm^3 1267

initial amounts of mole n_i 5.24×10^{-2}

The plots for obtaining the rate constant m are shown in Fig. 1.6.

The inclination of this line, m, is $1.53 \cdot 10^{-2}$.

5. Effect of temperature on the rate constant

The results are shown in Fig. 1.5 and 1.6 in the case of Musoshi copper
concentrate with 8.70 % moisture. The rate constant, m, is shown in
the next table. The rate constant becomes about two times when the
temperature raises 10 degree.

The effect of temperature on the rate constant m

Temp. C	Rate constant m/hr	$1/T$ (K^{-1})	m_{100}/hr 100 g
30	$2.20 \cdot 10^{-3}$	$3.30 \cdot 10^{-3}$	$7.33 \cdot 10^{-4}$
40	$3.80 \cdot 10^{-3}$	$3.19 \cdot 10^{-3}$	$1.27 \cdot 10^{-3}$
60	$1.53 \cdot 10^{-2}$	$3.00 \cdot 10^{-3}$	$5.10 \cdot 10^{-3}$

By Arrhenius plot of log m and reverse temperature, $1/T$, as shown in
Fig. 1.7, the linear relation can be obtained, that is, the next
formula is obtained;

$$\frac{d\,(\ln m)}{d\,T} = \frac{E}{R\,T^2}$$

From this relation, activation energy E is 12.9 Kcal/mole.
As shown in Fig. 1.6, the linear relation of the equation(1) for
obtaining m is not valid after a long run of the experiment at higher
temperature. At a relative high temperature, it is considered that the
moisture content of the concentrate changes during the experiment and
the rate constant m changes depending on the moisture.

5. Effect of moisture content on the rate constant

The effect of moisture content in concentrates on the oxygen consumption
is shown in Fig. 1.8. The samples are Musoshi concentrate and the
temperature is 60°C. The rate constant, calculated from this experi-
ment, is shown in the next table.

The effect of moisture content on the rate constant

moisture content w %	rate constant m	m_{100}/hr.100 g
0.37	$1.20 \cdot 10^{-3}$	$4.00 \cdot 10^{-4}$
3.70	$1.05 \cdot 10^{-2}$	$3.50 \cdot 10^{-3}$
8.70 —	$1.53 \cdot 10^{-2}$	$5.10 \cdot 10^{-3}$
15.8	$8.30 \cdot 10^{-3}$	$2.77 \cdot 10^{-3}$

The value of the rate constant is minimum at a bone dry state and it increases with moisture content and reaches at the maximum value between 3.70 and 8.70 % of moisture content, then it decreases again with more moisture content.

·7. Effect of species of concentrates

The various kinds of copper concentrates are examined and the experimental results are shown in Fig. 1.9. The rate constant m, calculated from these data, is shown in the next table.

Effects of species on the rate constant m

species	moisture %	rate constant m	m_{100}/hr 100 g
Musoshi	8.70	$1.53 \cdot 10^{-2}$	$5.10 \cdot 10^{-3}$
Gibraltar	6.34	$1.05 \cdot 10^{-2}$	$3.50 \cdot 10^{-3}$
Kenon	8.92	$3.85 \cdot 10^{-3}$	$1.28 \cdot 10^{-3}$
Lornex	6.04	$4.70 \cdot 10^{-3}$	$1.57 \cdot 10^{-3}$
Bougainville	5.70	$1.48 \cdot 10^{-2}$	$4.93 \cdot 10^{-3}$
Hitachi	10.58	$2.50 \cdot 10^{-4}$	$8.33 \cdot 10^{-4}$
Shimokawa	8.97	$6.20 \cdot 10^{-3}$	$2.07 \cdot 10^{-3}$

The moisture, listed in this table, is the value contained in concentrates, which were taken from the center part of the pile in ship holds for transportation.

Properties such as specific weight, size distribution, chemical and modal compositions are listed in the following tables.

Species	Specific weight
Musoshi	3.49
Gibraltar	4.13
Kenon	3.85
Lornex	4.01
Bougainville	3.83
Hitachi	3.92
Shimokawa	4.12

Size Distribution %

Mesh	Musoshi	Gibraltar	Kenon	Lornex	Bougainville	Hitachi	Shimok.
+48	0.71	2.47	0.11	0.27	0.39	1.06	4.5(
65	2.82	3.98	0.32	1.86	1.00	1.77	4.2;
100	4.06	6.84	2.93	7.39	2.52	2.81	5.1(
150	8.41	10.21	7.82	15.11	4.39	4.63	6.0!
200	16.38	12.58	12.63	16.43	8.25	12.07	7.1;
270	15.15	14.63	12.31	17.83	10.75	27.30	15.6(
-270	52.46	49.27	63.88	41.10	72.71	50.36	57.24

Chemical analysis of concentrates

Species	Cu	Fe	S	Pb	Zn	CaO	SiO_2 %
Musoshi	38.3	5.28	13.1	0.02	0.01	0.06	26.4
Gibraltar	25.8	29.6	34.7	-	0.04	-	-
Kenon	24.8	27.7	31.9	0.02	0.13	-	-
Lornex	32.6	22.7	28.1	0.03	0.17	-	-
Bougainville	28.55	28.48	28.73	0.04	0.19	0.47	6.04
Hitachi	24.67	28.47	26.0	0.11	4.68	0.14	1.42
Shimokawa	20.16	33.51	36.34	0.02	4.40	0.09	1.23

Modal Analysis

Musoshi		Bougainville	Gibraltar	Shimokawa	Lornex	Kenon	Hitachi
Cp	19.0	72.6	63.7	64.3	66.9	60.5	83.4
Bn	16.1	2.5	0.9	-	15.3	1.3	-
Cv	2.3	0.6	2.1	-	2.5	1.6	-
Cc	23.0	0.3	0.1	-	0.8	-	-
Cr	0.1	-	-	-	-	-	-
En	-	< 0.1	0.2	-	0.8	-	-
Tn	-	< 0.1	-	-	-	-	-
Mo	-	0.3	0.2	-	0.2	1.8	-
Sp	-	0.1	0.1	3.8	0.5	0.3	2.5
Py	0.1	7.5	17.9	25.1	4.7	13.4	5.4
Po	-	-	-	4.1	-	-	2.2
Hm	-	< 0.1	-	-	-	-	-
?	0.5	-	-	-	-	-	-
G	38.9	16.1	14.8	2.7	8.3	21.1	6.5

Cp: chalcopyrite   Bn: bornite   Cv: covellite

Cc: chalcocite   Cr: cuprite   En: enargite

Tn: tennantite   Mo: molybdenite   Sp: sphalerite

Py: pyrite   Po: pyrrhotite   Hm: hematite

? : umknown mineral   G : gangue mineral

8. Method for measuring volume change

Instead of measuring of oxygen concentration, explained in the term 3, the volume change of gas in the closed system may be measured in the same apparatus. Mole amounts of oxygen can be calculated from the data of the volume change.

8.1 The preparation before measurement

The preparation for the measurement of the volume change is the same as 3.1 to 3.4.

8.2 The measurement of the volume change

The level of the water surface in the pressure regulator is read by a scale attached outside the regulator at the constant interval during the experiment. The devise which is used for measuring the change of the volume automatically is now being prepared.

8.3 Calculation of mole amounts of oxygen, consumed.

The volume change of gas in the closed system ΔV is

$$\Delta V = S \mid A - B \mid$$

where, S; area of the cross section of the pressure regulator, cm^2

A; position of the level of the water surface in the pressure regulator before the experiment

B; position of the level after the constant interval

The mole amounts of oxygen, which are consumed in the closed system, can be obtained by the following formula.

$$x = \frac{P \cdot \Delta V}{R T'}$$

where, P; atmospheric pressure, 1030 cm H_2O

R; gas constant

T'; the average temperature of air in the closed system, obtained in term 2.9

II. Storing test with a constant temperature and humidity chamber

1. Experimental apparatus and method

In this test, the concentrate pile is stored in the constant temperature and humidity chamber, in which the atmosphere corresponding to that of vessels holds is reproduced artificially, and the occurence of heat in the pile is observed.

This chamber is one of the apparatus prepared for environmental test

in Japan and used normally, for instance, for the life or durability test of various materials and electric appliances in severe atmosphere. As shown in Fig. 2.1, it is 1,970mm long, 1,970mm wide and 2,100mm high in inner dimentions, and has following capability;

Control range; Temperature   -10 - +60°C

Humidity   30 - 95% (at 20 - 60°C)

Accuracy   ; Temperature   ±0.5°C

Humidity   ±3.0%

Temperature difference in chamber; ±1.0°C

A steel container of 1,500mm in diameter and 1,000mm in hight that contains approx. 2,500Kg sulphide concentrate is placed in this chamber, which is controlled at the desired constant temperature and the humidity for long time. Ten thermo-couples are inserted into the pile at selected positions and depth, and the temperature change of sulphide concentrate is recorded automatically. We have a program of investigating on the factor such as species of concentrate, temperature, humidity and bulk density which affect on the oxidation and spontaneous heating, and of researching on the influence of plastic sheeting, sealing method, etc. for protecting the cargo from oxidation.

2.   Results

Results obtained from the first test are as follows:

Sample   ; Gibraltar copper concentrate of Canada (Moisture content ⸗ 8.21%) (T.M.L. 10.6%)

Temperature; 40°C

Humidity   ; above 80%

2.1   As shown in Fig. 2.2 the concentrate temperature at the center part rised slowly from 40°C to near by 50°C, but since then the rising rate increased slightly, and on the 13th day it reached to 70°C, then dropped down slowly.

2.2   On that day, the ore temperature was the highest at depth of 10 - 15cm in vertical direction, and dropped lower with depth as shown in Fig.2.3. The distribution curve of ore temperature in horizontal direction at depth of 15cm was as shown in Fig. 2.4, and the temperature difference in the center part (about 50cm in diameter) was less than 1°C.

2.3   Results of analyses of ore samples taken from the pile are shown in Fig. 2.5 and Fig. 2.6. The compositions of water and acid soluble species increased and the moisture content decreased remarkably when

the ore temperature was high. It was confirmed that the concentrate at the depth of 5 - 15cm was more oxidized than that at the surface layer.

III. Practical survey on transportation of Bougainville copper concentrate by the carrying vessel.

This survey has been carried out by the expert who boarded on the carrying vessels, having laden with the cargo of Bougainville copper concentrate, in the sea way bound for Japan from the loading part.

The followings are covered within this survey in order to investigate reactive behavior of the cargo during transportion.

(1) Continuous measurement of the cargo; temperature at the depth of 23cm in concentrate, ambient temperature and humidity in the holds, and oxygen concentration in the compartments during transportation.

(2) Performance of further measurement, on arrival at the discharging port, about all the holds on board the cargo.

(3) Confirming the practical effects owing to varying such the designed stowage terms as trimming and ventilation and covering by plastic sheets, to each hold, and further considering these effects.

1. Condition of stowage and transportation

1.1 The subject cargo

Bougainville copper concentrate (T.M.L. 11.2%)

1.2 The name of the carrying vessel

M/V" Bougainville Maru (Nationality; Japan), concentrates carrier having four holds provided with two ventilators to each hold. With regard to dimentions and capacities of the holds, these are shown on table 3.1.

1.3 The conditions on stowage and transportation

The following method was conducted in order to re-confirm countersteps for preventing the spontaneous heating during transportation.

1.3.1 On the 1st survey

This survey was conducted conforming to the conditions which prevail as stowage practice of the cargo of concentrates, no trimming with fresh air therein.

1.3.2 On the 2nd survey. Surveyed holds, No.3 & No.4.

In the No.3 hold, the pile was made flat like an oval shape and covered by plastic sheets. In the No.4 hold, the pile was trimmed

and compacted only under the hatch square by a buldozer and the ventilators were closed tightly. (These conditions are shown in detail on Table 3.1).

1.3.3 The items carried out at the unloading port.

    a) Measuring temperatures in the concentrate at given points to each the hold.

    b) Measuring the gaseous composition in each the hold.

    c) Sampling for analysis from each the hold.

Results of the tests carried out on board the carrying vessel are shown in Fig. 3.1 and 3.2.

Results of the measurements performed on arrival at the unloading port are figured out on table 3.2 and 3.3.

2. General evaluation derived from the results

(1) When allowed free entry of air into the hold and provided no trimming, temperature in the concentrate had risen gradually at a certain rate irrelevant to that of the ambient temperature. A maximum temperature at around 80°C was recorded at some places on the 9th day after starting her voyage.

(2) In the case of the aforementioned item (1), a substantial variation in temperature between each location measured, was also recognized.

(3) In the case when provided no trimming and closed the ventilators, these were smaller increase and variation in temperature in comparison with that in the preceding paragraph of (1).

(4) When effective covering was applied, there was no rise in concentrate temperature, and the oxygen concentration could be also kept the normal one.

(5) In the tentative stowage which provided adequate compaction to the cargo stow and closed the ventilators, there was no rise of the concentrate temperature.

(6) When closed the ventilators on the second practical survey, the oxygen concentration in the compartment during transportation was recorded to decrease down to the level of 16 per cent.

(7) The maximum temperature was observed at the depth down to 15 - 30cm from the surface. The temperatures at the surface and at the deeper positions were rather low.

(8) From the results of the tests performed onboard the carrying vessel on arrival at the unloading port, in the portion of the

stow where the spontaneous heating in a max. temperature was observed in the preceding paragraph (7), formations of water and acid soluble components were markedly recognized associating with maximum values of Fe, Cu & SO4.

Table 3.1

No. of Hold	Dimensions (m) L x B x D	Capacities (m³)	Conditions at 2nd. Voy.	
			Trimming	Ventilators
1	26.4x13.0/11.2x10.5	3,561	no	1 open 1 close
2	28.0x " "	3,736	no	2 close
3	" " "		covered	1 open 1 close
4	" " "		compacted under hatch way	2 close

Table 3.2   Results of the Measurements on the Bougainville Concentrate (First Time)

Temperature, Water and Acid Soluble Components in Relation to Depth in the Pile and the Position

(No. 1 Hold)

No.	Pile Depth (cm)	Temp. (C)	Water Soluble (%) Cu	Fe	SO$_4$	Acid Soluble (%) Cu	Fe
1	15	29	0.95	0.016	1.77	1.17	1.18
2	15	32	0.74	0.015	1.40	0.97	1.16
3	15	49	1.05	0.013	1.89	1.21	1.15
4	15	42	0.97	0.010	1.73	1.29	1.22
5	15	41	0.86	0.007	1.57	0.97	1.00
2	0	-	0.26	0.016	0.57	0.62	1.07
2	15	32	0.74	0.015	1.40	0.97	1.16
2	30	45	0.59	0.008	1.16	0.84	0.92
2	50	42	0.36	0.001	0.81	0.64	0.96
2	70	47	0.16	0.001	0.42	0.47	0.77
2	400	48	0.03	0.000	0.30	0.32	0.64

(No.4 Hold)

No.	Pile Depth (cm)	Temp. (C)	Water Soluble (%) Cu	Fe	SO$_4$	Acid Soluble (%) Cu	Fe
1	15	55	1.58	0.009	2.76	1.79	0.93
2	15	73	1.97	0.564	4.42	-	1.60
3	15	74	1.94	0.662	4.13	1.99	1.57
4	15	78	2.55	0.842	4.27	-	2.01
5	15	46	1.48	0.050	3.01	-	0.86
6	15	54	2.24	0.254	3.79	2.25	1.37
7	15	36	1.36	0.005	2.38	1.50	1.23
6	0	-	0.57	0.004	1.14	0.80	0.96
6	15	54	2.24	0.254	3.79	2.25	1.37
6	30	70	1.43	0.008	2.65	1.51	0.91
6	50	70	0.38	0.000	0.93	0.74	0.65
6	70	68	0.55	0.002	1.23	1.24	0.67
6	400	36	0.13	0.001	0.53	0.59	0.62

Table 3.3   (Second Time)

(No.1 Hold)   (No.2 Hold)

No.	Pile Depth	Temp.	Water Soluble (%)			Acid Soluble (%)		No.	Pile Depth	Temp.	Water Soluble (%)			Acid Soluble (%)	
	(cm)	(C)	Cu	Fe	SO4	Cu	Fe		(cm)	(C)	Cu	Fe	SO4	Cu	Fe
1	15	38	0.66	0.00	1.21	1.02	1.07	1	15	72	1.96	0.03	3.44	2.20	1.36
2	15	67	1.71	0.02	2.87	1.93	0.92	2	15	63	1.49	0.00	2.55	2.22	1.30
3	15	46	1.42	0.00	2.55	2.08	1.12	3	15	73	1.73	0.00	2.98	2.49	1.30
4	15	52	0.99	0.00	1.87	1.52	0.89	4	15	66	2.05	0.07	3.86	2.43	1.21
5	15	56	1.52	0.00	2.32	1.68	0.83	5	15	68	2.32	0.13	4.33	2.49	1.54
6	15	48	1.13	0.01	2.02	1.89	1.12	6	15	50	0.82	0.02	1.55	1.05	1.18
7	15	50	1.12	0.01	2.00	1.59	1.18	7	15	47	0.70	0.00	1.32	0.97	1.12
2	15	67	1.71	0.02	2.87	1.93	0.92	3	15	73	1.73	0.00	2.98	2.49	1.30
2	30	62.5	1.54	0.01	2.83	1.84	0.80	3	30	66	0.21	0.00	0.59	0.43	0.71
2	50	60.5	0.33	0.01	0.80	0.48	0.59	3	50	66	0.21	0.01	0.61	0.36	0.68
2	70	62	0.20	0.06	0.72	0.36	0.62	3	70	68	0.25	0.14	1.00	0.38	0.95

(No.3 Hold)   (No.4 Hold)

No.	Pile Depth	Temp.	Water Soluble (%)			Acid Soluble (%)		No.	Pile Depth	Temp.	Water Soluble (%)			Acid Soluble (%)	
1	15	42	0.67	0.00	1.25	1.10	1.13	1	15	38	0.79	0.67	1.59	1.05	1.20
2	15	32	0.09	0.00	0.37	0.43	0.72	2	15	38	0.41	0.00	0.85	0.78	0.94
3	15	32	0.06	0.00	0.30	0.33	0.63	3	15	38	0.40	0.00	0.81	0.70	1.02
4	15	35	0.08	0.00	0.38	0.34	0.64	4	15	35	0.28	0.00	0.64	0.67	0.97
5	15	35	0.06	0.00	0.29	0.36	0.73	5	15	51	0.67	0.00	1.22	0.99	1.14
6	15	35	0.22	0.00	0.59	0.70	0.30	6	15	41	0.30	0.00	0.71	0.71	0.94
7	15	38	0.51	0.02	0.95	0.87	1.20	7	15	39	0.36	0.00	0.79	0.70	0.34
1	15	42	0.67	0.00	1.25	1.10	1.13	3	15	38	0.40	0.00	0.81	0.70	1.02
1	30	42	0.06	0.00	0.29	0.31	0.59	3	30	35	0.03	0.00	0.22	0.21	0.53
1	50	47	0.04	0.00	0.28	0.34	0.64	3	50	38	0.03	0.00	0.24	0.22	0.54
1	70	43	0.03	0.00	0.28	0.31	0.63	3	70	42	0.03	0.00	0.04	0.21	0.51

Fig. 1.1 Measurement apparatus of the rate of oxygen consumption
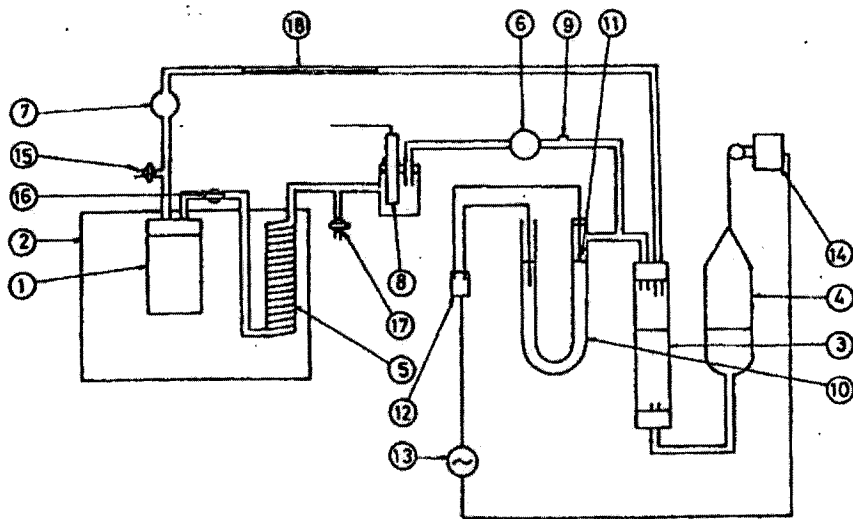
1. reaction vessel, stainless steel
2. thermostatic vessel
3. pressure regulator
4. water column
5. copper pipe coil
6. roller pump
7. water trap
8. probe for oxygen meter
9. outlet for gas sampling
10. mercury manometer
11. platinum contact
12. relay
13. power source
14. synchronous motor
15. stopcock
16. stopcock
17. stopcock
18. capillary tube
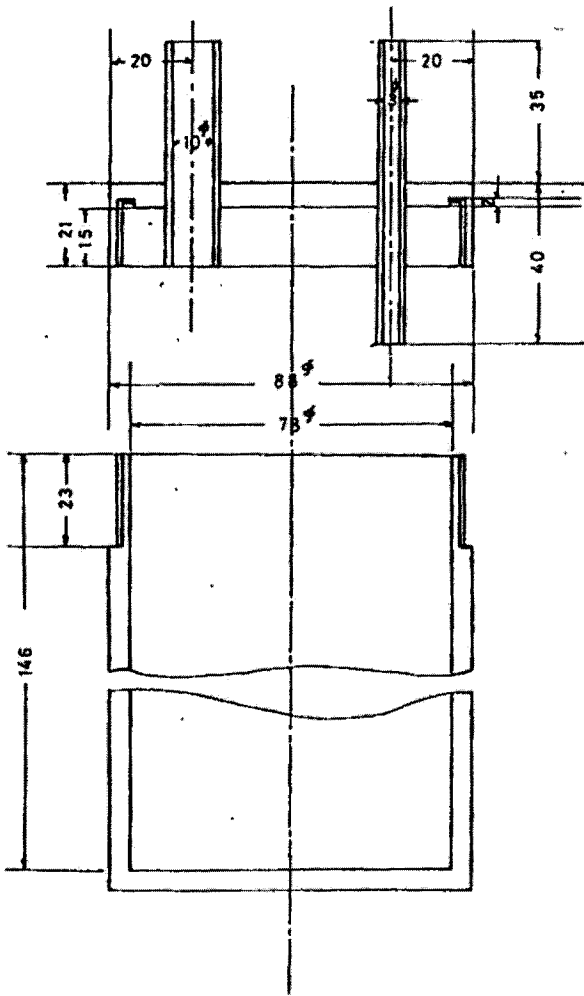
Fig. 1.2 Reaction vessel
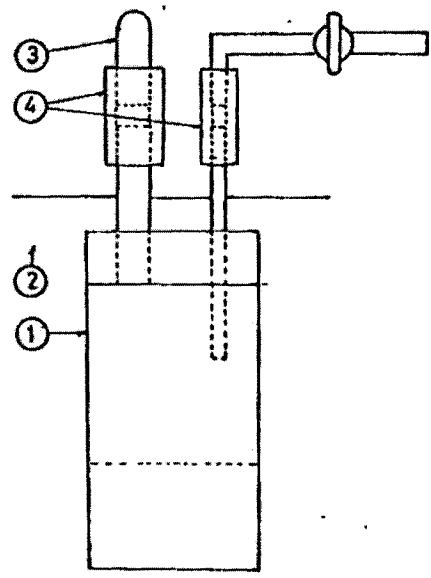
Fig. 1.3 Schematic diagram for procedure of pre-heating of concentrates before measurement

Temp	T	T_R (room temp)	T_R
Volume	V_t	$V_t - S|A-B|$	$V_t + S|C-A|$
Pressure	1030 cm H_2O	1030 cm H_2O	$1030 - h$ cm H_2O

Fig. 1.4 Schematic diagram for measurement of mole amounts of air

Fig. 1.5 Oxygen concentration (%) in closed system as function of time Musoshi copper concentrate
~ 0. 30 % moisture.

Fig. 1.6 Relation followed by equation (1)
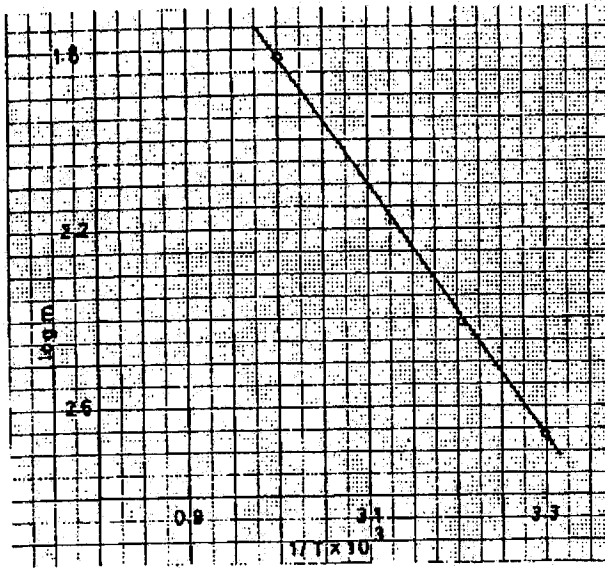
Fig. 1.7 Logarithmic plot of
reaction rate, m, against 1/T
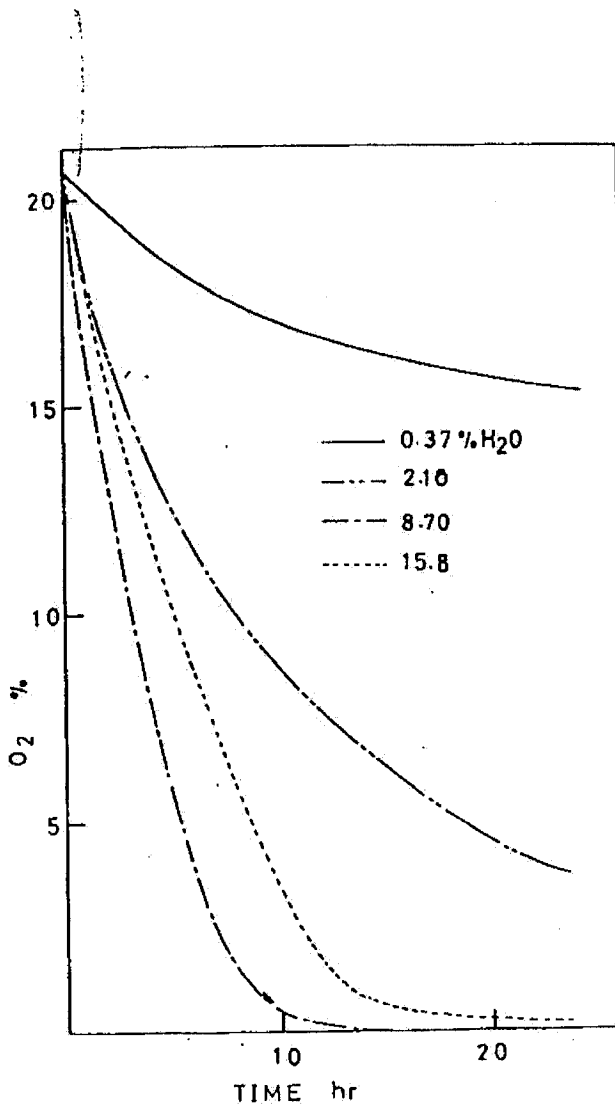
Fig. 1.8 Oxygen concentration (%)
in closed system as function of
time. Effect of moisture in
Musoshi copper concentrate
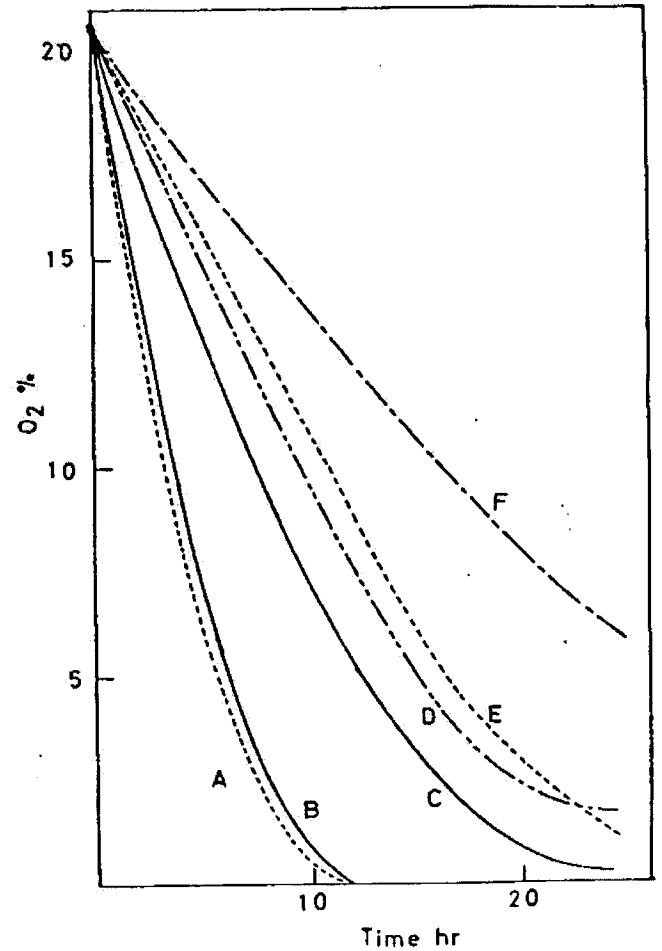
Fig. 1.9 Oxygen concentration (%)
in closed system as function of
time. Effect of species of
concentrates
A: Bougainville   B: Gibraltar
C: Shimokawa   D: Lornex
E: Kenon   F: Hitachi
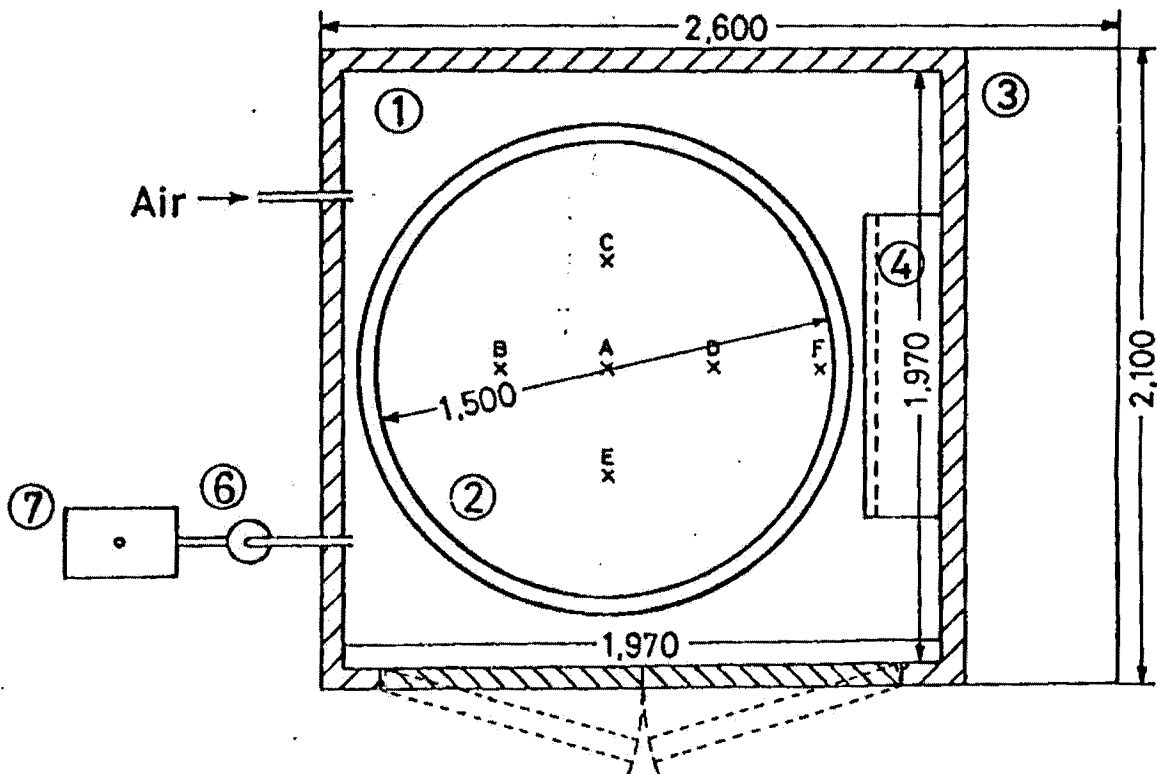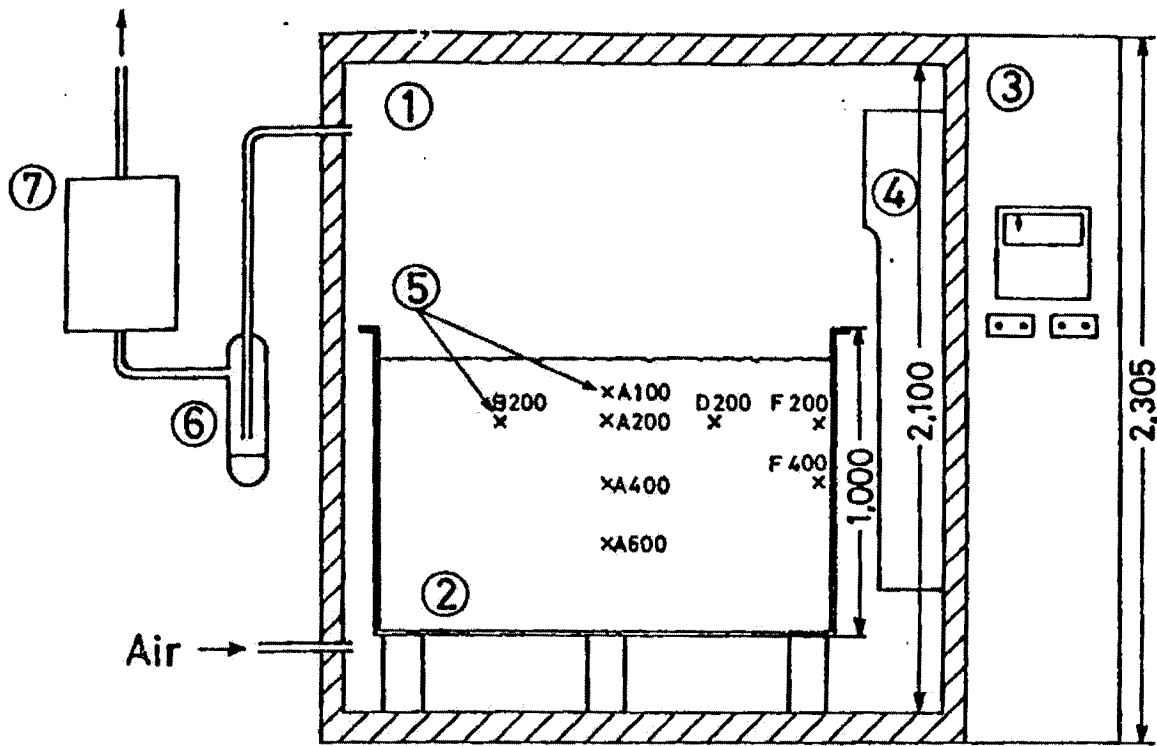
1 Constant temperature and humidity chamber
2 Container laded ore concentrate
3 Control box
4 Air conditioner
5 Thermo-couple
6 Steam trap
7 O - analyzer

Fig. 2.1   Apparatus for storing test (unit:mm)
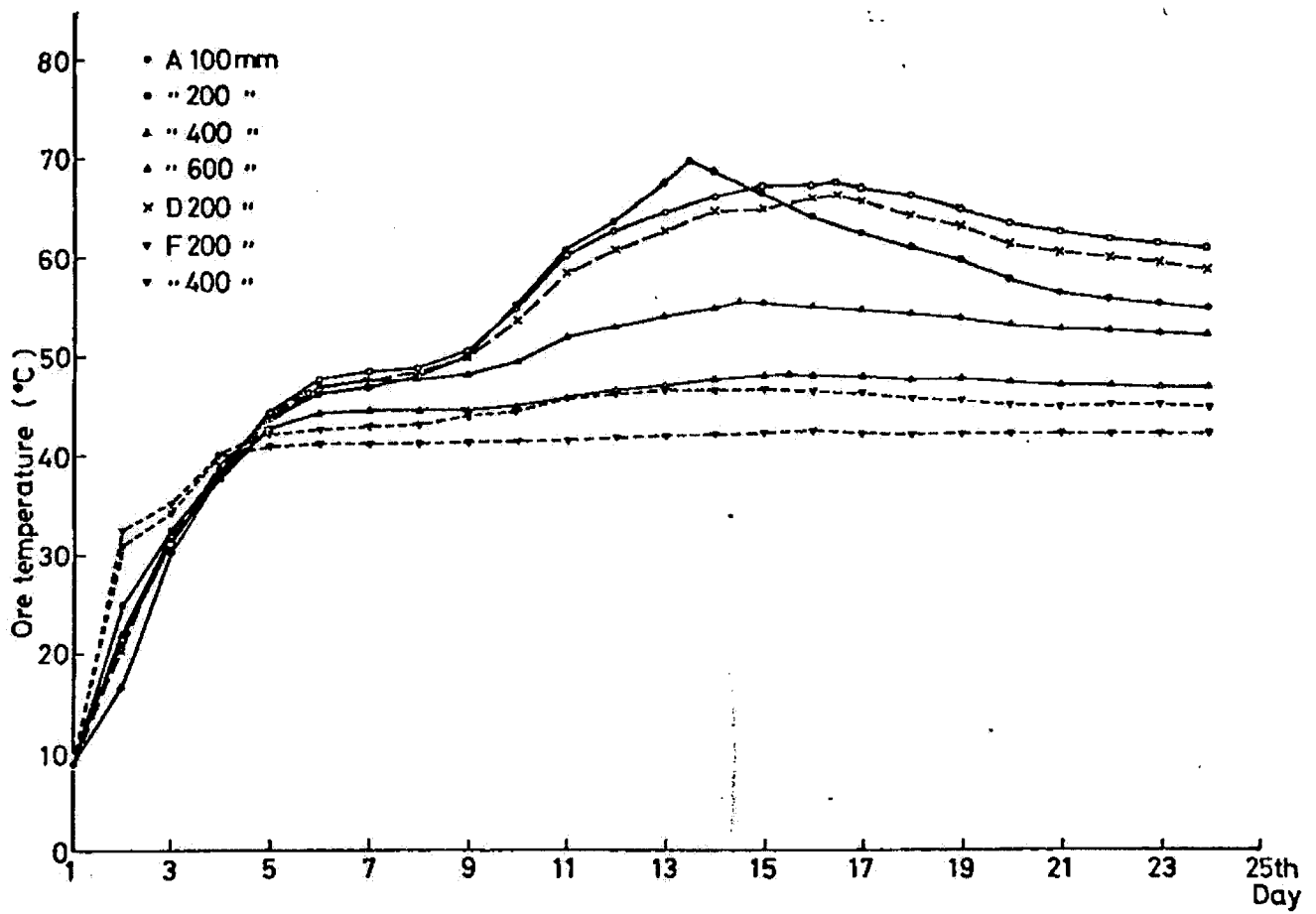
Fig. 2.2   Change of ore temperature in storing test
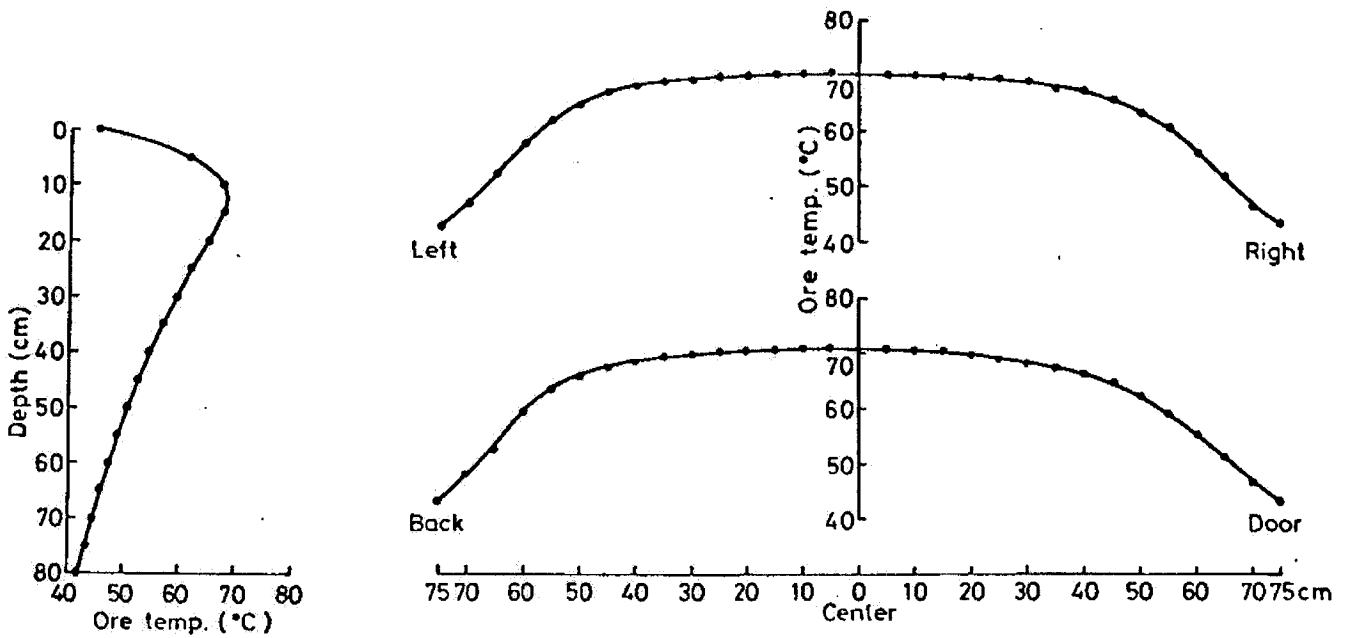
Fig. 2.3 Distribution curve of ore
temperature in vertical line.
(Center part: on the 13th day)

Fig. 2.4 Distribution curve of ore
temperature in horizontal line.
(Depth 15cm: on the 14th day)
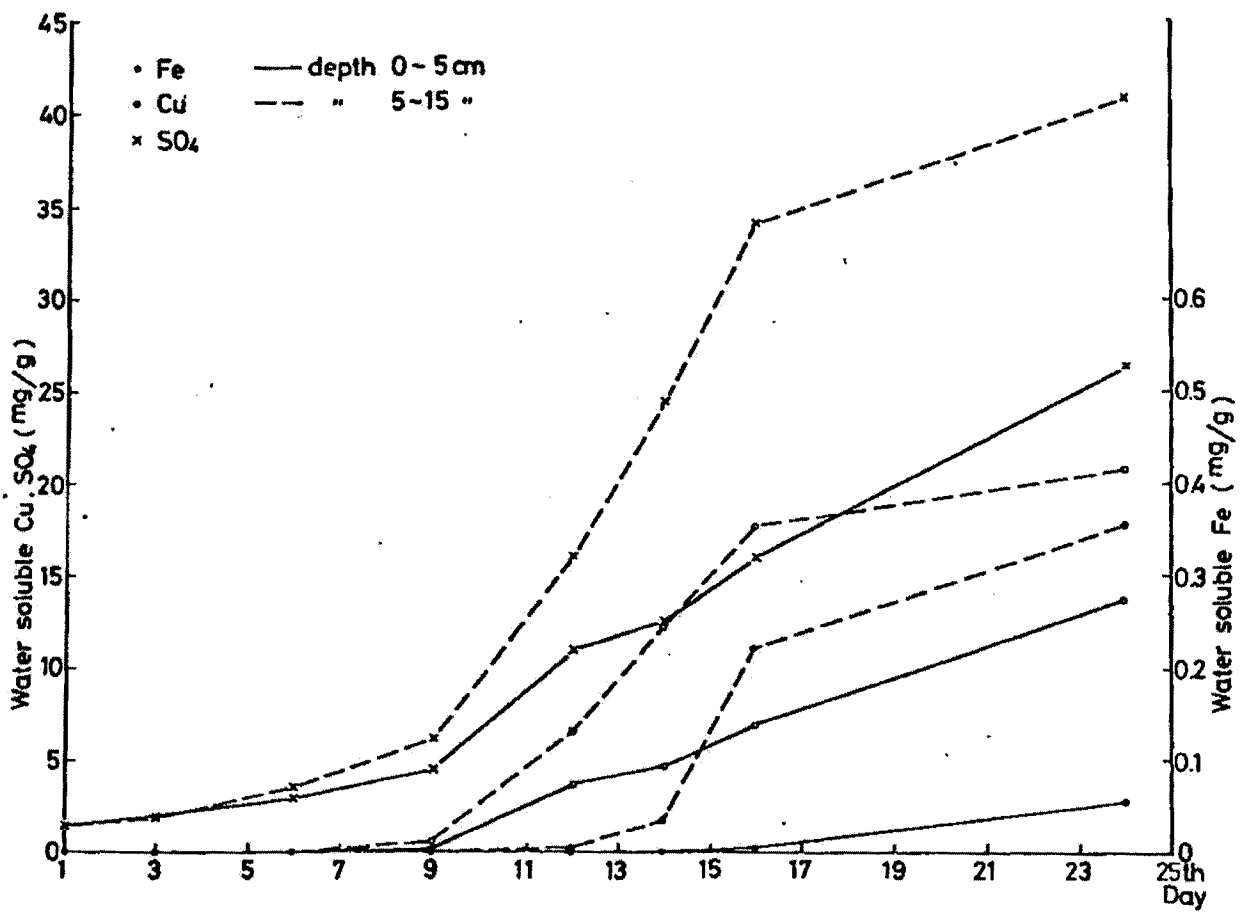
Fig. 2.5 Water soluble components of ore concentrate
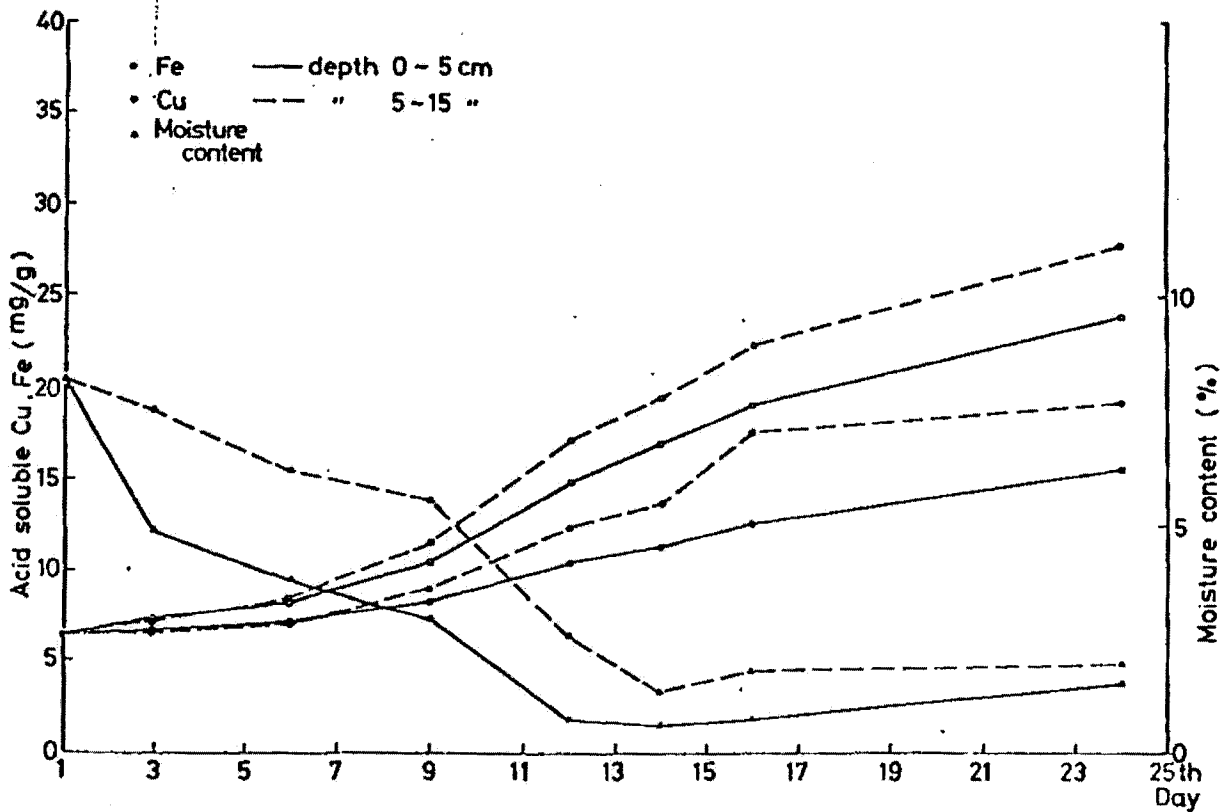
Fig. 2.6 Moisture content and acid soluble components of ore concentrate

°C

No.4 Hold

Temp.

50

30
0

°C

No.3 Hold

Temp.

Max. Temp. of Ore
Min.   ″   ″
Air Temp. in Hold

50

30
0

1   5   10
Date

Fig. 3.1   1st Voyage

°C

Max.Temp. ⎫ Compacted Ore
Min.   ″ ⎭
Max.Temp. ⎫ Noncompacted Ore
Min.   ″ ⎭
Air Temp. in Hold

No.4 Hold

Temp.

50

30
0

°C

No.3 Hold

Max. Temp. of Covered Ore
Min.   ″   ″
Air Temp. in Hold

Temp.

50

30
0

1   5   10
Date

Fig. 3.2   2nd Voyage